Fundamental Limits of Poisson Channels in Visible Light Communications

by

Ain-ul-Aisha

A Thesis

Submitted to the Faculty

of the

WORCESTER POLYTECHNIC INSTITUTE

In partial fulfillment of the requirements for the

Degree of Doctor of Philosophy

in

Electrical and Computer Engineering

by

May 2017

APPROVED:

_____

Professor Lifeng Lai, Major Thesis Advisor

_____

Professor Kaveh Pahlavan, Department of Electrical and Computer Engineering

_____

Professor Yingbin Liang, Syracuse University

Abstract

Visible Light Communications (VLC) has recently emerged as a viable solution for solving the spectrum shortage problem. The idea is to use artificial light sources as medium to communicate with portable devices. In particular, the light sources can be switched on and off with a very high-frequency corresponding to 1s and 0s of digital communication. The high-frequency on-off switching can be detected by electronic devices but not the human eyes, and hence will not affect the light sources' illumination functions.

In VLC, if a receiver is equipped with photodiodes that count the number of arriving photons, the channels can be modeled as Poisson channels. Unlike Gaussian channels that are suitable for radio spectrum and have been intensively investigated, Poisson channels are more challenging and are not that well understood. The goal of this thesis is to characterize the fundamental limits of various Poisson channels that models different scenarios in VLC.

We first focus on single user Poisson fading channels with time-varying background lights. Our model is motivated by indoor optical wireless communication systems, in which the noise level is affected by the strength of the background light. We study both the single-input single-output (SISO) and the multiple-input and multiple-output (MIMO) channels. For each channel, we consider scenarios with and without delay constraints. For the case without a delay constraint, we characterize the optimal power allocation scheme that maximizes the ergodic capacity. For the case with a strict delay constraint, we characterize the optimal power allocation scheme that minimizes the outage probability.

We then extend the study to the multi-user Poisson channels and analyze the sum-rate capacity of two-user Poisson multiple access channels (MAC). We first characterize the sum-rate capacity of the non-symmetric Poisson MAC when each transmitter has a single

antenna. We show that, for certain channel parameters, it is optimal for a single-user to transmit to achieve the sum-rate capacity. This is in sharp contrast to the Gaussian MAC, in which both users must transmit, either simultaneously or at different times, in order to achieve the sum-rate capacity. We then characterize the sum-rate capacity of the Poisson MAC with multiple antennas at each transmitter. By converting a non-convex optimization problem with a large number of variables into a non-convex optimization problem with two variables, we show that the sum-rate capacity of the Poisson MAC with multiple transmit antennas is equivalent to a properly constructed Poisson MAC with a single antenna at each transmitter.

We further analyze the sum-rate capacity of two-user Poisson MIMO multiple-access channels (MAC), when both the transmitters and the receiver are equipped with multiple antennas. We first characterize the sum-rate capacity of the Poisson MAC when each transmitter has a single antenna and the receiver has multiple antennas. We show that similar to Poisson MISO-MAC channels, for certain channel parameters, it is optimal for a single user to transmit to achieve the sum-rate capacity, and for certain channel parameters, it is optimal for both users to transmit. We then characterize the sum-rate capacity of the channel where both the transmitters and the receiver are equipped with multiple antennas. We show that the sum-rate capacity of the Poisson MAC with multiple transmit antennas is equivalent to a properly constructed Poisson MAC with a single antenna at each transmitter.

Acknowledgements

First of all I would like thank my advisor Professor Lifeng Lai for his guidance throughout my research. He made sure that I grow as a researcher and a problem solver and always believed in me.

I would also like to thank Professor Yingbin Liang and Professor Kaveh Pahlavan for not only serving as committee members for this thesis, but also taking personal interest to help me grow. I would like to thank Professor Shlomo Shamai (Shitz), as well, for his encouragement that helped me strive for improvement. I was able to observe these amazing researchers in their respective fields and learn a lot from them.

I would like to thank my peers and my friends specially Quratulain Shafi, Wenwen Tu, Wenwen Zhao, Bingwen Zhang, Jun Geng, Mostafa El Gamal and Bo Jiang, for keeping a healthy competitive environment around me and making sure that I push myself harder.

I would like thank the WPI ECE department office personnel, facilities, students and professors for maintaining a creative environment. I would like to personally thank Cathy and Colleen from the WPI ECE office their utmost support. I would like to thank Marlaine from WPI facilities for her smile and motherly persona.

Most importantly I would like to thank my husband Umair Ishaq Khan, who made sure that I remain intent on my final goal. Without his support, this journey would have been much more arduous. I would also like to thank my mother in law Salma Aslam Khan for her prayers and efforts that helped me get to this point. I would like to thank my aunts and uncles for their love, my siblings Ahmed, Noor and Hassan for always keeping things entertaining for me whenever I was having a bad day. Last but not the least, I would like to thank my father Haroon Anis and my mother Shaista Haroon for their unconditional love, nothing would have been possible without their support and faith in me.

Contents

List of Figures

List of Tables

Chapter 1

Introduction

Wireless networking technology has seen rapid development and wide deployment in the past few decades. However, one factor that is impeding the further development of wireless networks is the scarcity of radio spectrum. As shown in Figure. 1.1, the radio spectrum is highly congested. There has been significant recent research efforts to solve this challenge. Two of the promising emerging solutions are: i) Cognitive Radios (CR) [1], [2], [3]; and ii) Optical Communications.

The main idea of the cognitive radios is to divide spectrum users into two categories [4], [5], [6]: primary users, which are licensed users that are authorised to use certain channels and hence have the highest priority, and secondary users which are non-licensed users with lower priority. These secondary users use either any channel while keeping the interference to the primary users to an acceptable level or they use the channel when it is not being used by any primary user.

The second method being considered is to use optical communications. Among optical communications, Free Space Optics (FSO) is extremely popular but recently Visible Light Communications (VLC) has also gained a lot of attention and is considered as a viable alternative indoor wireless transmission technology [7], [8], [9], [10], [11].

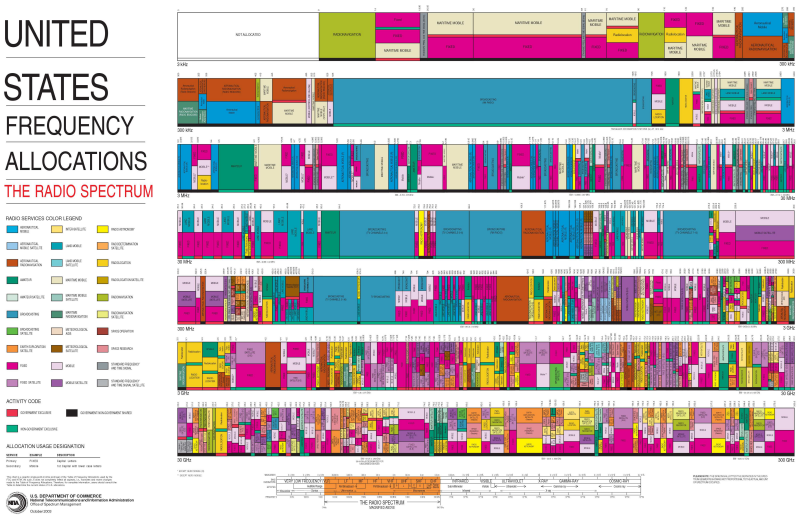

Figure 1.1: A Congested Radio Spectrum

Optical communication taps into a vast amount of untouched spectrum resources and also helps in scenarios in which radio frequency (RF) does not fit well [12]. FSO uses lasers as medium for communications, while VLC uses normal visible light as communication medium. Using lasers, communication in FSO is exceptionally directed, therefore it is not subjected to interference from nearby transmitters and receivers. However, it limits the communication to be point to point [13–16]. While the high dispersion of visible light in VLC imposes the need to deal with interference between transmitters and receivers in the range, it does not require strict point-to-point and hence is ideal for a much larger flavor of network topologies and channel models.

The idea of VLC is to use the abundantly available artificial light sources as a way to communicate with mobile devices. These light sources are turned on and off at such high rate that naked eyes will not notice these fluctuations (and hence they can still be used for illumination purpose). Photon detectors at the mobile devices, on the other hand, can detect these fluctuations, and hence can use them for communications' purpose.

In this thesis, we will investigate various design issues in VLC.

1.1 Comparison between VLC and Radio Frequency Systems

Compared with RF systems, VLC enjoys several advantages [17], [18]:

1. VLC has a much larger bandwidth. The bandwidth of the available RF spectrum is several Giga Hz, while the bandwidth of the available visible light bandwidth is Pico Hz.

2. VLC has very little regulatory restrictions compared to that of the RF. Use of RF equipment is restricted near sensitive devices to avoid interference, but there is no such restriction for VLC.

3. Due to limited transmission range, VLC is more secure. Lights can be easily confined in a room, while radio signal can be intercepted by attacker outside a room.

However, VLC has certain limitations as well. Such disadvantages are listed as:

1. The communication distance for VLC ranges from 1m to 100m, therefore small communication range is the biggest disadvantage of VLC.

2. Compared to RF, VLC can not penetrate walls and other obstacles so if the receiver is encapsulated then the sigal will not reach it.

3. VLC suffers from beam dispersion, therefore the signal reaching to the receiver might not be strong enough and be subjected to several forms of interference.

1.2 Introduction to the Poisson Channel

There are two major types of distributions that are widely used to model wireless communication channels: Gaussian model and Poisson model. Gaussian model is typically used

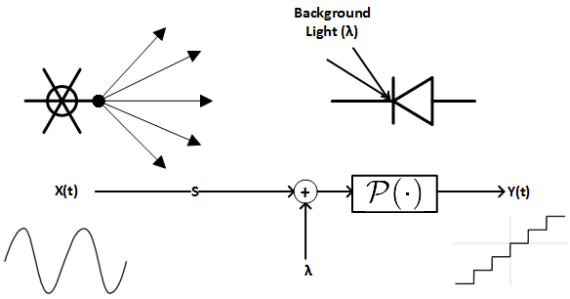

Figure 1.2: Poisson Channel

to model RF channels. Poisson Channel, whereby the arrival of photons is recorded by photon-sensitive devices incorporated in the receivers [19], is often used to model FSO and VLC [20–23]. [24] discusses that in an ideal photon counting detector, the probability of observing a photon is very small over a small time interval. Consequently the probability of observing two or more photons is even smaller and also the number of photons observed in the non-overlapping time intervals are independent of each other. These observations lay the foundation of the conclusion that the photon counting process for a VLC can be modeled as a Poisson counting process.

Figure 1.2 shows a standard single transmitter, single receiver Poisson channel. For a Poisson channel, the channel output $Y(t)$ is

$$Y(t) = \mathcal{P}\left(SX(t) + \lambda\right), \tag{1.1}$$

where $\mathcal{P}(\cdot)$ is the Poisson process, S is the channel gain and λ is the dark current that is the physical characteristics of the photodiode present at the receiver. Poisson process is defined by the probability of observing k photons at the receiver:

$$Pr\{Y(t+\tau) - Y(t) = k\} = \frac{e^{-\Lambda}\Lambda^k}{k!}, \tag{1.2}$$

where Λ is the arrival rate obtained by:

$$\Lambda = \int_{t}^{t+\tau} (SX(t') + \lambda)dt'.$$

In (1.1), $X(t)$ is the channel input that is subject to two types of constraints: maximum power constraint and average power constraint

$$0 \leq X(t) \leq A, \tag{1.3}$$

$$\frac{1}{T}\int_{0}^{T} X(t)dt \leq \sigma A, \tag{1.4}$$

in which A is the maximum power allowed, σ is the average to peak power ratio and T is the total time for transmission.

1.2.1 Gaussian Channels Vs. Poisson Channels

As mentioned above, Gaussian model is a popular choice for modeling RF channels, while Poisson model is considered more appropriate for the VLC. Compared to the Gaussian channel that has been extensively studied [25], the Poisson channel is less well understood due to several technical challenges.

1. Gaussian channels are linear where the channel output is given by $Y = SX + N$, whereas Poisson channel are non-linear $Y = \mathcal{P}(SX+\lambda)$, where $\mathcal{P}(\cdot)$ is the Poisson mapping, S is the channel gain, N is the channel noise for Gaussain channel and λ is the dark current for the Poisson channel. Therefore Poisson channels are not scale invariant like Gaussian channels.

2. The channel input to a Poisson channel is restricted to a positive value while the input to the Gaussian channel can be both positive and negative.

3. Gaussian channels are analog input and analog output channels while the Poisson channels are analog input digital output channels. Therefore the analysis of Poisson channel is much more complex.

Since, a Poisson channel is considered to be more complex than a traditional Gaussian channel, there are few approximations to make the analysis a little simpler. One such approximation is discussed in the next section, which would aid in the further analysis carried out in this study.

1.2.2 Capacity of a Poisson Channel

In this section, we first review existing results and techniques for the characterization of the capacity of a Poisson channel.

In particular, Wyner [26] developed a binary approximation method that converts the complicated continuous time continuous input discrete output Poisson channel into a discrete time binary input binary output channel. It is much simpler to handle the binary channel, and it is shown in [26] that this binary approximation does not reduce the capacity.

In this binary approximation, the time is divided into intervals, each with duration Δ. In each time interval $(i-1)\Delta \leq t \leq i\Delta$, the input waveform $X(t)$ is set to be a constant, which is equal to A with probability μ and is equal to 0 with probability $1-\mu$. Hence, μ can be viewed as the duty-cycle. Therefore, to satisfy the average power constraint (1.4), we require $\mu \leq \sigma$. Let X^{Δ} be a binary random variable with

$$X^{\Delta} = \begin{cases} 1 & \text{if } X(t) = A, \\ 0 & \text{if } X(t) = 0. \end{cases} \tag{1.5}$$

It is clear that $\Pr\{X^{\Delta} = 1\} = 1 - \Pr\{X^{\Delta} = 0\} = \mu$. At the receiver side, the receiver

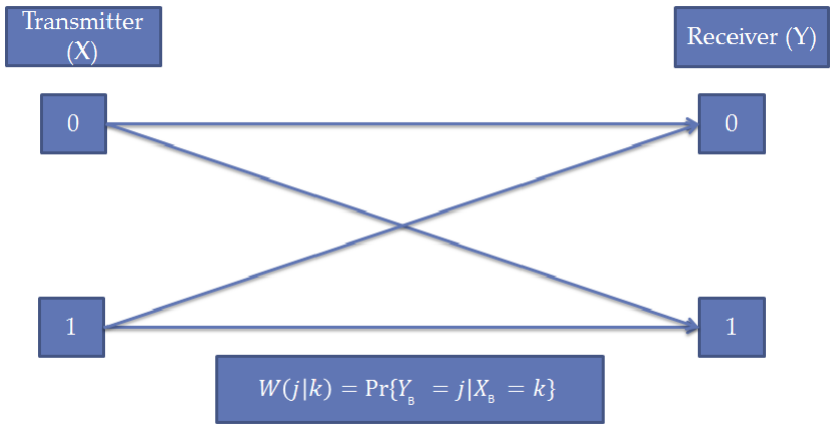

Figure 1.3: Binary Input and Binary Output Channel

records only whether or not there is exactly one photon arriving during each time interval $(i-1)\Delta \leq t \leq i\Delta$. Let Y^Δ be a binary random variable whose value is 1 if the receiver observes one photon in the small interval Δ, and is 0 otherwise. Using (1.2), one can easily compute the transition probabilities

$$\begin{aligned} \Pr\{Y^\Delta = 1|X^\Delta = 0\} &= \lambda\Delta e^{-\lambda\Delta}, \\ \Pr\{Y^\Delta = 1|X^\Delta = 1\} &= (SA+\lambda)\Delta e^{-(\lambda+SA)\Delta}. \end{aligned} \tag{1.6}$$

Figure 1.3 shows the transformed binary channel. It is easy to see that the capacity of the binary channel defined by $X^\Delta \to Y^\Delta$ is $\max\limits_{0\leq\mu\leq\sigma} I(X^\Delta;Y^\Delta)$, and the normalized value $\frac{1}{\Delta}\max\limits_{0\leq\mu\leq\sigma} I(X^\Delta;Y^\Delta)$ is an achievable rate for the original Poisson channel. Remarkably, [26] showed that this simple scheme is capacity achieving, and the capacity of the SISO Poisson non fading channel is given by

$$C_{SISO} = \lim_{\Delta\to 0}\frac{1}{\Delta}\max_{0\leq\mu\leq\sigma} I(X^\Delta;Y^\Delta). \tag{1.7}$$

Using (1.6), it was shown in [26] that

$$C_{SISO} = \max_{0\leq\mu\leq\sigma} \left[\mu\left(SA+\lambda\right)\log\left(SA+\lambda\right)\right. \\ \left. +(1-\mu)\lambda\log\lambda - (\mu SA+\lambda)\log\left(\mu SA+\lambda\right)\right]. \tag{1.8}$$

Intuitively, the first term in (1.8) corresponds to the case when the transmitter is on (i.e., $X(t) = A$ and the Poisson arrival rate at the receiver is $SA + \lambda$), which happens with probability μ. The second term corresponds to the case when the transmitter is off (i.e., $X(t) = 0$ and the Poisson arrival rate at the receiver is λ), which happens with probability $1 - \mu$. The third term corresponds to the average case (i.e., the average Poisson arrival rate at the receiver is $\mu SA + \lambda$). The optimal value of μ can be easily obtained by solving the optimization problem (1.8).

1.3 Literature Review

Recently, there have been great interests in analyzing Poisson channels. In this section, we will briefly discuss the existing literature on the Poisson channels.

The point-to-point single-user Poisson channel has been investigated from various perspectives, including single antenna [26–30], multiple antennas [31], fading channels [32], [33], in continuous-time [26, 34–37] and discrete-time [38–40]. There are two major types of fading models, that with time-varying channel gains and that with time-varying noise (e.g., background light) levels, for Poisson fading models. These two types of models are not equivalent and cannot be treated equivalently, because Poisson channels are not scale-invariant. This is different from Gaussian fading channels, in which channels with varying noise levels can be converted to channels with varying channel gains due to the scale-invariant property.

The first type of Poisson fading channels with time-varying channel gains have been studied in [31, 41–43], which characterized the ergodic and outage capacities. These studies developed useful information theoretic tools that will also be used in our thesis. Furthermore, [19] investigated this type of fading channels when the channel gains are log-normal random variables. The performance of the channel in both high and low signal to noise ratio regimes are studied based on lower and upper bounds on the channel capacity. [44] investigated the outage probabilities of several diversity schemes. [45] studied a single-input single-output (SISO) Poisson channel with channel state information (CSI) perfectly known at the receiver and partially known at the transmitter. The goal is to maximize the ergodic capacity of the channel, with partial information at the transmitter obtained by an error-free feedback link with a finite rate constraint from the receiver to the transmitter. [46] investigated the behavior of the outage capacity for the decode-and-forward multi-hop Poisson fading channel for FSO, where the atmospheric turbulence contributes to the fading in the channel. This study has characterized the optimal power control function under different assumptions on the availability of the CSI at the transmitter.

The second type of Poisson fading channels with time-varying noise levels have been much less studied with only a few exceptions as we describe below. In fact, such models arise in many practical scenarios. For instance, in indoor optical wireless communications, the noise levels at the receiver are affected by the temperature and the strength of the background light, as the noise level increases when the temperature or the strength of the background light increases. In addition, the noise level is higher when other light sources are also on. [47] studies optimal power allocation for 2 fold parallel poisson channel for constant dark current, which can be viewed as an equivalent SISO channel with time-varying noise levels. A recent study [48] also dealt with the channel with time-varying noise levels under an assumption that the transmitter knows the noise realization

at the receiver.

The Poisson channels with multiple users are not as well understood as single user Poisson Channels. [49–51] discuss that a Poisson broadcast channel can model an optical broadcast network, where [49] investigates the conditions under which the Poisson broadcast channel is stochastically degraded. [50] shows that the superposition coding is optimal much beyond the parameter ranges for which the channel is degraded. The superposition coding scheme is motivated by broadcast channels for which one receiver is much stronger than the other. [52] studies the Poisson multiple-access channels when users are equipped with a single antenna. It characterizes the sum-rate capacity and also characterizes the capacity region. [53] also studies the Poisson multiple-access channels and investigates the capacity region of Poisson MAC with respect to different power constraints. [54] considers the Poisson channel with side information at the transmitter, and argues that knowing the times at which the spurious counts occur only causally at the transmitter does not increase the channel capacity. Furthermore, [55] discusses Poisson interference channel, while [56] proposes a two-user discrete time Poisson (DTP) MAC model and proves the discreteness of sum capacity achieving distributions. [57] discusses the discrete-time Poisson channel and shows that sum-capacity achieving distributions of the Poisson MAC under peak amplitude constraints are discrete with a finite number of mass points.

1.4 Summary of Contributions

In this thesis, we analyze Poisson channels that model a variety of scenarios. In particular, we first consider Poisson channel for a single receiver and a single transmitter equipped with single antenna each and then expanded the analysis to when both are equipped with multiple antennas each. We then study Poisson channels when multiple users commu-

nicate with a single receiver and each user is equipped with a single antenna. Finally, we extend our analysis to the scenario when the users are equipped with multiple antennas each. Each of these scenarios are briefly discussed below, before elaborating them individually in subsequent chapters.

1.4.1 Single User Poisson Channel

In our research, Poisson fading channels with time-varying noise levels are studied. Our model is clearly different from the first type of Poisson fading models studied in [19, 31, 41–46, 58] due to the non-equivalence of the two types of models as we explain above. Our study is also different from [47], in which the model is equivalently SISO and the study focused on the case with two channels (equivalently two noise levels), whereas here we study the more general SISO case with arbitrary number of noise levels and MIMO channel. Our study also differentiates from [48] in that we make a mild assumption that only the noise level (a statistic quantity) rather than the realization of the noise is known at the transmitter.

More specifically, we study both the SISO and MIMO channels with and without delay constraints. Our contributions lie in a comprehensive characterization of the optimal power allocation schemes to achieve the ergodic capacity (for the case with no delay constraints) and to minimize the outage probability (for the case with delay constraints). Here, the delay constraint is measured by the number of fading blocks after which the receiver decodes information (i.e., codewords). The delay can also be viewed as the number of fading blocks that a codeword is allowed to span. If there is no delay constraint, then the codeword length is allowed to be infinite, in which case we use the ergodic capacity as the performance metric. If there is a delay constraint that requires the receiver to decode after a finite number of blocks, then we focus on the outage probability that captures the performance of such a scenario. For both scenarios, we assume that the transmitter knows

the noise level. As will be clear in the sequel, this is a reasonable assumption because the noise level here represents a statistic quantity but not the realization of the noise. Hence, the amount of feedback needed from the receiver to the transmitter is limited. In addition, as the noise level is affected by the background light, it can be effectively measured at the transmitter. This can further reduce the amount of feedback necessary for the transmitter to learn the value of the noise level.

For the case with no delay constraint, we establish the ergodic capacity, and characterize the corresponding optimal power allocation scheme as a function of the noise level that achieves the ergodic capacity. For the case with a strict delay constraint, our goal is to minimize the probability that the instantaneous achievable rate is less than a given threshold, i.e., the outage probability. Minimizing the outage probability directly is very challenging. In order to solve the problem, we apply the techniques developed in [59] to study a number of related optimization problems. From the solutions of these optimization problems, we then characterize the optimal power allocation scheme that minimizes the outage probability. Both problems are significantly more challenging than the corresponding problems in the Gaussian channels.

1.4.2 Multiple User Poisson Channel - Single Receiving Antenna

We further extend our research to multi-user Poisson channels. [52] is of particular relevance to our study, as it thoroughly investigates the continuous-time Poisson MAC with each user equipped with single antenna. [52] shows that the approximation of the complex continuous-time continuous-input discrete-output Poisson MAC by a discrete-time binary-input binary-output MAC does not result in a loss in terms of the capacity region. [52] determines the sum-rate capacity of the symmetric Poisson MAC, in which the channel gains and power constraints for all users are identical under the maximum power constraint. Furthermore, it characterizes the boundary points on the capacity region

of the symmetric MAC under maximum power constraint and analyzes the maximum-throughput under peak-power and average power constraints.

In our study, we first study the single antenna *non-symmetric* Poisson MAC, in which the channel gains and power constraints at the two users are not necessarily the same, though we consider a non-fading channel model i.e. channel gain and the dark current are not time varying. We refer to such a channel as Poisson SISO-MAC. This scenario naturally arises in multiuser optical communications when the transmitters have different distances to the receiver or have different transmission powers. Unfortunately, the method used in [52] to characterize the sum-rate capacity for the *symmetric* case does not apply to the *non-symmetric* case anymore. In particular, the method in [52] exploits the property that the objective function involved is a Schur concave function for the *symmetric* Poisson MAC. There is an interesting property of Schur concave functions where if $\phi(\cdot)$ is a Schur concave function, i.e. $\phi(x_1, x_2, ..., x_k) \leq \phi(\bar{x}, \bar{x}, ..., \bar{x})$, where $\bar{x} = (x_1 + x_2 + ... + x_k)/K$, which greatly simplifies the analysis. Hence, the multi-dimensional convex optimization problem can be converted into a single-dimensional convex optimization problem. However, in the *non-symmetric* channel, the objective function is not symmetric, and hence is not Schur concave anymore. As a result, we resort to a different approach from the one used in [52] to study the sum-rate capacity. More specifically, we show that characterizing the sum-rate capacity is equivalent to solving a non-convex optimization problem. We show that there are at most four possible candidates for the optimal solution to this optimization problem with two candidate solutions corresponding to the cases when only one user transmits. We further show that, for some channel parameters, it is indeed optimal to allow only one user to transmit in order to achieve the sum-rate capacity under the maximum power constraint. This is in sharp contrast to the Gaussian MAC with an average power constraint, in which it is always optimal for both users to transmit, either simultaneously or at different time, to achieve the sum-rate capacity. We

also identify conditions under which it is optimal for both users to transmit in order to achieve the sum-rate capacity.

We then extend the study to Poisson MAC with multiple antennas at each transmitter and one antenna at the receiver. We refer to this as Poisson MISO-MAC. Similarly to the Poisson SISO-MAC, the complex continuous-time continuous-input discrete-output Poisson MAC can be converted to a discrete-time binary-input binary-output Poisson MAC. However, the resulting problem is much more challenging than that of the Poisson SISO-MAC. In particular, to characterize the sum-rate capacity, we need to solve a non-convex optimization problem with $2^{J_1} + 2^{J_2}$ variables, in which J_n is the number of antennas at user n. Despite this challenge, we show that the optimal value obtained from this optimization problem with a large number of variables is the same as that of an optimization problem with only 2 variables. Furthermore, this reduced dimension optimization problem is equivalent to a problem arising in the Poisson SISO-MAC with properly chosen parameters. As the result, characterizing the sum-rate capacity of the Poisson MISO-MAC is equivalent to characterizing the sum-rate capacity of a Poisson SISO-MAC. Hence, the techniques and asymptotic analysis developed in the SISO-MAC case can be used for the MISO-MAC case. There are two major steps in our proof. In the first step, we show that the original optimization problem with $2^{J_1} + 2^{J_2}$ variables can be converted to a non-convex optimization problem with $J_1 + J_2$ variables by showing and exploiting the fact that, at the optimality, if the antenna with a smaller duty cycle is on, then the antenna with a larger duty cycle is also on. In the second step, we show that the optimization problem with $J_1 + J_2$ variables obtained in step 1 can be converted to an optimization problem with only 2 variables. The key ingredient in this step is to show that, at the optimality, all antennas at each transmitter have to be simultaneously on or off.

1.4.3 Multiple User Poisson Channel - Multiple Receiving Antennas

We further extend the study to the case where all users are equipped with multiple antennas (MIMO-MAC). Having multiple receiving antennas makes the problem considerably more complex than that of MISO-MAC [60]. In particular, in MISO-MAC [60], although the objective function is not convex, we are able to convert the set of nonlinear equations corresponding to KKT conditions, which are necessary but not sufficient conditions for optimality, into a set of linear equations along with a nonlinear but convex equation. This special structure of KKT conditions in MISO-MAC enables us to make further analysis. Unfortunately, this conversion technique developed for MISO-MAC does not work for MIMO-MAC anymore. As the result, we need to devise new technique to analyze MIMO-MAC. Despite this challenge, using a novel channel transformation argument, we show that characterizing the sum-rate capacity of MIMO-MAC can be reduced to characterizing the sum-rate capacity of SIMO-MAC, in which each transmitter has only one antenna. Similar to SISO-MAC considered, the SIMO-MAC has a non-convex objective function. After analyzing the KKT conditions for the case with two transmitters, we draw similar conclusion that there are three optimality scenarios for achieving the sum-rate capacity: 1) when only user 1 is active and user 2 is inactive, 2) when user 2 is active and user 1 is inactive and 3) when both users are active.

The remainder of the thesis is organized as follows. Chapter 2 presents the analysis of a single user Poisson channel. Chapter 3 discusses the Poisson channel with multiple users when the receiver is equipped with a single antenna. Chapter 4 discusses the multiple user Poisson channel when the receiver is also equipped with multiple antennas. Each chapter also contains the corresponding numerical analysis. Chapter 5 offers our concluding remarks.

Chapter 2

Single User Single Receiver

In this chapter, we consider a scenario when a single user communicates with the single receiver and we try to characterize the capacity for such a channel model.

2.1 System Model

In this section, we introduce the model considered in this chapter. As shown in Figure 2.1, we consider a MIMO Poisson channel with J transmitter antennas and M receiver antennas. Let $X_j(t)$ be the input of the j^{th} transmitter antenna and $Y_m(t)$ be the

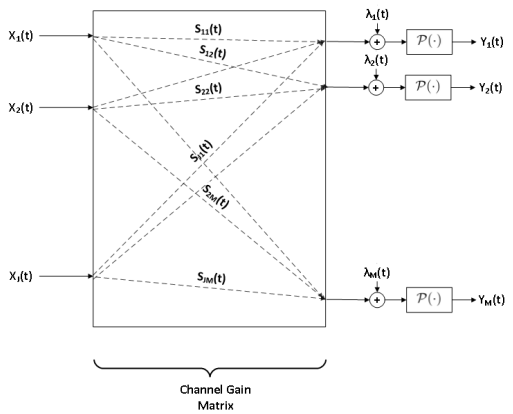

Figure 2.1: MIMO Poisson channel with time-varying background light

doubly-stochastic Poisson process observed at the m^{th} receiver antenna. The relationship between them can be described as:

$$Y_m(t) = \mathcal{P}\left(\sum_{j=1}^{J} S_{jm} X_j(t) + \lambda_m(t)\right), \tag{2.1}$$

as discussed in Chapter 1, S_{jm} is the channel response between the j^{th} transmitter antenna and m^{th} receiver antenna, $\lambda_m(t)$ is the dark current at the m^{th} receiver antenna, which signifies the background light, and $\mathcal{P}(\cdot)$ is the non-linear transformation converting the light strength to the doubly-stochastic Poisson process that records the timing and number of photon's arrivals. In particular, for any time interval $[t, t+\tau]$, the probability that there are k photons arriving at receiver antenna m is

$$\Pr\{Y_m(t+\tau) - Y_m(t) = k\} = \frac{e^{-\Lambda_m}\Lambda_m^k}{k!}, \tag{2.2}$$

$$\Lambda_m = \int_t^{t+\tau} \left[\sum_{j=1}^{J} S_{jm} X_j(t') + \lambda_m(t')\right] dt'. \tag{2.3}$$

We consider the sum power constraint, i.e. the transmitted signal $X_j(t)$ must satisfy the following constraints:

$$0 \le X_j(t) \le A_j, \tag{2.4}$$

$$\frac{1}{T}\int_0^T \sum_{j=1}^{J} X_j(t)dt \le \sigma \sum_{j=1}^{J} A_j, \tag{2.5}$$

in which A_j is the maximum power allowed for antenna j and σ is the average to peak power ratio. In our model, we assume that S_{jm} is constant while $\lambda_m(t)$ is time-varying. This model is motivated by the fact that the dark current is a physical parameter that depends on the temperature and the background lights in the environment, which naturally change throughout the day. We consider block fading model, in which $\lambda_m(t)$ is fixed for

a block of symbols and then changes to another independent value at the beginning of the next block. Furthermore, we assume that the transmitter knows λ_m. This can be justified for two reasons. Firstly, λ_m does not represent the realization of the noise, but is a statistical quantity that characterizes the average behavior of the noise process. Hence, it is reasonable that the receiver feeds back the information about λ_m albeit with a certain rate limit. Secondly, λ_m is affected by the background light and temperature, which can be measured at both the transmitter and the receiver. In this chapter, we assume that the distribution of λ satisfies the following properties: (i) $\Pr\{\lambda(t) > 0\} = 1$, (ii) $\mathbb{E}[\lambda(t)] < \infty$, and (iii) $\mathbb{E}[\lambda(t) \log \lambda(t)] < \infty$.

We note that the model considered here is different from the one considered in [41–43, 45, 46, 58], in which the channel gain S_{jm} is time-varying while λ_m is fixed. This is because the case of varying dark currents can not be converted to the case of varying channel gain, due to the nonlinearity of the Poisson channel unlike the Gaussian channels. However, some techniques developed in these studies are useful for solving the problems studied in our thesis.

2.2 SISO Channel Analysis

We first study a special case with $J = 1$ and $M = 1$, namely the SISO channel, to introduce main tools used in the MIMO case in Section 2.3. As $M = J = 1$, we drop the subscripts m and n in variables in this section for notational convenience.

2.2.1 Ergodic Capacity

In this section, we characterize the ergodic capacity of the Poisson fading channel. Following [26], it can be shown that the input $X(t)$ can be limited to be two levels without loss of optimality: either $X(t) = A$ or $X(t) = 0$. However, the probability that $X(t) = A$

can be adjusted depending on the noise level $\lambda(t)$. Let $\mu(t)$ be the time-varying duty cycle of the two-level waveform, then the average power constraint can be written as

$$\mathbb{E}[\mu(t)] \leq \sigma. \tag{2.6}$$

Using (1.8), the ergodic capacity can be characterized as

$$\begin{aligned} C_{SISO}^{f} &= \max_{\mu(t)} \mathbb{E}[I(\mu(t), \lambda(t))], && (2.7) \\ \text{s.t.} \quad & \mathbb{E}[\mu(t)] \leq \sigma, && (2.8) \\ & 0 \leq \mu(t) \leq 1, && (2.9) \end{aligned}$$

in which the expectation is over λ and

$$\begin{aligned} I(\mu(t), \lambda(t) &= \mu(t)\left(SA + \lambda(t)\right) \log\left(SA + \lambda(t)\right) + (1 - \mu(t))\lambda(t) \log \lambda(t) \\ &\quad - \left(\mu(t)SA + \lambda(t)\right) \log\left(\mu(t)SA + \lambda(t)\right) \\ &\triangleq \mu(t)\zeta(SA, \lambda(t)) - \zeta(\mu(t)SA, \lambda(t)), \end{aligned} \tag{2.10}$$

where $\zeta(x, y) = (x + y)\log(x + y) - y \log y$.

In the following, for notational convenience, we write $\mu(t)$ as μ. We characterize the optimal power allocation μ^{opt} for the constrained optimization problem (2.7)-(2.9).

For $0 \leq \mu \leq 1$, we note that $\frac{\partial^2 I(\mu, \lambda(t))}{\partial \mu^2}$ is negative, which implies that $I(\mu, \lambda(t))$ is a strictly concave function of μ in the range of our interest.

To obtain the optimal power allocation solution μ^{opt} for (2.7), we first consider the unconstrained version of (2.7) with (2.8) and (2.9) ignored. In particular, for any fading block with a given value of $\lambda(t)$, we examine the maximal rate that the channel can

support:

$$r_{max} = \max_{\mu} I(\mu, \lambda(t)). \tag{2.11}$$

Let μ^o be the corresponding maximizer. For this unconstrained problem, it is easy to obtain that

$$\mu^o = \frac{\left(1 + \frac{\lambda(t)}{SA}\right)^{\left(1+\frac{\lambda(t)}{SA}\right)}}{\left(\frac{\lambda(t)}{SA}\right)^{\left(\frac{\lambda(t)}{SA}\right)}} e^{-1} - \frac{\lambda(t)}{SA}. \tag{2.12}$$

Now, we examine (2.12) in detail. We first have the following result, which can be proved easily.

Lemma 1.

$$0 \leq \mu^o \leq 1. \tag{2.13}$$

Proof. The proof is provided in Appendix A.1. □

This result implies that μ^o satisfies the constraint (2.9).

In the following, we consider the constraint (2.8). We have two cases.

Case 1): If

$$\mathbb{E}[\mu^o] \leq \sigma. \tag{2.14}$$

In this case, μ^o also satisfies condition (2.8). Since $I(\mu, \lambda(t))$ is a strictly concave function of μ in the range of our interest, it is clear that μ^o is the maximizer for the original problem with constraints. That is

$$\mu^{opt} = \mu^o \text{ and } C^f_{SISO} = \mathbb{E}[r_{max}]. \tag{2.15}$$

Case 2): If

$$\mathbb{E}[\mu^o] > \sigma. \tag{2.16}$$

In this case, μ^o does not satisfy the condition (2.8). Hence μ^o is not the maximizer for the problem (2.7) with the average power constraint. To obtain the optimal solution for (2.7), we consider the Lagrangian function:

$$\mathcal{L}(\mu, \eta) = \mathbb{E}[\psi(\mu)] \triangleq \mathbb{E}[I(\mu, \lambda(t)) - \eta\mu]. \tag{2.17}$$

Since $I(\mu, \lambda(t))$ is a strictly concave function of μ and $-\eta\mu$ is a linear function of μ, we know that $\psi(\mu)$ is a strictly concave function of μ. From the Euler-Lagrange equation:

$$\begin{aligned}\frac{\partial\psi(\mu)}{\partial\mu} &= SA\left[-\left(\log\left(\mu+\frac{\lambda(t)}{SA}\right)+1\right)+\left(1+\frac{\lambda(t)}{SA}\right)\log\left(1+\frac{\lambda(t)}{SA}\right)\right. \\ &\quad \left.-\frac{\lambda(t)}{SA}\log\frac{\lambda(t)}{SA}\right]-\eta \\ &= 0,\end{aligned}$$

we have

$$\mu_\eta = \frac{\left(1+\frac{\lambda(t)}{SA}\right)^{\left(1+\frac{\lambda(t)}{SA}\right)}}{\left(\frac{\lambda(t)}{SA}\right)^{\left(\frac{\lambda(t)}{SA}\right)}} e^{-1} e^{\frac{-\eta}{SA}} - \frac{\lambda(t)}{SA}. \tag{2.18}$$

Now, we consider the constraint $0 \leq \mu \leq 1$. It is easy to see that $\mu_\eta \leq \mu^o$ for any positive η. From Lemma 1, we know that $\mu_\eta \leq 1$. However, μ_η might be smaller than 0. If this occurs, from the fact that $\psi(\mu)$ is a strictly concave function of μ, we know that $\psi(\mu)$ is a strictly decreasing function of μ in the range $\mu > 0$. Hence, if $\mu_\eta < 0$, the constraint $\mu \geq 0$ implies that $\mu^{opt} = 0$. If $\mu_\eta > 0$, we have $\mu^{opt} = \mu_\eta$. Hence, we can write $\mu^{opt} = \mu^+_{\eta^*}$, in which η^* should be chosen such that $\mathbb{E}[\mu^+_{\eta^*}] = \sigma$.

We summarize the above analysis with the following Theorem.

Theorem 2. *The optimal power allocation scheme that solves* (2.7) *(i.e., achieves the*

ergodic capacity of the Poisson fading channel) is given by

$$\mu^{opt} = \begin{cases} \mu^{+}_{\eta^*} & \textit{if } \mathbb{E}[\mu^o] > \sigma \\ \mu^o & \textit{if } \mathbb{E}[\mu^o] \leq \sigma \end{cases}. \tag{2.19}$$

2.2.2 Outage Probability

In this section, we study the scenario with a strict delay constraint. In particular, we assume that each codeword needs to be transmitted within a fading block. Let r_0 be the target rate. Then an outage event occurs if $I(\mu, \lambda(t)) < r_0$. Our goal is to find the optimal power allocation strategy that minimizes the outage probability. Hence, we solve the following optimization problem.

Problem-1 (P1-S):

$$\min \quad \Pr\{I(\mu, \lambda(t)) < r_0\}, \tag{2.20}$$

$$\text{s.t.} \quad \mathbb{E}[\mu] \leq \sigma, \tag{2.21}$$

$$0 \leq \mu \leq 1. \tag{2.22}$$

Again, we use μ^{opt} to denote the solution for this optimization problem.

Directly solving **P1-S** is challenging. Following a similar strategy as used for the Gaussian channel [59], we first solve several related optimization problems, from which we obtain the optimal solution for (2.20).

In the first step, we examine the maximal rate r_{max}, obtained in (2.11), that the channel can support for any given value of $\lambda(t)$. Following the discussion on (2.11), the optimal duty cycle that achieves r_{max} is μ^o given in (2.12). From Lemma 1 it is clear that $0 \leq \mu^o \leq 1$. We now compare r_{max} with r_0. Intuitively, for a given block with $\lambda(t)$, if $r_{max} < r_0$, then we should not transmit at this fading block and save the power for the

future use, because an outage event will occur no matter what the value of μ we choose. On the other hand, if $r_{max} > r_0$, there exist choices of μ such that the achievable rate is larger than r_0. These are the regions of interest in the second step below.

In the second step, we investigate for any given value of $\lambda(t)$, what is the minimal value of μ that achieves the target rate r_0 or higher.

Problem-2 (P2-S):

$$\min \quad \mu, \tag{2.23}$$

$$\text{s.t.} \quad I(\mu, \lambda(t)) \geq r_0. \tag{2.24}$$

Let $\hat{\mu}$ be the minimizer for **P2-S**. Clearly, for those values of $\lambda(t)$s such that r_{max} is less than r_0, **P2-S** does not have a solution. For other values of $\lambda(t)$s, using the solution μ^o specified in (2.12), we have the following two cases:

- If $r_{max} = r_0$, then $\hat{\mu}$ must be equal to μ^o.
- If $r_{max} > r_0$, then the optimal power $\hat{\mu}$ equals $\check{\mu}$ that satisfies the following equation so as to reduce the power consumption

$$r_0 = I(\check{\mu}(\lambda), \lambda(t)), \tag{2.25}$$

  from which $\check{\mu}$ can be solved easily.

With the solutions to **P2-S**, we can obtain the optimal solution for an unconstrained version of **P1-S**. In the unconstrained version of **P1-S**, the average power constraint is

ignored. It is easy to see that

$$\mu^*(\lambda) = \begin{cases} 0 & \text{if } r_{max} < r_0 \\ \mu^o & \text{if } r_{max} = r_0 \\ \breve{\mu} & \text{if } r_{max} > r_0. \end{cases} \tag{2.26}$$

is a solution for the unconstrained version of **P1-S**. It is also clear that $0 \leq \mu^*(\lambda) \leq 1$ due to Lemma 1.

Now, we include the average power constraint into consideration.

Theorem 3. *The optimal power allocation μ^{opt} of **P1** that achieves the smallest outage probability is characterized as follows.*

If $\mathbb{E}[\mu^*] \leq \sigma$, then $\mu^{opt} = \mu^*$.

If $\mathbb{E}[\mu^*] > \sigma$, then μ^{opt} is given by

$$\mu^{opt}(\lambda) = \begin{cases} \mu^*(\lambda) \ \textit{with probability } \hat{w}, \\ 0 \quad \textit{with probability } (1-\hat{w}), \end{cases} \tag{2.27}$$

where $\hat{w}$ is given by

$$\hat{w} = \begin{cases} 1 & \textit{if } \mu^*(\lambda) < p^* \\ w^* & \textit{if } \mu^*(\lambda) = p^* \\ 0 & \textit{if } \mu^*(\lambda) > p^*, \end{cases} \tag{2.28}$$

with

$$w^* = \frac{\sigma - \Sigma(p^*)}{\overline{\Sigma}(p^*) - \Sigma(p^*)}, \tag{2.29}$$

and

$$p^* = \textit{sup}\{p : \Sigma(p) < \sigma\}, \tag{2.30}$$

and

$$\Sigma(p) = \int_{R(p)} \mu dF(\lambda),$$
$$\overline{\Sigma}(p) = \int_{\overline{R}(p)} \mu dF(\lambda),$$

Here $F(\lambda)$ is the distribution of the dark current and the regions are defined by:

$$R(p) = \{\lambda \in \mathbb{R} \backslash r_0 : \mu < p\},$$
$$\overline{R}(p) = \{\lambda \in \mathbb{R} \backslash r_0 : \mu \leq p\}.$$

Proof. The proof follows similar steps as those in [59] and [41], and is presented in Appendix A.2. □

Theorem 3 implies that if $\mu^*(\lambda)$ specified in (2.26) does not satisfy the average power constraint, the optimal solution can be obtained by setting it to be equal to μ^* with a probability $\hat{w}$, and we should choose $\hat{w}$ properly so that the average power constraint is satisfied.

2.3 MIMO channel Analysis

For the ease of the presentation, we will present the results for $M = 1$ and $J = 2$ in details. We will briefly discuss how to extend the results to the case with general values of M and J in Section 2.3.4.

2.3.1 With Constant λ

In this subsection, we will first focus on the case in which λ is a constant. Hence, the power allocation is only among transmitters. The solution to this problem will be used to study the general case with time-varying λ.

As discussed in Section 2.2, without loss of optimality, the input of a single antenna Poisson channel can be limited to two levels, i.e., $X(t) = A$ or $X(t) = 0$. The same idea can be extended to the channel with two transmitter antennas and the input of each antenna can be restricted to two levels, i.e. $X_j(t) = A_j$ or $X_j(t) = 0$. Let μ_j be duty-cycle of antenna j, i.e., the probability of $X_j(t) = A_j$. Similar to Section 2.2, the capacity of the Poisson channel with two transmitter antennas, one receiver antenna, and a fixed dark current level with a total power constraint is given by

$$\begin{aligned} C_{MIMO} = \quad & \max \quad I(\mu_1, \mu_2, \lambda), \\ & \mu_1 A_1 + \mu_2 A_2 \leq \sigma(A_1 + A_2) \\ & 0 \leq \mu_1 \leq 1 \\ & 0 \leq \mu_2 \leq 1 \end{aligned} \tag{2.31}$$

in which

$$I(\mu_1, \mu_2, \lambda) \tag{2.32}$$

$$\begin{aligned} &\triangleq (\mu_1 - \kappa)\left(S_1 A_1 + \lambda\right) \log\left(S_1 A_1 + \lambda\right) + (\mu_2 - \kappa)\left(S_2 A_2 + \lambda\right) \log\left(S_2 A_2 + \lambda\right) \\ &+\kappa\left(S_1 A_1 + S_2 A_2 + \lambda\right) \log\left(S_1 A_1 + S_2 A_2 + \lambda\right) + (1 - (\mu_1 + \mu_2 - \kappa))\lambda \log \lambda \\ &- \left(\mu_1 S_1 A_1 + \mu_2 S_2 A_2 + \lambda\right) \log\left(\mu_1 S_1 A_1 + \mu_2 S_2 A_2 + \lambda\right) \\ &= (\mu_1 - \kappa)\zeta(S_1 A_1, \lambda) + (\mu_2 - \kappa)\zeta(S_2 A_2, \lambda) \\ &+\kappa\zeta(S_1 A_1 + S_2 A_2, \lambda) - \zeta(\mu_1 S_1 A_1 + \mu_2 S_2 A_2, \lambda), \end{aligned} \tag{2.33}$$

where κ is the probability with which both antenna 1 and 2 remain active. Each term in (2.32) has the same interpretation as the corresponding formula for the single antenna case (1.8). In particular, in (2.32), the first term corresponds to the case when only antenna 1 is active (i.e. $X_1(t) = A_1$ and the Poisson arrival rate at the receiver is $S_1A_1 + \lambda$), which happens with probability $\mu_1 - \kappa$. The second term corresponds to the case where only antenna 2 is active (i.e. $X_2(t) = A_2$ and the Poisson arrival rate at the receiver is $S_2A_2 + \lambda$), which happens with probability $\mu_2 - \kappa$. The third term corresponds to the case when both antennas 1 and 2 are active (i.e. $X_1(t) = A_1$ and $X_2(t) = A_2$ and the Poisson arrival rate at the receiver is $S_1A_1 + S_2A_2 + \lambda$), which happens with probability κ and the fourth term corresponds to the case when both of the transmitters are off and only the dark current is observed at the receiver. The last term corresponds to the average case (i.e. the average Poisson arrival rate at the receiver is $\mu_1S_1A_1 + \mu_2S_2A_2 + \lambda$).

Unlike the single antenna case in (1.8), it needs a bit of work to solve the optimization problem (2.31). First, using the property of $\zeta(x, y)$, it has been proved in [42], that if the antenna with the smaller duty cycle is on (i.e., the antenna with the smaller value of μ_n), the other antenna should also be active for the optimality. This implies that $\kappa = \min\{\mu_1, \mu_2\}$. Hence to calculate the optimal solution of (2.31), we consider the following two cases:

Case 1): $\mu_1 \geq \mu_2$. In this case, (2.33) can be simplified as

$$\begin{aligned} I(\mu_1 - \mu_2, \mu_2, \lambda) &= (\mu_1 - \mu_2)\zeta(S_1A_1, \lambda) \\ &\quad +\mu_2\zeta(S_1A_1 + S_2A_2, \lambda) \\ &\quad -\zeta(\mu_1S_1A_1 + \mu_2S_2A_2, \lambda). \end{aligned} \tag{2.34}$$

Case 2): $\mu_1 \leq \mu_2$. In this case, (2.33) can be simplified as

$$\begin{aligned} I(\mu_2 - \mu_1, \mu_1, \lambda) &= (\mu_2 - \mu_1)\zeta(S_2 A_2, \lambda) \\ &\quad + \mu_1 \zeta(S_1 A_1 + S_2 A_2, \lambda) \\ &\quad - \zeta(\mu_1 S_1 A_1 + \mu_2 S_2 A_2, \lambda). \end{aligned} \tag{2.35}$$

Hence, (2.31) can be written as

$$C_{MIMO} = \max\{C_{\mu_1 \geq \mu_2}, C_{\mu_2 \geq \mu_1}\}, \tag{2.36}$$

in which $C_{\mu_1 \geq \mu_2}$ is given by (corresponds to case 1 above)

$$C_{\mu_1 \geq \mu_2} = \max I(\mu_1 - \mu_2, \mu_2, \lambda) \tag{2.37}$$

$$\text{s.t.} \quad \mu_1 - \mu_2 \geq 0, \tag{2.38}$$

$$\mu_1 \leq 1, \tag{2.39}$$

$$\mu_2 \geq 0, \tag{2.40}$$

$$\mu_1 A_1 + \mu_2 A_2 \leq \sigma(A_1 + A_2), \tag{2.41}$$

and $C_{\mu_2 \geq \mu_1}$ corresponds to case 2 above and can be written in a similar manner.

Hence, to solve (2.31), we need to find $C_{\mu_1 \geq \mu_2}$ and $C_{\mu_2 \geq \mu_1}$. Due to the symmetry, one can focus on case 1 and solve (2.37), as case 2 is similar. The solution to $C_{\mu_1 \geq \mu_2}$ can be obtained using following steps. First, we will solve (2.37) by ignoring the total power constraint (2.41). Then, we check whether the obtained solution satisfies the total power constraint or not. If yes, the solution is optimal. If not, we then need to do further calculation.

Step 1: Following the strategy outlined above, we first consider the following optimiza-

tion problem

$$\begin{aligned} C_{\mu_1 \geq \mu_2} &= \max I(\mu_1 - \mu_2, \mu_2, \lambda) && (2.42) \\ \text{s.t.} \quad & \mu_1 - \mu_2 \geq 0, && (2.43) \\ & \mu_1 \leq 1, && (2.44) \\ & \mu_2 \geq 0. && (2.45) \end{aligned}$$

To solve this problem, we further ignore (2.44) and (2.45). We will discuss at the end of step 1 that ignoring these conditions does not affect the solution.

Setting $q_1 = \mu_1 - \mu_2$ and $q_2 = \mu_2$, the Lagrangian for (2.42) with the constraint (2.43) only is given by:

$$\mathcal{L}(q_1, q_2, \eta) = I(q_1, q_2, \lambda) - \eta q_1.$$

Let (q_1^*, q_2^*, η^*) be the optimizer, and the corresponding KKT conditions are:

$$\begin{aligned} \left.\frac{\partial \mathcal{L}}{\partial q_1}\right|_{q_1^*, q_2^*} = \left.\frac{\partial I}{\partial q_1}\right|_{q_1^*, q_2^*} - \eta^* &= 0, \\ \left.\frac{\partial \mathcal{L}}{\partial q_2}\right|_{q_1^*, q_2^*} = \left.\frac{\partial I}{\partial q_2}\right|_{q_1^*, q_2^*} &= 0, \\ \eta^* q_1^* &= 0. \end{aligned}$$

After solving the KKT conditions, we conclude that $x_1^* = 0$ and q_2^* can be obtained from

$$\left.\frac{\partial I}{\partial q_2}\right|_{q_1^* = 0, q_2^*} = \lambda B \log\left(\frac{1 + B\alpha(B)}{1 + q_2^* B}\right) = 0,$$

where

$$\alpha(x) = \frac{1}{x}\left(e^{-1}(1+x)^{(1+\frac{1}{x})} - 1\right), \tag{2.46}$$

$$B = \frac{S_1A_1 + S_2A_2}{\lambda}. \tag{2.47}$$

Hence, $q_2^* = \alpha(B)$.

In summary, the solution to (2.42) with only the constraint (2.43) is $\mu_1^* = \mu_2^* = \alpha(B)$. It is easy to show that $0 \leq \alpha(B) \leq 1$. Hence, $\mu_1^* = \mu_2^* = \alpha(B)$ satisfy conditions (2.44) and (2.45). As the result, $(\alpha(B), \alpha(B))$ is the solution to (2.42) with constraints (2.43), (2.44) and (2.45).

Step 2: In this step, we follow similar steps as those in [42] to check whether the solution $(\alpha(B), \alpha(B))$ obtained in Step 1 satisfies the sum power constraint (2.41) or not. If $\alpha(B) \leq \sigma$, then $(\alpha(B), \alpha(B))$ also satisfies the sum power constraint, hence is the optimal solution to (2.37). On the other hand, if $\alpha(B) > \sigma$, $(\alpha(B), \alpha(B))$ violates the sum power constraint, and hence can not be the solution. In this case, the sum power constraint is active in the optimal solution. To solve for optimality, we convert the given problem into a single variable optimization problem: $\max_{\mu_1^*} I(\mu_1^*) = I((1+a)(\mu_1^*-\sigma), (1+a)\sigma - a\mu_1^*, \lambda)$, which is obtained by writing μ_2^* as function of μ_1^* using the average power constraint $\mu_1^*A_1 + \mu_2^*A_2 = \sigma(A_1 + A_2)$. Here, $a = A_1/A_2$. By simple calculations, the optimal solution for $\max_{\mu_1^*} I(\mu_1^*)$ is found out to be:

$$\omega = \frac{e^{-1}}{A_1(S_1 - S_2)}\left(\frac{(S_1A_1 + \lambda)^{(S_1A_1+\lambda)(1+a)}}{\lambda^{\lambda}(S_1A_1 + S_2A_2 + \lambda)^{(S_1A_1+S_2A_2+\lambda)a}}\right)^{\frac{1}{A_1(S_1-S_2)}} - \frac{(1+a)\sigma S_2A_2 + \lambda}{A_1(S_1 - S_2)}. \tag{2.48}$$

Now, we check whether ω satisfies the corresponding constraint or not. If yes, ω is the

optimal solution to $I(\mu_1^*)$ (therefore, it is also optimal for (2.37)). If not, we need to modify the solution. First, it is easy to check that $I(\mu_1^*)$ is a concave function of μ_1^*. Hence, if $\omega < \sigma$, we set $\mu_1^* = \sigma$, which implies $\mu_2^* = \sigma$. Similarly, if $\omega > (1 + 1/a)\sigma$, we set $\mu_1^* = (1 + 1/a)\sigma$, which implies $\mu_2^* = 0$.

We have the following Lemma regarding the optimal duty cycle that maximize $C_{\mu_1 \geq \mu_2}$.

Lemma 4. *The optimal solution to the optimization problem* (2.37) *is given by*

$$(\mu_1^*, \mu_2^*) = \begin{cases} (\alpha(B), \alpha(B)) & \textit{if } \alpha(B) \leq \sigma, \\ (\omega, (1+a)\sigma - a\omega) & \textit{if } \alpha(B) > \sigma \textit{ and} \\ & \sigma \leq \omega \leq (1 + 1/a)\sigma, \\ (\sigma, \sigma) & \textit{if } \alpha(B) > \sigma \textit{ and} \\ & \omega < \sigma, \\ ((1 + 1/a)\sigma, 0) & \textit{if } \alpha(B) > \sigma \textit{ and} \\ & \omega > (1 + 1/a)\sigma. \end{cases}$$

We can obtain $C_{\mu_2 \geq \mu_1}$ in a similar manner and therefore finally obtain C_{MIMO} via (2.36).

2.3.2 Ergodic Capacity

We now study the case in which $\lambda(t)$ is a time varying random variable and characterize the ergodic capacity. We derive the optimal power allocation strategy using the results developed Section 2.3.1. To maximize the ergodic capacity in the presence of the time-varying dark current, we have:

$$\begin{aligned} C_{MIMO}^f = \max \quad & \mathbb{E}[\Phi(t)], \\ \mathbb{E}[\mu_1(t)A_1 + \mu_2(t)A_2] &\leq \sigma(A_1 + A_2) \\ 0 \leq \mu_1(t) &\leq 1 \\ 0 \leq \mu_2(t) &\leq 1 \end{aligned} \tag{2.49}$$

where the expectation is over random variable $\lambda(t)$ and $\Phi(t) = I(\mu_1(t), \mu_2(t), \lambda(t))$ and we use $(\mu_1^{opt}, \mu_2^{opt})$ to denote the maximizer for (2.49). We follow the same strategy developed in the SISO case, and use a two-step approach to solve this problem.

Step 1: First, we ignore the average power constraint, and find the maximal rate that the channel can support for any given value of $\lambda(t)$.

$$\begin{aligned} r_{max} &= \max I(\mu_1, \mu_2, \lambda(t)), && (2.50)\\ \text{s.t.} \quad & 0 \le \mu_1 \le 1, && (2.51)\\ & 0 \le \mu_2 \le 1. && (2.52) \end{aligned}$$

We use (μ_1^o, μ_2^o) to denote the maximizer of this problem.

As shown in Section 2.3.1, for any given value of $\lambda(t)$,

$$\max_{\mu_1,\mu_2} I(\mu_1, \mu_2, \lambda(t)) = \max\left\{\Theta_1(t), \Theta_2(t)\right\},$$

where $\Theta_1(t) = \max_{\mu_1,\mu_2} I(\mu_1 - \mu_2, \mu_2, \lambda(t))$ and $\Theta_2(t) = \max_{\mu_1,\mu_2} I(\mu_2 - \mu_1, \mu_1, \lambda(t))$. Therefore, problem (2.50) can be split into two separate problems. Due to the symmetry, we focus on $\Theta_1(t)$ (the other case being similar), which can be written as:

$$\begin{aligned} \max \quad & I(\mu_1 - \mu_2, \mu_2, \lambda(t)), && (2.53)\\ \text{s.t.} \quad & \mu_1 \le 1, && (2.54)\\ & \mu_2 \ge 0, && (2.55)\\ & \mu_1 \ge \mu_2. && (2.56) \end{aligned}$$

For a given value of $\lambda(t)$, problem (2.53) is the same as the problem (2.42). Following the analysis of (2.42), it is clear that $\mu_1 = \mu_2 = \alpha(B(t))$ is the solution to (2.53), where

$\alpha(\cdot)$ is defined in (2.46) and $B(t)$ is defined in (2.47) with λ replaced by $\lambda(t)$. Similarly, $\mu_1 = \mu_2 = \alpha(B(t))$ is also the solution to the problem $\Theta_2(t)$. As the result, the solution to the problem (2.50) is $(\mu_1^o, \mu_2^o) = (\alpha(B(t)), \alpha(B(t)))$.

Step 2: Now we check whether the solution (μ_1^o, μ_2^o) obtained in Step 1 satisfies the average power constraint or not, i.e., we check whether the following inequality holds or not:

$$\mathbb{E}[\mu_1^o A_1 + \mu_2^o A_2] \leq \sigma(A_1 + A_2). \tag{2.57}$$

If (2.57) holds, the optimal solution to (2.49) is $(\mu_1^{opt}, \mu_2^{opt}) = (\mu_1^o, \mu_2^o)$, and $C_{MIMO}^f = \mathbb{E}[r_{max}]$.

If (2.57) does not hold, then (μ_1^o, μ_2^o) can not be the optimal solution to (2.49), as it violates the average power constraint. Therefore, in the optimal solution, the average power constraint is active, and hence the problem (2.49) is equivalent to:

$$C_{MIMO}^f = \max_{\substack{\mathbb{E}[\sigma'(t)] = \sigma \\ 0 \leq \sigma'(t) \leq 1}} \mathbb{E}[\Psi(t)], \tag{2.58}$$

where $\Psi(t) = \max_{\substack{\mu_1(t)A_1 + \mu_2(t)A_2 = \sigma'(t)(A_1 + A_2) \\ 0 \leq \mu_1(t) \leq 1 \\ 0 \leq \mu_2(t) \leq 1}} \Phi(t)$. We note that, in the optimization problem inside $\mathbb{E}[\cdot]$, the value of $\lambda(t)$ is fixed, and hence the results in Section 2.3.1 are applicable. More specifically, we use results in step 2 of Section 2.3.1, because the sum power constraint is active here. Using the results in Section 2.3.1, we can write the mutual information term inside $\mathbb{E}[\cdot]$ as a function of $\sigma'(t)$, and hence the problem is converted into an optimization problem of $\sigma'(t)$. Due to its complex form (as shown in

Lemma 4), it is difficult to obtain an analytical form of the optimal solution. However, one can set $\mu_1(t) = \mu_2(t)$ and obtain a computable solution, which is optimal when σ is large.

In summary, we have the following proposition regarding the optimal power allocation scheme for the ergodic capacity.

Proposition 5. *The optimal power allocation strategy that achieves the ergodic capacity (namely the optimization problem in* (2.49)*) is given by*

$$(\mu_1^{opt}, \mu_2^{opt}) = \begin{cases} (\alpha(B(t)), \alpha(B(t))) & \textit{if } \mathbb{E}[\alpha(B(t))] \leq \sigma, \\ \textit{solution of } (2.58) & \textit{if } \mathbb{E}[\alpha(B(t))] > \sigma. \end{cases} \tag{2.59}$$

As we can see here, when the average power constraint σ is large, we obtain the closed form expression for the optimal allocation scheme. When σ is small, we do not have the closed form solution as the form of the function is too complicated. Alternatively, suboptimal solutions with good properties can be numerically computed easily as discussed in the paragraph after (2.58).

2.3.3 Outage Probability

In this section, we consider the case with a strict delay constraint, for which the strategy developed in Section 2.2.2 for the SISO case is useful. Let r_0 be the target rate, hence an outage event occurs if $I(\mu_1, \mu_2, \lambda(t)) < r_0$. The goal is to minimize the outage probability.

Problem-1-*MIMO* (P1-M):

$$\min \quad \Pr\{I(\mu_1, \mu_2, \lambda(t)) < r_0\}, \tag{2.60}$$

$$\text{s. t.} \quad \mathbb{E}[\mu_1 A_1 + \mu_2 A_2] \leq \sigma(A_1 + A_2). \tag{2.61}$$

We use $(\mu_1^{opt}, \mu_2^{opt})$ to denote the minimizer of this problem.

Similar to the SISO case studied in Section 2.2, we first solve several related optimization problems, which help to obtain the optimal solution for **P1-M**.

We first examine the maximal rate r_{max} that the channel can support for any given value of $\lambda(t)$, namely, the optimization problem (2.50). Following Step 1 in Section 2.3.2, $(\mu_1^o, \mu_2^o) = (\alpha(B(t)), \alpha(B(t)))$ is the power allocation strategy that achieves r_{max} for each block.

Similar to Section 2.2, we then compare r_{max} with r_0. If $r_{max} < r_0$, then the transmitter should not transmit anything and save the power for the future use. If $r_{max} = r_0$, then the only choice of power control that avoids outage is the power that achieves r_{max}. The interesting case is when $r_{max} > r_0$. In this case, there are multiple (in fact infinitely many) power control choices that can avoid outage. In the following, we find the minimal sum power that avoids the outage.

Problem-2-*MIMO* (P2-M):

$$\min \quad \mu_1 A_1 + \mu_2 A_2, \tag{2.62}$$

$$\text{s.t.} \quad I(\mu_1, \mu_2, \lambda(t)) \geq r_0. \tag{2.63}$$

We use $(\hat{\mu}_1, \hat{\mu}_2)$ to denote the optimal solution to **P2-M**.

For those $\lambda(t)$s such that r_{max} is less than r_0, **P2-M** does not have a solution. For other values of $\lambda(t)$s, we consider the following two cases:

- If $r_{max} = r_0$ then $\hat{\mu}_1 = \hat{\mu}_2 = \alpha(B(t))$.
- If $r_{max} > r_0$ then $(\hat{\mu}_1, \hat{\mu}_2) = (\check{\mu}_1, \check{\mu}_2)$, such that $(\check{\mu}_1, \check{\mu}_2)$ is the solution of the following problem **P2a-M**.

Problem-2a-*MIMO* (P2a-M):

$$\min \quad \mu_1 A_1 + \mu_2 A_2, \tag{2.64}$$

$$\text{s.t.} \quad I(\mu_1, \mu_2, \lambda(t)) = r_0. \tag{2.65}$$

To solve this problem, we consider two subproblems.

The first subproblem is:

P2a-M-sub1:

$$\min \quad \mu_1 A_1 + \mu_2 A_2, \tag{2.66}$$

$$\text{s.t.} \quad I(\mu_1 - \mu_2, \mu_2, \lambda(t)) = r_0, \tag{2.67}$$

$$\mu_1 \geq \mu_2. \tag{2.68}$$

Let $(\tilde{\mu}_1, \tilde{\mu}_2)$ be the solution.

The second subproblem of **P2a-M** is

P2a-M-sub2:

$$\min \quad \mu_1 A_1 + \mu_2 A_2, \tag{2.69}$$

$$\text{s.t.} \quad I(\mu_2 - \mu_1, \mu_1, \lambda(t)) = r_0, \tag{2.70}$$

$$\mu_2 \geq \mu_1. \tag{2.71}$$

Let $(\bar{\mu}_1, \bar{\mu}_2)$ be the solution. Following the similar approach in Corollary 1 of [41], the solutions to these sub problems can be found using KKT conditions.

As $I(\mu_1, \mu_2, \lambda) = \max\{I(\mu_1 - \mu_2, \mu_2, \lambda),$
$I(\mu_2 - \mu_1, \mu_1, \lambda)\}$, then from the solutions to the two subproblems **P2a-M-sub1** and

P2a-M-sub2, the optimal solution of **P2a-M** is given by

$$(\check{\mu}_1, \check{\mu}_2) = \begin{cases} (\tilde{\mu}_1, \tilde{\mu}_2) \text{ if } \tilde{\mu}_1 A_1 + \tilde{\mu}_2 A_2 \leq \bar{\mu}_1 A_1 + \bar{\mu}_2 A_2, \\ (\bar{\mu}_1, \bar{\mu}_2) \text{ otherwise.} \end{cases}$$

Therefore, the solution to problem **P-1M** with the absence of the average power constraint can be written as:

$$(\mu_1^*(\lambda), \mu_2^*(\lambda)) = \begin{cases} (0,0) \text{ if } r_{max}(\lambda) < r_0 \\ (\mu_1^o, \mu_2^o) \text{ if } r_{max}(\lambda) = r_0 \\ (\check{\mu}_1, \check{\mu}_2) \text{ if } r_{max}(\lambda) > r_0 \end{cases} . \tag{2.72}$$

Now, we check the average power constraint. Depending on whether (μ_1^*, μ_2^*) satisfies $\mathbb{E}[\mu_1^* A_1 + \mu_2^* A_2] \leq \sigma(A_1 + A_2)$ or not, we have the following two cases.

Case 1): $\mathbb{E}[\mu_1^* A_1 + \mu_2^* A_2] \leq \sigma(A_1 + A_2)$. In this case, we have $(\mu_1^{opt}, \mu_2^{opt}) = (\mu_1^*, \mu_2^*)$.

Case 2): $\mathbb{E}[\mu_1^* A_1 + \mu_2^* A_2] > \sigma(A_1 + A_2)$. In this case, we need to modify (μ_1^*, μ_2^*) to obtain $(\mu_1^{opt}, \mu_2^{opt})$. Following similar arguments as in Section 2.2, we can conclude that, if $\mathbb{E}[\mu_1^* A_1 + \mu_2^* A_2] > \sigma(A_1 + A_2)$, then the optimal solution $(\mu_1^{opt}, \mu_2^{opt})$ of **P1-M** is given by

$$(\mu_1^{opt}, \mu_2^{opt}) = \begin{cases} (\mu_1^*, \mu_2^*) \text{ with probability } \hat{w} \\ (0,0) \quad \text{with probability } (1 - \hat{w}) \end{cases} , \tag{2.73}$$

in which $\hat{w}$ is explained in (2.28) and has the following form

$$\hat{w} = \begin{cases} 1 \text{ if } \bar{\sigma}(t) < p^* \\ w^* \text{ if } \bar{\sigma}(t) = p^* \\ 0 \text{ if } \bar{\sigma}(t) > p^* \end{cases}, \tag{2.74}$$

where w^* is given by (2.29), p^* is given by (2.30) and $\bar{\sigma} = \frac{\mu_1^* A_1 + \mu_2^* A_2}{A_1 + A_2}$.

In summary, we have the following proposition regarding the optimal power allocation strategy that minimize the outage probability.

Proposition 6. *The optimal power allocation strategy that minimizes the outage probability is given by*

$$(\mu_1^{opt}, \mu_2^{opt}) = \begin{cases} \textit{specified in } (2.72) & \textit{if} \quad \mathbb{E}[\mu_1^* A_1 + \mu_2^* A_2] \leq \sigma(A_1 + A_2), \\ \textit{specified in } (2.73) & \textit{if} \quad \mathbb{E}[\mu_1^* A_1 + \mu_2^* A_2] > \sigma(A_1 + A_2). \end{cases}$$

2.3.4 Extension to General MIMO Case

For the case with an arbitrary number of transmit and receive antennas, i.e., general values of J and M, we can follow the similar steps as in the previous sections to obtain the optimal power control policy that maximizes the ergodic capacity and the optimal power control policy that minimizes the outage probability. In particular, for any J, if the transmitter antenna with the smallest duty cycle is active, then the other antennas should also be active. Hence, there are $J + 1$ states. As the result, the mutual information $I(\mu^J(t), \lambda(t))$ has $J + 1$ terms, each corresponding to one state. Thus in order to obtain the ergodic capacity, we solve

$$C_{MIMO}^f = \max_{\mathbb{E}[\sum_i \mu_i(t) A_i] \leq \sigma \sum_i A_i} \mathbb{E}[I(\mu^J(t), \lambda(t))], \tag{2.75}$$

where

$$I(\mu^J(t),\lambda(t)) \;=\sum_{m=1}^{M}\left[\sum_{j=1}^{J}\nu_j\zeta\left(\sum_{k=1}^{j}S_{km}A_k,\lambda_m(t)\right)\;-\zeta\left(\sum_{j=1}^{J}\nu_j\sum_{k=1}^{j}S_{km}A_k,\lambda_m(t)\right)\right], \tag{2.76}$$

and when $\mu_j > \mu_{j+1}, j = 1, ..., J-1$,

$$\nu_j = \begin{cases} \mu_j - \mu_{j+1} & j = 1, ..., J-1 \\ \mu_J & j = J \end{cases}. \tag{2.77}$$

The solution of (2.75) can be obtained following the same approach as in Section 2.3.2 by examining cases with different ordering of duty cycles.

To minimize the outage probability, we consider

$$\min \quad Pr\{I(\mu^J(t),\lambda(t))\}, \tag{2.78}$$

$$s.t. \quad \mathbb{E}\left[\sum_i \mu_i(t)A_i\right] \le \sigma\sum_i A_i, \tag{2.79}$$

which can be solved following the similar steps as explained in Section 2.3.3 by examining cases with different ordering of duty cycles.

2.4 Numerical Analysis

In the simulations for single transmitting user, we set $M = 1$, and consider two cases respectively with $J = 1$ and $J = 2$. Furthermore, $\lambda(t)$ is chosen as a uniform random variable such that $\lambda(t) \sim \mathcal{U}[1, 2]$. For fair comparison between $J = 1$ and the $J = 2$ case, we have ensured that both the total power constraints and average power constraints are equal by setting $A = 30$ for $J = 1$ and $A_1 = A_2 = 15$ for $J = 2$.

2.4.1 Ergodic Capacity

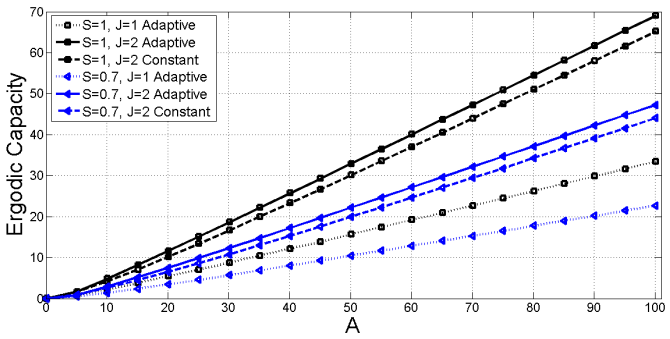

Figure 2.2: The ergodic capacity vs. A

Figure 2.2 illustrates the ergodic capacity as a function of the maximum amplitude for both $J = 1$ and $J = 2$, for $\lambda(t) \sim \mathcal{U}[1, 2]$. It is evident from the figure that as A increases, the ergodic capacity increases monotonically. If the number of antennas at the transmitter is larger, the increment in the ergodic capacity is more evident. For comparison, in the figure, we also plot curves for the ergodic capacity when the constant power allocation strategy is employed (refer to the Appendix B). The figure shows that the adaptive power allocation for multiple transmitting antennas observe a significant improvement in the ergodic capacity when A is increased, compared to the case with constant power control for multiple transmitting antennas and adaptive power control for a single transmitting antenna.

Figure 2.3 further illustrates the comparison between the ergodic rate achieved with and without adaptive power control. In this figure, we plot the rate as a function of σ for $A_1 = A_2 = 15$, $J = 2$ and $M = 1$ when $\lambda(t) \sim \mathcal{U}[0.5, 8.0]$. It can be observed from the figure that initially as σ increases, the ergodic capacity increases. But after reaching a certain threshold point, increasing σ does not affect the ergodic capacity. This is due to the fact that once σ is large enough, as discussed in (2.59), $(\alpha(B(t)), \alpha(B(t)))$ satisfy the total power constraint $\mathbb{E}[\mu_1 A_1 + \mu_2 A_2] \leq \sigma(A_1 + A_2)$, and then the optimal power allocation

strategy and the ergodic capacity do not depend on σ. It is shown in the figure that the gain achieved by adaptive power allocation is more obvious when $\mathbb{E}[\mu_1 A_1 + \mu_2 A_2] \leq \sigma(A_1 + A_2)$ is satisfied and for the smaller values of S. From the figure, it is clear that when σ is small, both the adaptive and constant power control have the same rate. This can be explained as follows. In the adaptive power control case, solving (2.48) shows that for the given parameters, $\omega < 0$. Therefore, from Lemma 4, we know that the optimal power allocation strategy is $(\mu_1, \mu_2) = (\sigma, \sigma)$, which is the same as the constant power control case.

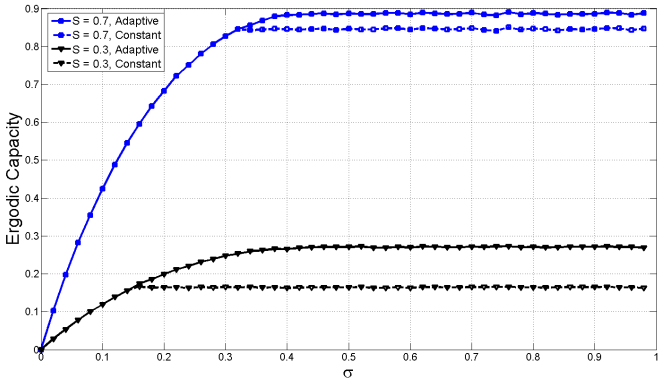

Figure 2.3: The ergodic capacity vs. σ for $J = 2$, comparing the adaptive and the constant power allocation

Figure 2.4 illustrates the ergodic capacity as a function of the total power for both $J = 1$ and $J = 2$ with $A = 30$ and $A_1 = A_2 = 15$. As the total power (i.e. σA for $J = 1$ and $\sigma(A_1 + A_2)$ for $J = 2$) increases, the ergodic capacity also increases. As discussed above, after reaching a certain threshold, the increase in power does not affect the ergodic capacity.

Figure 2.5 compares the ergodic capacity of two transmitter antennas and one receiver with one transmitter and two receiver antennas while keeping the power constraints (i.e. total power and average power constraint) to be the same when $S = 0.5$. For both cases we assume that for each receiver, the corresponding dark current is uniformly distributed

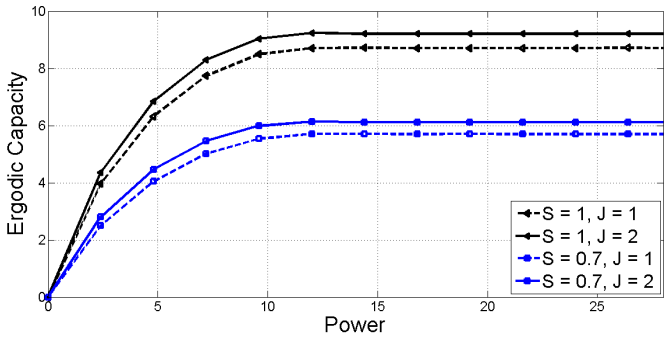

Figure 2.4: The ergodic capacity vs. power for both multi-antenna and single-antenna cases

in the interval $[1, 2]$. It is clear from the figure that the two receiver antennas case has a better performance.This can be explained by the mutual information formulas. For $(M = 1, J = 2)$, when $\mu_1 \geq \mu_2$, the mutual information is given by $(\mu_1 - \mu_2)\zeta(S_1A_1, \lambda) + \mu_2\zeta(S_1A_1 + S_2A_2, \lambda) - \zeta(\mu_1 S_1A_1 + \mu_2 S_2A_2, \lambda)$, while for $(M = 2, J = 1)$, it is given by: $\mu\zeta(SA, \lambda_1) - \zeta(\mu SA, \lambda_1) + \mu\zeta(SA, \lambda_2) - \zeta(\mu SA, \lambda_2)$.

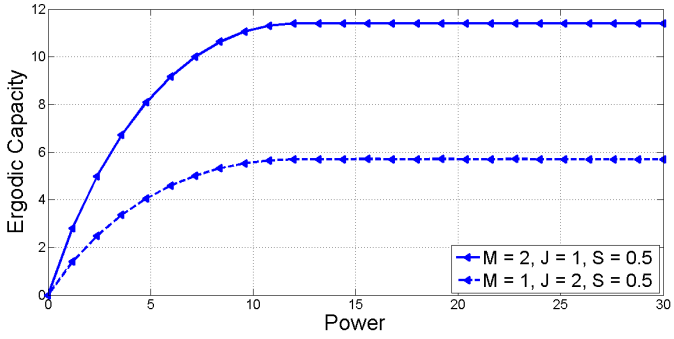

Figure 2.5: The ergodic capacity vs. power for $M = 1, J = 2$ and $M = 2, J = 1$

2.4.2 Outage Probability

Figure 2.6 plots the outage probability as a function of the target rate r_0. For this simulation, $A = 30$, $A_1 = A_2 = 15$ and $\sigma = 0.03725$ for both $J = 1$ and $J = 2$, for the fair comparison between $J = 1$ and $J = 2$. It is evident from the figure that as r_0 increases,

P_{out} also increases. Furthermore, the outage probability for $J = 1$ increases more rapidly than that of $J = 2$. As the figure is in logarithmic scale and $\log 0$ is not defined, hence the figure only shows the values when the outage probability is > 0. Figure 2.7 compares

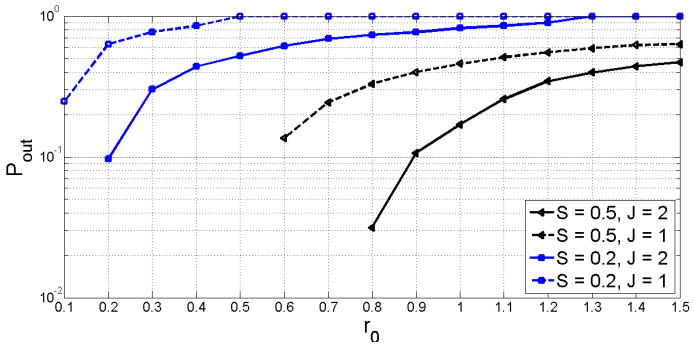

Figure 2.6: P_{out} vs. r_0, comparing $J = 1$ with $J = 2$

the relationship between the target rate r_0 and the probability for the adaptive power allocation and the constant power allocation when $A_1 = A_2 = 15$ and $\sigma = 0.03725$. It shows that the outage probability of the adaptive power allocation responds gradually to the increase in the target rate as compared to the constant power allocation where the outage probability abruptly increases when r_0 increases. This figure also shows the values of outage probability when $P_{out} > 0$. Figure 2.8 shows that as the power increases,

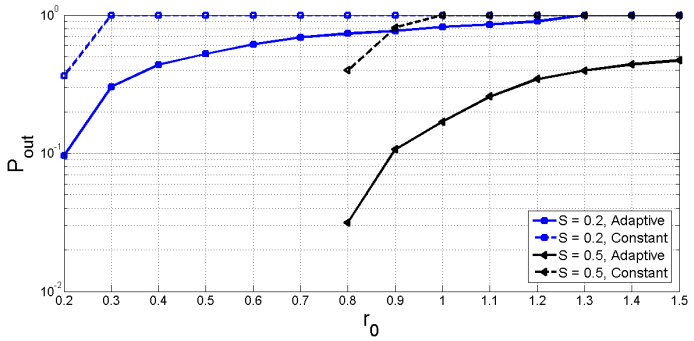

Figure 2.7: P_{out} vs. r_0, comparing the adaptive power allocation with the constant power allocation

P_{out} decreases and $r_0 = 1.2$. Furthermore, we can observe that, after a certain point, the

increase in power does not lead to further decrease in P_{out}. Similar to the ergodic case, the reason for this phenomena is that once the available power is large enough, the optimal power allocation strategy and hence the outage probability does not depend on the available power anymore. From the figure, we also see that when $S = 0.2$, the outage probability for $J = 1$ is always 1. The value of $P_{out} = 0$ for $S = 0.5, J = 2$ when power is larger than 2.45 and $P_{out} = 0$ for $S = 0.5, J = 1$, when power is larger than 3.

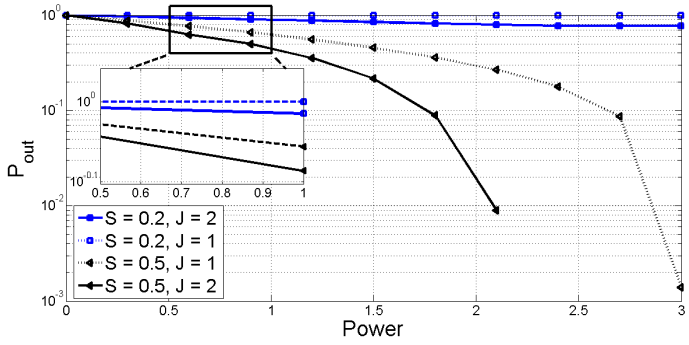

Figure 2.8: P_{out} vs. power, comparing $J = 1$ with $J = 2$

Figure 2.9 shows the improvement achieved by the multi-antenna dynamic power allocation as compared to multi-antenna constant power allocation and shows that when the available power increases, the adaptive power allocation scheme reduces the outage probability more significantly as compared to the constant power allocation for $A_1 = A_2 = 15$ and $r_0 = 1.2$. $P_{out} = 0$ when power is larger than 2.45.

Figure 2.10 compares the outage probabilities for the cases with $(M = 1, J = 2)$ and $(M = 2, J = 1)$ with $S = 0.2$. From the figure, it is clear that P_{out} is higher for $M = 1, J = 2$ case than for the $M = 2, J = 1$, which is consistent with the mutual information formula and the comparison in Figure 2.5. It is clear from the examples shown above that the performance of the single user Poisson channel can be improved by increasing the number of antennas at both transmitting and receiving user.

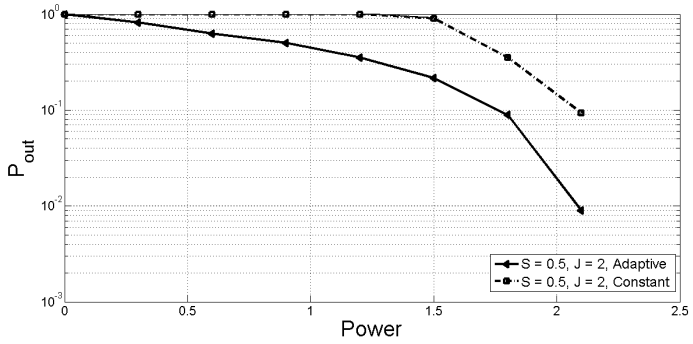

Figure 2.9: P_{out} vs. power, comparing the adaptive power allocation with the constant power allocation

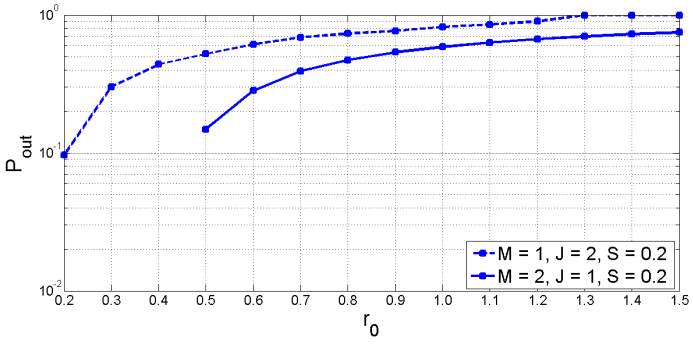

Figure 2.10: P_{out} vs. r_0, Comparing $M = 1, J = 2$ with $M = 2, J = 1$ with adaptive power allocation

Chapter 3

Multi User Single Receiver

In this chapter, we extend the analysis to a non-fading Poisson channel where multiple transmitting users communicate with a single receiver. In this chapter we will restrict our analysis to the scenario where the receiver has only one antenna (the transmitters can have either one or multiple antennas).

3.1 System Model

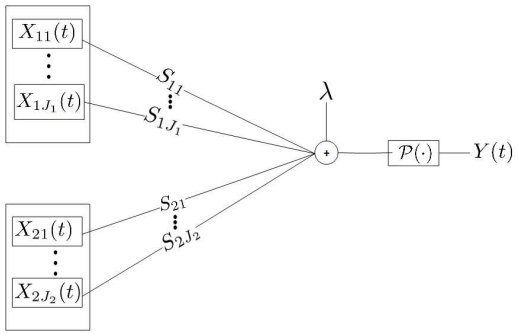

Figure 3.1: The Poisson MISO-MAC model.

In this section, we introduce the model considered in this chapter. As shown in the Fig. 3.1, we consider the continuous-time two-user Poisson MISO-MAC with two users

communicating with a single antenna receiver. For transmitter n, it is equipped with J_n transmit antennas. Let $X_{nj}(t)$ be the input of the j^{th} transmitter from n^{th} user and $Y(t)$ be the doubly-stochastic Poisson process observed at the receiver antenna. The input-output relationship can be described as:

$$Y(t) = \mathcal{P}\left(\sum_{n=1}^{2}\sum_{j=1}^{J_n} S_{nj}X_{nj}(t) + \lambda\right), \tag{3.1}$$

in which S_{nj} is the channel response between the j^{th} antenna of the n^{th} user to the receiver, λ is the dark current at receiver antenna, and $\mathcal{P}(\cdot)$ is the nonlinear transformation converting the light strength to the doubly-stochastic Poisson process that records the timing and number of photon's arrivals. In particular, for any time interval $[t, t+\tau]$, the probability that there are k photons arriving at the receiver is

$$\Pr\{Y(t+\tau) - Y(t) = k\} = \frac{e^{-\Lambda}\Lambda^k}{k!}, \tag{3.2}$$

where

$$\Lambda = \int_t^{t+\tau}\left[\sum_{n=1}^{2}\sum_{j=1}^{J_n} S_{nj}X_{nj}(t') + \lambda\right]dt'. \tag{3.3}$$

We consider the peak power constraint, i.e., the transmitted signal $X_{nj}(t)$ must satisfy the following constraint:

$$0 \le X_{nj}(t) \le A_{nj}, \tag{3.4}$$

where A_{nj} is the maximum power allowed by the j^{th} antenna of the n^{th} transmitter. We use μ_{nj} to denote the duty cycle of each transmitting antenna, i.e., μ_{nj} is the percentage of time at which the j^{th} antenna of the n^{th} user is on. We use $\boldsymbol{\mu}$ to denote the vector of all μ_{nj}s.

Throughout the chapter, we use the following notation:

$$\varphi(x) \triangleq x\log(x), \tag{3.5}$$

$$\zeta(x,y) \triangleq (x+y)\log(x+y) - y\log y, \tag{3.6}$$

$$\alpha(x) \triangleq \frac{1}{x}\left(e^{-1}(1+x)^{\left(1+\frac{1}{x}\right)} - 1\right). \tag{3.7}$$

As shown in Chapter 2, it is easy to check that $0 < \alpha(x) < 1$ for $x \geq 0$.

Our goal is to characterize the sum-rate capacity of this Poisson MAC.

3.2 SISO-MAC Analysis

In this section, we focus on the special case in which each transmitter has only one antenna, i.e., $J_1 = 1$ and $J_2 = 1$. Hence for the sake of convenience, we drop the subscript j in this section. The techniques developed in this section will be used in the more complicated setup considered in Section 3.3.

3.2.1 Optimality Conditions

It has been shown in [52] that the continuous-time continuous-input discrete-output Poisson MAC can be converted to a much simpler discrete-time binary-input binary-output MAC. In particular, the input waveform can be limited to be piecewise constant waveforms with two levels 0 or A_n for the n^{th} transmitter. Let μ_n be the duty cycle of the n^{th} transmitter (i.e., μ_n is the fraction of the time that transmitter n is on). It has been shown in [52] that the sum-rate capacity is given by

$$\textbf{(P0):} \quad C_{sum}^{SISO-MAC} = \max_{0\leq\mu_1,\mu_2\leq 1} \quad I_{X_1,X_2;Y}(\mu_1,\mu_2), \tag{3.8}$$

in which

$$I_{X_1,X_2;Y}(\mu_1,\mu_2) = (1-\mu_1)(1-\mu_2)\varphi(\lambda)+\mu_1(1-\mu_2)\varphi(S_1A_1+\lambda)$$
$$+(1-\mu_1)\mu_2\varphi(S_2A_2+\lambda)+\mu_1\mu_2\varphi(S_1A_1+S_2A_2+\lambda)-\varphi(S_1A_1\mu_1+S_2A_2\mu_2+\lambda).$$

The optimization problem (3.8) has been solved by [52] for the symmetric case with $S_1A_1 = S_2A_2$. In particular, [52] shows that the objective function $I_{X_1,X_2;Y}(\mu_1,\mu_2)$ is a Schur concave function when $S_1A_1 = S_2A_2$. As the result, if $(\hat{\mu}_1,\hat{\mu}_2)$ is the optimal solution to (3.8) for the symmetric case, $\hat{\mu}_1$ must be equal to $\hat{\mu}_2$. Hence, the problem can be converted into a one-dimensional optimization problem, which can be solved easily.

However, the situation for the non-symmetric case is different. In particular, if $S_1A_1 \neq S_2A_2$, then $I_{X_1,X_2;Y}(\mu_1,\mu_2)$ is not a Schur concave function anymore. This can be observed from the fact that a Schur concave function must be a symmetric function (see page 258 of [61]), while $I_{X_1,X_2;Y}(\mu_1,\mu_2)$ is not a symmetric function when $S_1A_1 \neq S_2A_2$. Therefore, the techniques developed in [52] for the symmetric case cannot be extended to the non-symmetric case. Furthermore, for general values of S_nA_n and λ, $I_{X_1,X_2;Y}(\mu_1,\mu_2)$ is not necessarily a concave function of (μ_1,μ_2), (see the proof in Appendix C.1). Hence, (3.8) is a non-convex optimization problem in general.

In the following, we solve this non-convex optimization problem. We start with the necessary KKT conditions (since the problem is not convex, these conditions are not sufficient for optimality). For convenience, we write $I_{X_1,X_2;Y} = I$ and hence the corresponding Lagrangian equation is given by:

$$\mathcal{L} = -I+\eta_1(\mu_1-1)-\eta_2\mu_1+\eta_3(\mu_2-1)-\eta_4\mu_2. \tag{3.9}$$

The optimal solution $(\hat{\mu}_1, \hat{\mu}_2)$ must satisfy the following KKT constraints:

$$\begin{aligned}
\frac{\partial I}{\partial \mu_1}\Big|_{(\hat{\mu}_1,\hat{\mu}_2)} - \eta_1 + \eta_2 &= 0, \\
\frac{\partial I}{\partial \mu_2}\Big|_{(\hat{\mu}_1,\hat{\mu}_2)} - \eta_3 + \eta_4 &= 0, \\
\eta_1(\hat{\mu}_1 - 1) &= 0, \\
\eta_2\hat{\mu}_1 &= 0, \\
\eta_3(\hat{\mu}_2 - 1) &= 0, \\
\eta_4\hat{\mu}_2 &= 0,
\end{aligned}$$

where

$$\begin{aligned}
\frac{\partial I}{\partial \mu_1} &= -(1-\mu_2)\varphi(\lambda) + (1-\mu_2)\varphi(S_1A_1+\lambda) - \mu_2\varphi(S_2A_2+\lambda) \\
&+\mu_2\varphi(S_1A_1+S_2A_2+\lambda) - S_1A_1\log(S_1A_1\mu_1 + S_2A_2\mu_2 + \lambda) - S_1A_1, \qquad (3.10)
\end{aligned}$$

and

$$\begin{aligned}
\frac{\partial I}{\partial \mu_2} &= -(1-\mu_1)\varphi(\lambda) - \mu_1\varphi(S_1A_1+\lambda) + (1-\mu_1)\varphi(S_2A_2+\lambda) \\
&+\mu_1\varphi(S_1A_1+S_2A_2+\lambda) - S_2A_2\log(S_1A_1\mu_1 + S_2A_2\mu_2 + \lambda) - S_2A_2. \qquad (3.11)
\end{aligned}$$

In order to further analyze the above KKT conditions, we need to consider 16 cases corresponding to different combinations of active constraints (i.e., whether $\eta_i = 0$ or not for $i = 1, \cdots, 4$). For example, if $\eta_1 = 0, \eta_2 = 0, \eta_3 \neq 0, \eta_4 = 0$, then the above KKT

conditions can be simplified to

$$\begin{aligned} \frac{\partial I}{\partial \mu_1}\Big|_{(\hat{\mu}_1,\hat{\mu}_2)} &= 0, \\ \frac{\partial I}{\partial \mu_2}\Big|_{(\hat{\mu}_1,\hat{\mu}_2)} - \eta_3 &= 0, \\ \eta_3(\hat{\mu}_2 - 1) &= 0, \end{aligned}$$

from which we obtain

$$\begin{aligned} \hat{\mu}_1 &= \alpha\left(\frac{S_1 A_1}{S_2 A_2 + \lambda}\right), \\ \hat{\mu}_2 &= 1. \end{aligned} \tag{3.12}$$

Since $\max I(\hat{\mu}_1, 0) > \max I(\hat{\mu}_1, 1)$, (3.12) is clearly not an optimal solution.

Using similar arguments, we can show that among these 16 possible combinations, 13 constraint combinations result in non-optimal solutions. We are then left with the following three possible scenarios:

Scenario 1: $\eta_1 = 0, \eta_2 = 0, \eta_3 = 0, \eta_4 = 0$**:**

The KKT conditions are simplified to

$$\frac{\partial I}{\partial \mu_1}\Big|_{(\mu_1,\mu_2)} = 0, \tag{3.13}$$

$$\frac{\partial I}{\partial \mu_2}\Big|_{(\mu_1,\mu_2)} = 0. \tag{3.14}$$

This scenario corresponds to the case where both users are active. From (3.10) and (3.11), we can see that both $\frac{\partial I}{\partial \mu_1}\Big|_{(\mu_1,\mu_2)}$ and $\frac{\partial I}{\partial \mu_2}\Big|_{(\mu_1,\mu_2)}$ are nonlinear functions of (μ_1, μ_2). Hence, there can be multiple (μ_1, μ_2) pairs satisfying (3.13) and (3.14) simultaneously. However, we now show that there are in fact at most 2 possible (μ_1, μ_2) pairs that satisfy (3.13) and (3.14) simultaneously.

First, by (3.13)$\times S_2A_2-$ (3.14)$\times S_1A_1$, we have

$$\begin{aligned}
&S_2A_2(-(1-\mu_2)\varphi(\lambda)+(1-\mu_2)\varphi(S_1A_1+\lambda)-\mu_2\varphi(S_2A_2+\lambda)\\
&+\mu_2\varphi(S_1A_1+S_2A_2+\lambda)=S_1A_1(-(1-\mu_1)\varphi(\lambda)-\mu_1\varphi(S_1A_1+\lambda)\\
&-(1-\mu_1)\varphi(S_2A_2+\lambda)+\mu_1\varphi(S_1A_1+S_2A_2+\lambda). \qquad (3.15)
\end{aligned}$$

Using (3.15), we can write μ_2 in terms of μ_1:

$$\mu_2=\frac{V}{W}+\frac{S_1A_1}{S_2A_2}\mu_1\triangleq f(\mu_1), \qquad (3.16)$$

where

$$\begin{aligned}
W &\triangleq \varphi(\lambda)-\varphi(S_1A_1+\lambda)-\varphi(S_2A_2+\lambda)+\varphi(S_1A_1+S_2A_2+\lambda), \qquad (3.17)\\
V &\triangleq -\varphi(S_1A_1+\lambda)+\varphi(\lambda)-\frac{S_1A_1}{S_2A_2}\varphi(\lambda)+\frac{S_1A_1}{S_2A_2}\varphi(S_2A_2+\lambda). \qquad (3.18)
\end{aligned}$$

It is clear that $f(\mu_1)$ is a linear function of μ_1.

Using $\frac{\partial I}{\partial \mu_2}=0$, we can write μ_2 in terms of μ_1:

$$\begin{aligned}
\mu_2 &= \frac{1}{S_2A_2}\Bigg(\exp\left(\frac{1}{S_2A_2}\left(-(1-\mu_1)\varphi(\lambda)-\mu_1\varphi(S_1A_1+\lambda)+(1-\mu_1)\varphi(S_2A_2+\lambda)\right.\right.\\
&\quad\left.\left.+\mu_1\varphi(S_1A_1+S_2A_2+\lambda)-S_2A_2\right)\right)-\frac{S_1A_1\mu_1+\lambda}{S_2A_2}\\
&\triangleq g(\mu_1). \qquad (3.19)
\end{aligned}$$

It is easy to check that $g^{''}(\mu_1)>0$, and hence $g(\mu_1)$ is a strictly convex function of μ_1.

We have just converted (3.13) and (3.14) into equivalent forms:

$$\mu_2 = f(\mu_1), \tag{3.20}$$

$$\mu_2 = g(\mu_1). \tag{3.21}$$

Hence, (μ_1, μ_2) pairs where $f(\mu_1)$ and $g(\mu_1)$ intersect with each other satisfy (3.13) and (3.14) simultaneously. As $f(\mu_1)$ is a linear function of μ_1, while $g(\mu_1)$ is a strictly convex function of μ_1, they can have at most two intersecting points as shown in Fig. 3.2.

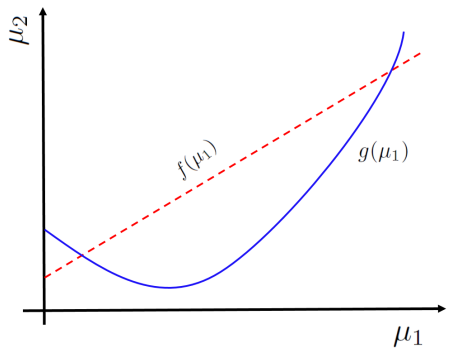

Figure 3.2: $f(\mu_1)$ and $g(\mu_1)$ have at most two intersecting points.

Therefore, there can be at most two pairs of (μ_1, μ_2) that satisfy both conditions simultaneously. Let these solutions be $(\tilde{\mu}_1, \tilde{\mu}_2)$ and $(\tilde{\mu}_1', \tilde{\mu}_2')$. We then need to check whether $(\tilde{\mu}_1, \tilde{\mu}_2)$ is in $[0, 1] \times [0, 1]$ or not. If yes, we keep it. If not, then for the presentation convenience, we replace it with $(0, 0)$. We do the same for $(\tilde{\mu}_1', \tilde{\mu}_2')$.

Scenario 2: $\eta_1 = 0, \eta_2 = 0, \eta_3 = 0, \eta_4 \neq 0$**:**

Solving the corresponding KKT conditions, we obtain

$$\begin{aligned} \bar{\mu}_1 &= \alpha(S_1 A_1/\lambda), \\ \bar{\mu}_2 &= 0. \end{aligned} \tag{3.22}$$

From the property of $\alpha(\cdot)$, we know that $0 \leq \bar{\mu}_1 \leq 1$, and hence $(\bar{\mu}_1, 0)$ is a valid input. This scenario corresponds to the case where only user 1 is active.

Scenario 3: $\eta_1 = 0, \eta_2 \neq 0, \eta_3 = 0, \eta_4 = 0$**:**

Solving the corresponding KKT conditions, we obtain

$$\begin{aligned} \mu_1^* &= 0, \\ \mu_2^* &= \alpha(S_2 A_2/\lambda). \end{aligned} \tag{3.23}$$

Similarly, we have $0 \leq \mu_2^* \leq 1$, and hence $(0, \mu_2^*)$ is a valid input. This scenario corresponds to the case where only user 2 is active.

In summary, we have the following theorem.

Theorem 7. *The optimal value $(\hat{\mu}_1, \hat{\mu}_2)$ that achieves the sum-rate capacity for the general Poisson MAC is given by*

$$(\hat{\mu}_1, \hat{\mu}_2) = \begin{cases} (0, \mu_2^*) & \textit{if} \quad I(0, \mu_2^*) \geq \max\left(I(\bar{\mu}_1, 0), I(\tilde{\mu}_1, \tilde{\mu}_2), I(\tilde{\mu}_1', \tilde{\mu}_2')\right) \\ (\bar{\mu}_1, 0) & \textit{if} \quad I(\bar{\mu}_1, 0) \geq \max\left(I(0, \mu_2^*), I(\tilde{\mu}_1, \tilde{\mu}_2), I(\tilde{\mu}_1', \tilde{\mu}_2')\right) \\ (\tilde{\mu}_1', \tilde{\mu}_2') & \textit{if} \quad I(\tilde{\mu}_1', \tilde{\mu}_2') \geq \max\left(I(0, \mu_2^*), I(\bar{\mu}_1, 0), I(\tilde{\mu}_1, \tilde{\mu}_2)\right) \\ (\tilde{\mu}_1, \tilde{\mu}_2) & \textit{otherwise} \end{cases} \tag{3.24}$$

It is interesting to note that unlike the Gaussian MAC with an average power constraint, it can be optimal to allow only one user to transmit in order to achieve the sum-rate capacity in the Poisson MAC with a maximum power constraint. For example, when $S_1 A_1 = 5, S_2 A_2 = 50, \lambda = 0.5$, there is no solution for (3.20) and (3.21) in the desired range of $0 \leq \mu_1 \leq 1$ and $0 \leq \mu_2 \leq 1$, because (3.20) and (3.21) do not intersect (as shown in Fig. 3.3). Hence, for such a set of parameters, it is optimal to allow only one user (in this case, user 2) to transmit to achieve the sum-rate capacity.

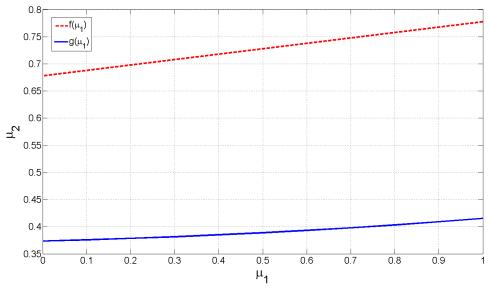

Figure 3.3: $f(\mu_1)$ and $g(\mu_1)$ have no intersection in $0 \leq \mu_1 \leq 1$ and $0 \leq \mu_2 \leq 1$, when $S_1A_1 = 5, S_2A_2 = 50$, and $\lambda = 0.5$.

On the other hand, there are scenarios under which it is optimal for both users to transmit. For example, when $S_1A_1 = 10, S_2A_2 = 15, \lambda = 0.5$, it is easy to check that it is optimal for both users to transmit in order to achieve the sum-rate capacity.

Motivated by these observations, we further analyze (3.24) to characterize conditions under which it is optimal to either allow one user or two users to transmit.

3.2.2 Single-User or Two-User Transmission?

In this subsection, we present conditions under which it is optimal for a single-user to transmit and conditions under which it is optimal for two-user transmission.

We first focus on the optimality of single-user transmission. As discussed above, the solution for two-user transmission is characterized by the intersections of (3.20) and (3.21). The following simple proposition characterize the conditions under which (3.20) and (3.21) do not have an intersection in the desired region $[0, 1] \times [0, 1]$ and hence two-user transmission is not optimal.

Proposition 8. *If $g(0) < f(0)$ and $g(1) < f(1)$, then single-user transmission is optimal to achieve the sum-rate capacity.*

Proof. It suffices to argue that two-user transmission is not optimal under the assumption of the proposition. This happens when (3.20) and (3.21) do not intersect. Therefore we

prove that $g(\mu_1)$ does not intersect with $f(\mu_1)$ when $g(0) < f(0)$ and $g(1) < f(1)$ for $\mu_1 \in [0, 1]$. For any $\mu_1 \in [0, 1]$, we have

$$\begin{aligned} f(\mu_1) &\overset{(a)}{=} (1-\mu_1)f(0) + \mu_1 f(1) \\ &\overset{(b)}{>} (1-\mu_1)g(0) + \mu_1 g(1) \\ &\overset{(c)}{>} g(\mu_1). \end{aligned}$$

Here, (a) follows from the linearity of $f(\cdot)$, (b) follows from the assumption $g(0) < f(0)$ and $g(1) < f(1)$, and (c) follows from the strict convexity of $g(\cdot)$. □

For any given S_1A_1 and S_2A_2 we can determine whether single-user transmission is optimal or not by using Proposition 8. In the following, we will show that if one of the S_iA_is is sufficiently large, then it is optimal for one user to transmit. As the roles of users are symmetric, we restrict our analysis to $S_2A_2 \to \infty$ as an example. We show that as $S_2A_2 \to \infty$, the conditions in Proposition 8 are satisfied and hence $f(\mu_1)$ and $g(\mu_1)$ do not intersect.

Lemma 9. *The functions $f(\mu_1)$ and $g(\mu_1)$ have the following properties:*

$$\lim_{S_2A_2\to\infty} f(\mu_1) = \lim_{S_2A_2\to\infty} f(0) = \lim_{S_2A_2\to\infty} f(1) = 1$$

and

$$\lim_{S_2A_2\to\infty} g(\mu_1) = \lim_{S_2A_2\to\infty} g(1) = \lim_{S_2A_2\to\infty} g(0) = \frac{1}{e}.$$

Therefore, (3.20) *and* (3.21) *do not intersect as $S_2A_2 \to \infty$.*

Proof. Please refer to Appendix C.2. □

Lemma 9 is illustrated in Fig. 3.4. As discussed in Scenario 1 of Section 3.2.1, (3.20) and (3.21) do not intersect in our region of interest, and hence we replace $(\tilde{\mu}_1', \tilde{\mu}_2')$ and

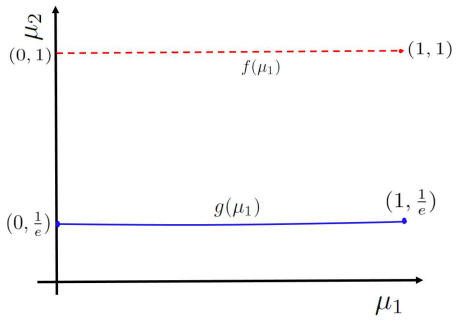

Figure 3.4: μ_2 vs. μ_1 as $S_2A_2 \to \infty$

$(\tilde{\mu}_1, \tilde{\mu}_2)$ by $(0,0)$ when $S_2A_2 >> S_1A_1$. This implies that either $(0, \mu_2^*)$ or $(\bar{\mu}_1, 0)$ is the possible solutions. With $S_2A_2 >> S_1A_1$, solving (3.24) yields $(0, \mu_2^*)$ as the optimal solution, i.e., only user 2 transmitting achieves the sum-rate capacity.

Now, we discuss the conditions under which it is optimal for both users to transmit. In particular, the following proposition characterizes conditions under which single-user transmission is not optimal.

Proposition 10. *User 1 transmitting alone is not optimal if*

$$\alpha(S_1A_1/\lambda) > \gamma_1 \triangleq \frac{\left(1 - \frac{S_2A_2}{S_1A_1}\right)\varphi(\lambda) - \varphi(S_2A_2 + \lambda) + \frac{S_2A_2}{S_1A_1}\varphi(S_1A_1 + \lambda)}{W},$$

in which W is defined in (3.17)*. Similarly, user* 2 *transmitting alone is not optimal if*

$$\alpha(S_2A_2/\lambda) > \gamma_2 \triangleq \frac{\left(1 - \frac{S_1A_1}{S_2A_2}\right)\varphi(\lambda) - \varphi(S_1A_1 + \lambda) + \frac{S_1A_1}{S_2A_2}\varphi(S_2A_2 + \lambda)}{W}.$$

Furthermore, if both conditions above are satisfied, it is optimal for both users to be active.

Proof. To prove this proposition, we will find out conditions under which a single-user transmission can be eliminated as a candidate for optimality. To eliminate $(0, \mu_2^*)$, which is obtained in (3.23), as a candidate for the optimal solution, we check whether $\frac{\partial I}{\partial \mu_1}\Big|_{(\mu_1=0,\mu_2^*)}$

is larger than 0 or not. If it is larger than 0, then we know that $(0, \mu_2^*)$ cannot be the optimal solution. By replacing the value of $\log(S_2A_2\mu_2^* + \lambda)$ from the $\frac{\partial I}{\partial \mu_2}\Big|_{\mu_1=0,\mu_2^*} = 0$ in $\frac{\partial I}{\partial \mu_1}\Big|_{(\mu_1=0,\mu_2^*)} = 0$, we have

$$\begin{aligned}\frac{\partial I}{\partial \mu_1}\Big|_{(\mu_1=0,\mu_2^*)} &= -(1-\mu_2^*)\varphi(\lambda) + (1-\mu_2^*)\varphi(S_1A_1+\lambda) - \mu_2^*\varphi(S_2A_2+\lambda) \\ &\quad +\mu_2^*\varphi(S_1A_1+S_2A_2+\lambda) - \frac{S_1A_1}{S_2A_2}\varphi(S_2A_2+\lambda) \\ &\quad +\frac{S_1A_1}{S_2A_2}\varphi(\lambda). \end{aligned} \tag{3.25}$$

Hence the condition for $\frac{\partial I}{\partial \mu_1}\Big|_{(\mu_1=0,\mu_2^*)} > 0$ to hold true is $\mu_2^* > \gamma_2$, where $\gamma_2 = \frac{r_2}{W}$ with $r_2 = (1 - \frac{S_1A_1}{S_2A_2})\varphi(\lambda) - \varphi(S_1A_1 + \lambda) + \frac{S_1A_1}{S_2A_2}\varphi(S_2A_2 + \lambda)$. Therefore, the case $(0, \mu_2^*)$ is not optimal if $\mu_2^* > \gamma_2$.

Following similar arguments, we can conclude that $(\bar{\mu}_1, 0)$, which is obtained in (3.22), is not optimal when $\bar{\mu}_1 > \gamma_1$, in which $\gamma_1 = \frac{r_1}{W}$ with $r_1 = (1 - \frac{S_2A_2}{S_1A_1})\varphi(\lambda) - \varphi(S_2A_2 + \lambda) + \frac{S_2A_2}{S_1A_1}\varphi(S_1A_1 + \lambda)$.

If $\bar{\mu}_1 > \gamma_1$ and $\mu_2^* > \gamma_2$, two-user transmission is the optimal solution. □

3.2.3 Special Case: Symmetric Channel

In this section we show that the results obtained in Section 3.2.1 can recover the results obtained in [52] for the symmetric case. We show this using the following three steps.

Step 1: Among the four possible solutions in (3.24), we first rule out $(0, \mu_2^*)$ and $(\bar{\mu}_1, 0)$. It is easy to check that, when $S_1A_1 = S_2A_2$, $\gamma_1 = 0$ and $\gamma_2 = 0$. Hence, as discussed in Section 3.2.2, $(0, \mu_2^*)$ is not optimal, as we clearly have $\mu_2^* > \gamma_2 = 0$. Similarly, $(\bar{\mu}_1, 0)$ is not optimal, as $\bar{\mu}_1 > \gamma_1 = 0$. Hence, scenario 2 and scenario 3 cannot be optimal, and we are left with only scenario 1.

Step 2: We show that, if (μ_1, μ_2) is a solution to (3.20) and (3.21) of scenario 1, then

μ_1 must be equal to μ_2. This can be easily seen by setting $S_1A_1 = S_2A_2$ in (3.16), which yields $\mu_1 = \mu_2$.

Step 3: We show that there is a unique pair (μ_1, μ_2) that satisfies (3.20) and (3.21) of scenario 1. To prove the uniqueness of the solution, as illustrated in Fig. 3.5, we show

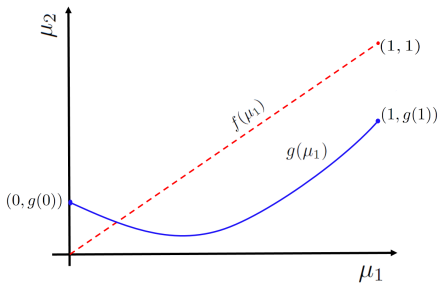

Figure 3.5: $f(\mu_1)$ and $g(\mu_1)$ has a single intersecting point in the region of interest when $S_1A_1 = S_2A_2$.

that $g(0) > 0 = f(0)$ and $g(1) < 1 = f(1)$. Since $g(\cdot)$ is a strictly convex function while $\mu_2 = \mu_1$ is a linear function, $f(\mu_1)$ and $g(\mu_1)$ have a single intersecting point in the range $0 \leq \mu_1 \leq 1$.

Lemma 11. *If* $S_1A_1 = S_2A_2$, $g(1) < 1$ *and* $g(0) > 0$.

Proof. Please refer to Appendix C.3. □

Hence it can be concluded that if $S_1A_1 = S_2A_2$, then there is a unique solution to the problem and at optimality $\hat{\mu}_1 = \hat{\mu}_2$. This result is consistent with the one shown in [52].

3.3 MISO-MAC Analysis

In this section, we extend the analysis to the case when the transmitters are equipped with more than one antennas.

3.3.1 Sum-rate Capacity of MISO-MAC

Similarly to the single-antenna case studied in Section 3.2, the continuous-time continuous-input discrete-output Poisson MAC can be converted to discrete-time binary-input binary-output MAC. In particular, the input waveform of each antenna can be limited to be piecewise constant waveforms with two levels 0 or A_{nj} for the j^{th} antenna of the n^{th} transmitter. Depending on the on-off states of each antenna of user n, there are 2^{J_n} states at user n. In the following, we use $i_n \in [1, \cdots, 2^{J_n}]$ to index each of these 2^{J_n} states at user n. We will use $P_n(i_n)$ to denote the probability that user n lies in state i_n and $\mathbf{p}_n \triangleq [P_n(1), \cdots, P_n(2^{J_n})]$ to denote the vector of probabilities of states at user n. We will use the binary variable $b_{nj}(i_n)$ to indicate whether the j^{th} antenna of the n^{th} user is on or off at state i_n, i.e., $b_{nj}(i_n) = 1$ if the j^{th} antenna of the n^{th} user is on for state i_n and is 0 otherwise. The sum-rate achievable using $(\mathbf{p}_1, \mathbf{p}_2)$ is given by

$$I_{\mathbf{X}_N;Y}(\mathbf{p}_1, \mathbf{p}_2) = \sum_{i_1=1}^{2^{J_1}} \sum_{i_2=1}^{2^{J_2}} \left[P_1(i_1) P_2(i_2) \zeta \left(\sum_{n=1}^{2} \sum_{j=1}^{J_n} S_{nj} A_{nj} b_{nj}(i_n), \lambda \right) \right] - \zeta \left(\sum_{n=1}^{2} \sum_{j=1}^{J_n} S_{nj} A_{nj} \mu_{nj}, \lambda \right). \tag{3.26}$$

It is easy to see that

$$\mu_{nj} = \sum_{i_n=1}^{2^{J_n}} P_n(i_n) b_{nj}(i_n). \tag{3.27}$$

Fig 3.6 (a) shows 4 possible states for user 2 with 2 antennas.

To characterize the sum-rate capacity, we need to solve the following optimization

problem:

$$\textbf{(P1):} \quad C_{sum}^{MISO-MAC} = \max_{\mathbf{p}_1,\mathbf{p}_2} I_{\mathbf{X}_N;Y}(\mathbf{p}_1,\mathbf{p}_2), \tag{3.28}$$

$$\text{s.t} \qquad 0 \le P_n(i_n) \le 1,\ i_n = 1,\cdots,2^{J_n}, n = 1,2, \tag{3.29}$$

$$\sum_{i_n=1}^{2^{J_n}} P_n(i_n) = 1, n = 1,2. \tag{3.30}$$

Problem (P1) is a complex non-convex optimization problem with a large number of variables. In particular, the number of variables $2^{J_1} + 2^{J_2}$ increases exponentially with the number of antennas. The main result of this section is the following theorem.

Theorem 12. *Solving problem (P1) is equivalent to solving the following problem*

$$\textbf{(P2):} \quad C_{sum}^{MISO-MAC} = \max_{0\le\mu_1,\mu_2\le 1} I(\mu_1,\mu_2), \tag{3.31}$$

with

$$\begin{aligned} I(\mu_1,\mu_2) &= (1-\mu_1)(1-\mu_2)\varphi(\lambda) + \mu_1(1-\mu_2)\varphi(B_1+\lambda) + (1-\mu_1)\mu_2\varphi(B_2+\lambda) \\ &\quad +\mu_1\mu_2\varphi(B_1+B_2+\lambda) - \varphi(B_1\mu_1 + B_2\mu_2 + \lambda), \end{aligned} \tag{3.32}$$

where

$$B_n \triangleq \sum_{j=1}^{J_n} S_{nj}A_{nj}. \tag{3.33}$$

Remark 1. *Compared with (P1), there are only 2 variables in (P2). Although (P2) is still a non-convex optimization problem, it has the same form as the problem (P0) solved in Section 3.2.1 and hence all techniques and results there (e.g., the analysis on whether single-user transmission is optimal or not) can be applied here. Intuitively, this theorem says that the sum capacity of a MISO-MAC (with channel gains (S_{n1}, S_{n2}) and power*

constraints (A_{n1}, A_{n2}) *for each transmitter* n*) is the same as the sum capacity of a SISO-MAC (with channel gain* $S_{n1}A_{n1} + S_{n2}A_{n2}$ *and power constraint* 1 *for each transmitter* n*).*

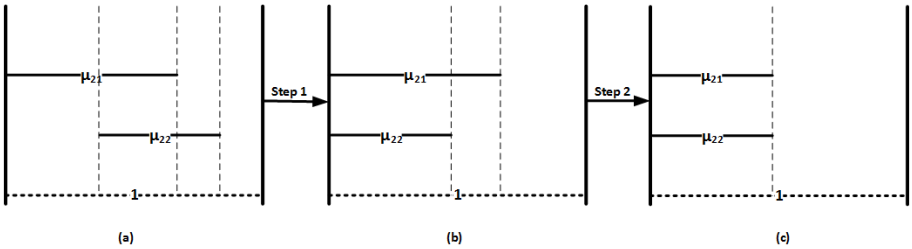

Figure 3.6: (a) Four possible states for user 2; (b) Step 1 shows, at the optimality, the timing of antennas being on is aligned; (c) Step 2 shows, at the optimality, the duty cycles of both antennas are the same and are aligned.

The proof of Theorem 12 has the following two major steps.

In Step-1, we prove the following proposition that simplifies the optimization problem from $(\mathbf{p}_1, \mathbf{p}_2)$ to $\boldsymbol{\mu}$.

Proposition 13. *At the optimality, for each user, if the antenna with a smaller duty cycle is on then all antennas with a larger duty cycle must also be on.*

This proposition shows that, at the optimality, instead of being a function of $(\mathbf{p}_1, \mathbf{p}_2)$, the objective function can be simplified to a function of $\boldsymbol{\mu}$. As the result, the dimension of the problem is reduced from $2^{J_1} + 2^{J_2}$ to $J_1 + J_2$. The central issue addressed here is that, for a given $\boldsymbol{\mu}$, there are infinite number of combinations of $(\mathbf{p}_1, \mathbf{p}_2)$ that satisfy (3.27). The main idea is to show that, for any user n, if the antenna with a smaller duty cycle is on, then the antenna with a larger duty cycle is also on at the optimality. As the result, at the optimality, the value of $(\mathbf{p}_1, \mathbf{p}_2)$ is determined by $\boldsymbol{\mu}$. Detailed proof of this proposition can be found in Section 3.3.2. For the example shown in Figure 3.6, assuming $\mu_{21} \geq \mu_{22}$, there are four initial states shown in Fig. 3.6 (a): only the antenna with the larger duty cycle is on, both of the antennas are on, only the antenna with the smaller duty cycle is on

and none of the antennas is on. We argue that a state with only the antenna having smaller duty cycle to be on is not optimal. Hence, at the optimality, we have the scenario shown in Fig. 3.6 (b).

In Step-2, we show the following proposition that characterizes the optimal value of $\boldsymbol{\mu}$.

Proposition 14. *At the optimality, for each user, all antennas must have the same duty cycle and they must be on or off simultaneously.*

This proposition shows that, at the optimality, the antennas of each user must have the same duty cycle (i.e., $\mu_{n1} = \cdots = \mu_{nJ_n} \triangleq \mu_n$) and are aligned. Hence, the dimension of the problem is further reduced from $J_1 + J_2$ to 2. The main idea of this step is to show that, at the optimality, all antennas of user n are either simultaneously on or off. Hence, from receiver's perspective, transmitter n can be viewed as a single antenna with power constraint 1 and channel gain $\sum_{j=1}^{J_n} S_{nj} A_{nj}$. Step 2 is illustrated Fig. 3.6 (b) and Fig. 3.6 (c). The proof can be found in Section 3.3.3.

In order to prove Theorem 12, Propositions 13 and 14 need to be proved. In the following subsections, we prove these propositions in detail.

3.3.2 Proof of Proposition 13

In this subsection, we prove Proposition 13 by characterizing the optimal value of $(\mathbf{p}_1, \mathbf{p}_2)$ for any given $\boldsymbol{\mu}$. Hence, in this subsection, $\boldsymbol{\mu}$ is fixed. More specifically, we show that, at the optimality in the MISO-MAC, if the antenna with the smaller duty cycle is on, then the other antenna should also be on.

From (4.22), it is clear that to optimize over $(\mathbf{p}_1, \mathbf{p}_2)$ for a given $\boldsymbol{\mu}$, we only need to

focus on

$$\begin{aligned}\mathcal{H} &\triangleq \sum_{i_1=1}^{2^{J_1}}\sum_{i_2=1}^{2^{J_2}} P_1(i_1)P_2(i_2)\zeta\left(\sum_{n=1}^{2}\sum_{j=1}^{J_n} S_{nj}A_{nj}b_{nj}(i_n),\lambda\right) \\ &= \sum_{i_1=1}^{2^{J_1}} P_1(i_1)\underbrace{\sum_{i_2=1}^{2^{J_2}} P_2(i_2)\,\underbrace{\zeta\left(\sum_{j=1}^{J_1} S_{1j}A_{1j}b_{1j}(i_1)+\sum_{j=1}^{J_2} S_{2j}A_{2j}b_{2j}(i_2),\lambda\right)}_{d(i_1,i_2)}}_{\mathcal{H}_1(i_1)}. \end{aligned} \quad (3.34)$$

We focus on finding the optimal values of $\mathbf{p}_2$ first. To facilitate the understanding, we list the labeling of states of user 2 and the corresponding values of b_{2j}s in Table 3.1.

	b_{21}	b_{22}
$(i_1,1)$	0	0
$(i_1,2)$	0	1
$(i_1,3)$	1	0
$(i_1,4)$	1	1

Table 3.1: The states of user 2 and the corresponding values of b_{2j}s.

Using the definition of ζ function in (3.6), we can easily check that

$$d(i_1,1) < \min\{d(i_1,2),d(i_1,3)\} \le \max\{d(i_1,2),d(i_1,3)\} < d(i_1,4),$$

which is simultaneously true for any value of i_1. As $\mathcal{H}_1(i_1)$ is simply a linear combination of $d(i_1,i_2)$s, hence, for any given $\boldsymbol{\mu}$, maximizing $\mathcal{H}_1(i_1)$ is a linear programming problem, for which we have the following (assuming $\mu_{21} \ge \mu_{22}$, the other case being similar):

1. As $d(i_1,4)$ is the largest, $P_2(4)$ should be as large as possible. Therefore, we assign $P_2(4) = \mu_{22}$.

2. As μ_{22} has been all used, we should set $P_2(2) = 0$.

3. As $d(i_1, 3) > d(i_1, 1)$, we assign the remaining part of μ_{21} to state $(i_1, 3)$ and hence $P_2(3) = \mu_{21} - \mu_{22}$.

4. For the last state related to the term $d(i_1, 1)$, allot the remaining probability. Hence $P_2(1) = 1 - \mu_{21}$.

This assignment implies that if the antenna with a smaller duty cycle is on, the antenna with a larger duty cycle should also be on. This is illustrated in Fig. 3.6 (b). Note that the above arguments are true for all i_1s, and hence this assignment maximizes $\mathcal{H}_1(i_1)$ for all i_1 simultaneously. Furthermore, this assignment is independent of $\mathbf{p}_1$.

Notice that the above discussion for $J_2 = 2$, can be extended for $J_2 > 2$.

Similarly, by writing

$$\mathcal{H} \;=\; \sum_{i_2=1}^{2^{J_2}} P_2(i_2) \sum_{i_1=1}^{2^{J_1}} P_1(i_1)\zeta \left(\sum_{j=1}^{J_1} S_{1j} A_{1j} b_{1j}(i_1) + \sum_{j=1}^{J_2} S_{2j} A_{2j} b_{2j}(i_2), \lambda \right),$$

then following the same procedure as above, we can calculate the optimal values of $\mathbf{p}_1$.

As the result, we know that (3.26) can be simplified to a function $\boldsymbol{\mu}$ depending on the relationships between the values of μ_{nj}s. For example, in the case of two transmitter antennas, we have four symmetric cases, i.e. $(\mu_{11} \geq \mu_{12}, \mu_{21} \geq \mu_{22}), (\mu_{11} \leq \mu_{12}, \mu_{21} \geq \mu_{22}), (\mu_{11} \geq \mu_{12}, \mu_{21} \leq \mu_{22})$ and $(\mu_{11} \leq \mu_{12}, \mu_{21} \leq \mu_{22})$. For the case of $(\mu_{11} \geq$

$\mu_{12}, \mu_{21} \geq \mu_{22}$), $I_{\mathbf{X}_N;Y}$ can be simplified to

$$
\begin{aligned}
&I(\mu_{11}-\mu_{12}, \mu_{12}, \mu_{21}-\mu_{22}, \mu_{22}) = \\
&(1-\mu_{11})((1-\mu_{21})\varphi(\lambda) + (\mu_{21}-\mu_{22})\varphi(S_{21}A_{21}+\lambda) + \mu_{22}\varphi(B_2+\lambda)) + \\
&(\mu_{11}-\mu_{12})((1-\mu_{21})\varphi(S_{11}A_{11}+\lambda) + (\mu_{21}-\mu_{22})\varphi(S_{21}A_{21}+S_{11}A_{11}+\lambda) + \mu_{22}\varphi(B_2+S_{11}A_{11}+\lambda)) \\
&+\mu_{12}((1-\mu_{21})\varphi(B_1+\lambda) + (\mu_{21}-\mu_{22})\varphi(S_{21}A_{21}+B_1+\lambda) + \mu_{22}\varphi(B_2+B_1+\lambda)) \\
&-\varphi\left(\sum_{n=1}^{2}\sum_{j=1}^{J_n} S_{nj}A_{nj}\mu_{nj} + \lambda\right).
\end{aligned}
\tag{3.35}
$$

As the result, the objective function is simplified to characterizing

$$
C_{sum}^{MISO-MAC} = \max\left(C_{\mu_{11}\geq\mu_{12},\mu_{21}\geq\mu_{22}}, C_{\mu_{11}\leq\mu_{12},\mu_{21}\geq\mu_{22}}, C_{\mu_{11}\geq\mu_{12},\mu_{21}\leq\mu_{22}}, C_{\mu_{11}\leq\mu_{12},\mu_{21}\leq\mu_{22}}\right),
\tag{3.36}
$$

in which

$$
\begin{aligned}
\textbf{(P3):} \quad C_{\mu_{11}\geq\mu_{12},\mu_{21}\geq\mu_{22}} &= \max I(\mu_{11}-\mu_{12}, \mu_{12}, \mu_{21}-\mu_{22}, \mu_{22}), && (3.37)\\
\text{s.t.} \quad & 0 \leq \mu_{12} \leq \mu_{11} \leq 1, && (3.38)\\
& 0 \leq \mu_{22} \leq \mu_{21} \leq 1. && (3.39)
\end{aligned}
$$

Other terms in (3.36) are defined in a similar manner. Due to symmetry, in the following, we only provide details on how to solve (P3).

3.3.3 Proof of Proposition 14

In this subsection, we prove Proposition 14 by solving (P3). For the ease of calculation, we define $q_1 = \mu_{11}-\mu_{12}$, $q_2 = \mu_{12}$, $q_3 = \mu_{21}-\mu_{22}$ and $q_4 = \mu_{22}$ and let $\mathbf{q} = [q_1, q_2, q_3, q_4]$.

Then (4.35) can be re-written as

$$
\begin{aligned}
&I(\mathbf{q}) = (1-(q_1+q_2))((1-(q_3+q_4))\varphi(\lambda) + q_3\varphi(S_{21}A_{21}+\lambda) + q_4\varphi(B_2+\lambda)) \\
&+q_1((1-(q_3+q_4))\varphi(S_{11}A_{11}+\lambda) + q_3\varphi(S_{21}A_{21}+S_{11}A_{11}+\lambda) + q_4\varphi(B_2+S_{11}A_{11}+\lambda)) \\
&+q_2((1-(q_3+q_4)\varphi(B_1+\lambda) + q_3\varphi(S_{21}A_{21}+B_1+\lambda) + q_4\varphi(B_2+B_1+\lambda)) \\
&-\varphi(S_{11}A_{11}q_1 + B_1q_2 + S_{21}A_{21}q_3 + B_2q_4 + \lambda). \qquad (3.40)
\end{aligned}
$$

Correspondingly, (P3) is equivalent to

$$
\begin{aligned}
\textbf{(P4):} \quad C_{\mu_{11}\geq\mu_{12},\mu_{21}\geq\mu_{22}} &= \max I(\mathbf{q}) && (3.41)\\
\text{s.t.} \quad & q_k \geq 0,\ k=1,\cdots,4, && (3.42)\\
& q_1+q_2 \leq 1, && (3.43)\\
& q_3+q_4 \leq 1. && (3.44)
\end{aligned}
$$

Similarly to (3.8), the objective function (3.41) is not a convex function in general. We use the KKT conditions as necessary conditions to characterize the set of possible candidates for the optimal solution. In the following, we consider only the constraint (3.42) explicitly. We check (3.43) and (3.44) after obtaining the solution.

The Langrangian equation for (P4) with constraint (3.42) is given by

$$
\mathcal{L} = -I - \sum_{k=1}^{4} \eta_k q_k.
$$

The corresponding KKT conditions are:

$$
\begin{aligned}
\frac{\partial I}{\partial q_k} + \eta_k = 0, \quad & k=1,\cdots,4, && (3.45)\\
\eta_k q_k = 0, \quad & k=1,\cdots,4, && (3.46)
\end{aligned}
$$

where

$$\frac{\partial I}{\partial q_1} = \zeta(S_{11}A_{11}, \lambda) + q_3(\zeta(S_{21}A_{21}, S_{11}A_{11} + \lambda) - \zeta(S_{21}A_{21}, \lambda)) + q_4(\zeta(B_2, S_{11}A_{11} + \lambda) - \zeta(B_2, \lambda))$$
$$-S_{11}A_{11}(\log(S_{11}A_{11}q_1 + B_1q_2 + S_{21}A_{21}q_3 + B_2q_4 + \lambda) + 1),$$
$$\frac{\partial I}{\partial q_2} = \zeta(B_1, \lambda) + q_3(\zeta(S_{21}A_{21}, B_1 + \lambda) - \zeta(S_{21}A_{21}, \lambda)) + q_4(\zeta(B_2, B_1 + \lambda) - \zeta(B_2, \lambda))$$
$$-B_1(\log(S_{11}A_{11}q_1 + B_1q_2 + S_{21}A_{21}q_3 + B_2q_4 + \lambda) + 1),$$
$$\frac{\partial I}{\partial q_3} = (1 - (q_1 + q_2))\zeta(S_{21}A_{21}, \lambda) + q_1\zeta(S_{21}A_{21}, S_{11}A_{11} + \lambda) + q_2\zeta(S_{21}A_{21}, B_1 + \lambda)$$
$$-S_{21}A_{21}\left(\log(S_{11}A_{11}q_1 + B_1q_2 + S_{21}A_{21}q_3 + B_2q_4 + \lambda) + 1\right),$$

and

$$\frac{\partial I}{\partial q_4} = (1 - (q_1 + q_2))\zeta(B_2, \lambda) + q_1\zeta(B_2, S_{11}A_{11} + \lambda) + q_2\zeta(B_2, B_1 + \lambda)$$
$$-B_2\left(\log(S_{11}A_{11}q_1 + B_1q_2 + S_{21}A_{21}q_3 + B_2q_4 + \lambda) + 1\right).$$

Now in order to find the set of optimal solutions, we may solve the above KKT conditions (3.45) and (3.46). As we can see from the expressions of $\frac{\partial I}{\partial q_k}$s, we need to solve a set of nonlinear equations, which are in general difficult to solve and may have infinite number of solutions. Nevertheless, by exploring the structure of problem, we obtain the following result.

Proposition 15. *There are only three possible cases for the solution to Problem (P4):*

1. $\mathbf{q} = (0, \alpha(B_1/\lambda), 0, 0)$*, which implies that both antennas of user 1 are active with the same duty cycle* $\alpha(B_1/\lambda)$ *while both antennas of user 2 are off.*

2. $\mathbf{q} = (0, 0, 0, \alpha(B_2/\lambda))$*, which implies that both antennas of user 1 are off while while both antennas of user 2 are active with the same duty cycle* $\alpha(B_2/\lambda)$*.*

3. $\mathbf{q} = (0, \mu_1, 0, \mu_2)$*, which implies that both antennas of user 1 are active with the*

same duty cycle μ_1 and both antennas of user 2 are active with the same duty cycle μ_2. Furthermore, there are only two possible pairs of (μ_1, μ_2) and can be obtained by solving (3.13) *and* (3.14) *with S_1A_1 being replaced with B_1 and S_2A_2 being replaced with B_2.*

Proof. Please refer to Appendix C.4. □

Proposition 15 states that the solution to (P4) is the same as the solution to (P2), and hence Theorem 12 is proved.

3.4 Numerical Analysis

In this section, we provide numerical examples to illustrate the results for MISO-MAC. As discussed in the Chapter 3, the case of Poisson MISO-MAC can be converted to a Poisson SISO-MAC. Hence, in this subsection, we provide only example related to the SISO-MAC case.

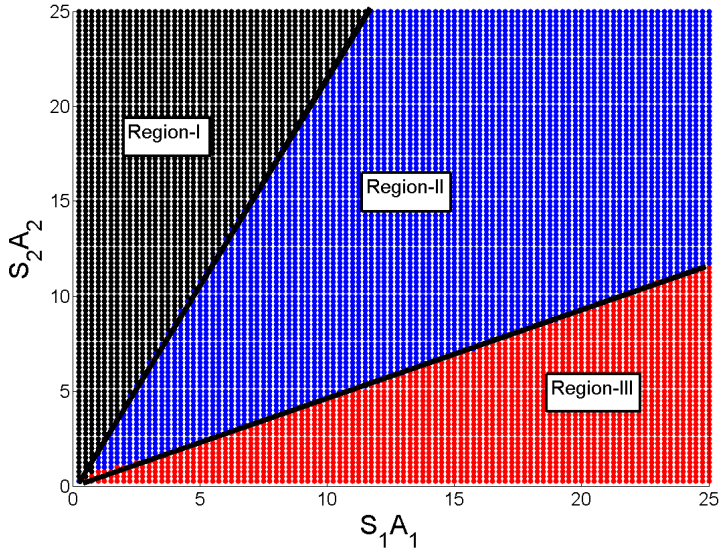

Figure 3.7: Optimal operating schemes over the ranges of S_1A_1 and S_2A_2

Fig. 3.7 shows the optimal operating scenarios for different combinations of S_1A_1

and S_2A_2 when they range from 0 to 25. In generating this figure, we set $\lambda = 0.5$. In Region-I, it is optimal for user 2 to transmit alone. Region-II corresponds to the case in which it is optimal for both users to transmit. In Region-III, it is optimal for user 1 to transmit alone.

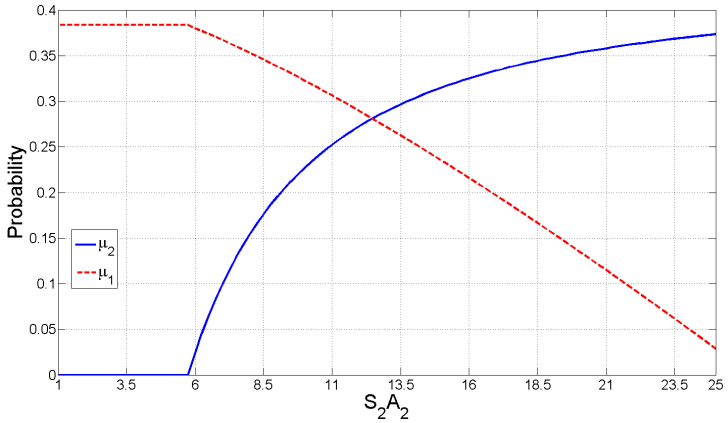

Figure 3.8: $(\hat{\mu}_1, \hat{\mu}_2)$ vs. S_2A_2

Fig. 3.8 illustrates the effect of increasing S_2A_2 on the optimal value of $(\hat{\mu}_1, \hat{\mu}_2)$ when S_1A_1 is constant. In this figure, $S_1A_1 = 12.5$. We can see that when S_2A_2 is small, the optimal value $\hat{\mu}_2$ is equal to 0, i.e., it is optimal for user 2 to stay silent. We also observe that once S_2A_2 starts to increase and has noticeable value compared to S_1A_1, $\hat{\mu}_1$ starts to decrease while $\hat{\mu}_2$ starts to increase. Furthermore, μ_1 and μ_2 intersect with each other, i.e. $\hat{\mu}_1 = \hat{\mu}_2$, when $S_1A_1 = S_2A_2$. This is consistent with the result obtained in [52] for the symmetric case.

Chapter 4

Multi User Multi Receiver

This chapter is a continuation to the Chapter 3, and we extend our analysis to the scenario when receiver is also equipped with multiple antennas.

4.1 System Model

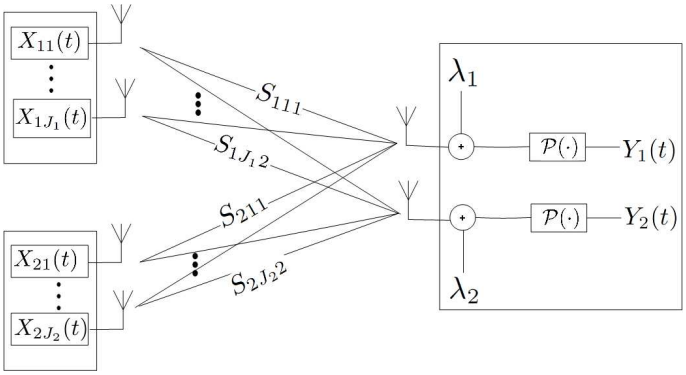

Figure 4.1: The Poisson MISO-MAC model.

In this section, we introduce the model studied in this chapter. As shown in Fig. 4.1, we consider a two-user Poisson MIMO MAC. The analysis can be extended to the scenario with more than two transmitting users. Let J_n be the number of antennas at transmitter n, and M be the number of antennas at the receiver. Let $X_{nj_n}(t)$ be the input of the j_n^{th}

transmitting antenna of the n^{th} user and $Y_m(t)$ be the doubly-stochastic Poisson process observed at the m^{th} receiving antenna. The input-output relationship can be described as:

$$Y_m(t) = \mathcal{P}\left(\sum_{n=1}^{2}\sum_{j=1}^{J_n} S_{njm}X_{nj}(t) + \lambda_m\right), \forall m \tag{4.1}$$

in which S_{nj_nm} is the channel response between the j_n^{th} antenna of the n^{th} user and the m^{th} receiving antenna, λ_m is the dark current at the m^{th} receiving antenna, and $\mathcal{P}(\cdot)$ is the non-linear transformation converting the light strength to the doubly-stochastic Poisson process that records the timing and number of photon's arrivals. In particular, for any time interval $[t, t+\tau]$, the probability that there are k photons arriving at the m^{th} receiving antenna is

$$\Pr\{Y_m(t+\tau) - Y_m(t) = k\} = \frac{e^{-\Lambda_m}\Lambda_m^k}{k!}, \tag{4.2}$$

$$\Lambda_m = \int_t^{t+\tau}\left[\sum_{n=1}^{2}\sum_{j=1}^{J_n} S_{njm}X_{nj}(t') + \lambda_m\right]dt'. \tag{4.3}$$

We consider the peak power constraint, i.e., the transmitted signal $X_{nj_n}(t)$ must satisfy the following constraint:

$$0 \le X_{nj_n}(t) \le A_{nj_n}, \tag{4.4}$$

where A_{nj_n} is the maximum power allowed for antenna j_n of user n.

We use μ_{nj} to denote the duty cycle of each transmitting antenna, i.e., μ_{nj} is the percentage of time at which the j^{th} antenna of the n^{th} user is on. We use $\boldsymbol{\mu}$ to denote the vector of all μ_{nj}s.

Throughout the chapter, we will use the following substitutions to simplify the nota-

tions:

$$a_{jm} \triangleq S_{1jm}A_{1j}, \tag{4.5}$$

$$b_{jm} \triangleq S_{2jm}A_{2j}, \tag{4.6}$$

$$\phi(x) \triangleq x\log(x), \tag{4.7}$$

$$\zeta(x,y) \triangleq \phi(x+y) - \phi(y). \tag{4.8}$$

The goal of this chapter is to characterize the sum-rate capacity of this Poisson MIMO MAC.

4.2 SIMO-MAC Analysis

To simplify the presentation of main ideas, in this section, we focus on the case with $M = 2$ and $J_1 = J_2 = 1$. That is each transmitter has only one antenna while the receiver has 2 antennas. The solution of this special case is a building block to the solution to the general case where the transmitters also have multiple antennas. This general case will be considered in Section 4.3. As $J_1 = J_2 = 1$, to lighten the notation, we omit the j_n subscript in the remainder of this section.

4.2.1 Optimality Conditions

As discussed before, it has been shown in [52] that the continuous-input discrete-output Poisson MAC channel can be converted to a binary-input binary-output MAC channel. In particular, the input waveform can be limited to a two level waveform i.e. 0 or A_n for the n^{th} user. Let μ_n be the duty cycle of each transmitting user. Therefore, the sum-rate

capacity of of such a channel is given by

$$C_{sum} = \max_{0 \leq \mu_1, \mu_2 \leq 1} I_{X_1, X_2; Y}. \tag{4.9}$$

where

$$I_{X_1, X_2; Y} = \sum_{m=1}^{M} I_{X_1, X_2; Y_m} \tag{4.10}$$

with

$$\begin{aligned} I_{X_1, X_2; Y_m} &= (1-\mu_1)(1-\mu_2)\phi(\lambda_m) + \mu_1(1-\mu_2)\phi(a_m + \lambda_m) \\ &\quad + \mu_2(1-\mu_1)\phi(b_m + \lambda_m) + \mu_1\mu_2\phi(a_m + b_m + \lambda_m) \\ &\quad - \phi(a_m\mu_1 + b_m\mu_2 + \lambda_m). \end{aligned} \tag{4.11}$$

The problem to calculate the sum-rate capacity can be rewritten as

$$\begin{aligned} \textbf{P0-Multi:} \quad & \max I_{X_1, X_2; Y}, \\ \text{s.t} \quad & 0 \leq \mu_1 \leq 1, \\ & 0 \leq \mu_2 \leq 1. \end{aligned} \tag{4.12}$$

The problem **(P0-Multi)** has been solved for the special case of $M = 1$ (i.e., when the receiver has only one antenna) in Chapter 3. The main idea in [62] is to convert a set of nonlinear equations that appear in the analysis into a set of linear equations and a convex function, which then can be solved. However, when $M > 1$ (i.e., when the receiver has multiple antennas) as considered in this chapter, this technique will not work anymore.

It can be easily shown that (4.10) is not a convex function. Accordingly, **(P0-Multi)** is a non-convex optimization problem. Therefore, KKT conditions, being necessary but

sufficient conditions for non-convex optimization problem, can only be used to identify candidates for the optimal solution. In the following, we use I to denote $I_{X_1,X_2;Y}$.

The Lagrangian equation from (**P0-Multi**) is

$$\mathcal{L} = -I + \eta_1(\mu_1 - 1) - \eta_2\mu_1 + \eta_3(\mu_2 - 1) - \eta_4\mu_2,$$

where $\eta_i, i = 1, \cdots, 4$ are Lagrangian multipliers.

These KKT conditions are

$$\begin{aligned}
\frac{\partial I}{\partial \mu_1}\Big|_{(\hat{\mu}_1,\hat{\mu}_2)} - \eta_1 + \eta_2 &= 0,\\
\frac{\partial I}{\partial \mu_2}\Big|_{(\hat{\mu}_1,\hat{\mu}_2)} - \eta_3 + \eta_4 &= 0,\\
\eta_1(\hat{\mu}_1 - 1) &= 0,\\
\eta_2\hat{\mu}_1 &= 0,\\
\eta_3(\hat{\mu}_2 - 1) &= 0,\\
\eta_4\hat{\mu}_2 &= 0,
\end{aligned}$$

where

$$\begin{aligned}
\frac{\partial I}{\partial \mu_1} &= \sum_{m=1}^{2}\Big(-(1-\mu_2)\phi(\lambda_m) + (1-\mu_2)\phi(a_m+\lambda_m) - \mu_2\phi(b_m+\lambda_m)\\
&\quad +\mu_2\phi(a_m+b_m+\lambda_m) - a_m(\log(a_m\mu_1 + b_m\mu_2 + \lambda_m) + 1)\Big), \qquad (4.13)
\end{aligned}$$

and

$$\begin{aligned}
\frac{\partial I}{\partial \mu_2} &= \sum_{m=1}^{2}\Big(-(1-\mu_1)\phi(\lambda_m) - \mu_1\phi(a_m+\lambda_m) + (1-\mu_1)\phi(b_m+\lambda_m)\\
&\quad +\mu_1\phi(a_m+b_m+\lambda_m) - b_m(\log(a_m\mu_1 + b_m\mu_2 + \lambda_m) + 1)\Big). \qquad (4.14)
\end{aligned}$$

To find the solution for this non-convex optimization problem, the KKT conditions can be solved while considering different combinations of constraints being active at a given time. This leaves us with 16 possible cases, each corresponding to whether $\eta_i, i = 1, \cdots, 4$ being zero or not. Out of these 16 cases, in Appendix D.1, we show that 13 cases are not valid candidates for the optimal solution. For example when $\eta_1 = 0, \eta_2 = 0, \eta_3 \neq 0, \eta_4 = 0$, we have

$$\begin{aligned} \frac{\partial I}{\partial \mu_1} &= 0, \\ \frac{\partial I}{\partial \mu_2} - \eta_3 &= 0, \\ \eta_3 \neq 0 \Rightarrow \mu_2 &= 1. \end{aligned}$$

Then the optimal solution must satisfy $\frac{\partial I}{\partial \mu_1}\Big|_{(\mu_1,1)} = 0$. In this case having $\mu_2 = 1$ means that user 2 is transmitting constantly and just imposing interference for the user 1. Hence, $I(\mu_1, 0) \geq I(\mu_1, 1)$. Therefore we may conclude that this case does not result in a candidate for the optimal solution. Detailed analysis on how to exclude these 13 cases is listed in Appendix D.1.

The feasible candidates for the optimal solution are listed below.

Case-1: $\eta_1 = 0, \eta_2 \neq 0, \eta_3 = 0, \eta_4 = 0 \Rightarrow$

$$\begin{aligned} \frac{\partial I}{\partial \mu_1} + \eta_2 &= 0, \\ \frac{\partial I}{\partial \mu_2} &= 0, \\ \eta_2 \neq 0 \Rightarrow \mu_1 &= 0. \end{aligned}$$

The candidate for the optimal solution is $(0, \mu_2)$, where μ_2 satisfies $\frac{\partial I}{\partial \mu_2}\Big|_{(0,\mu_2)} = 0 \Rightarrow$

$$\sum_{m=1}^{2} \Big(b_m \log(b_m \mu_2 + \lambda_m) \Big) = \sum_{m=1}^{2} \Big(-\phi(\lambda_m) + \phi(b_m + \lambda_m) - b_m \Big). \tag{4.15}$$

This case corresponds to the scenario when only user 2 is active and user 1 is inactive. (4.15) shows that the optimal value of μ_2 that satisfies the KKT conditions will be the intersection between the right side function of the equation and left side of the equation. It is easy to check that the left side of (4.15) is a monotonically increasing function of μ_2, while the right side of (4.15) is a constant. Therefore there can be at most one value of μ_2 that satisfies this equation. We use $\tilde{\mu}_2$ to denote the solution to (4.15). If such solution does not exist or if the solutions lies out of $[0, 1]$, we simply set $\tilde{\mu}_2 = 0$. Hence, a candidate obtained from this case is $(0, \tilde{\mu}_2)$.

Case-2: $\eta_1 = 0, \eta_2 = 0, \eta_3 = 0, \eta_4 \neq 0 \Rightarrow$

$$\begin{aligned} \frac{\partial I}{\partial \mu_1} &= 0, \\ \frac{\partial I}{\partial \mu_2} + \eta_4 &= 0, \\ \eta_4 \neq 0 \Rightarrow \mu_2 &= 0. \end{aligned}$$

Therefore the optimal pair must satisfy $\frac{\partial I}{\partial \mu_1}\Big|_{(\mu_1,0)} = 0$. We have

$$\sum_{m=1}^{2} \Big(a_m \log(a_m \mu_1 + \lambda_m) \Big) = \sum_{m=1}^{2} \Big(-\phi(\lambda_m) + \phi(a_m + \lambda_m) - a_m \Big). \tag{4.16}$$

This case corresponds to the scenario when only user 1 is active and user 2 is inactive. It is clear that, similar to Case-1, μ_1 is the intersection point of a monotonically increasing function and a constant. Therefore there could only be at most one such value of μ_1 that

satisfy this equation. Let $(\bar{\mu}_1, 0)$ be the obtained solution, with $\bar{\mu}_1$ setting to zero if such solution does not exist or the solution lies outside of $[0, 1]$.

Case-3: $\eta_1 = 0, \eta_2 = 0, \eta_3 = 0, \eta_4 = 0 \Rightarrow$

$$\frac{\partial I}{\partial \mu_1} = 0, \tag{4.17}$$

$$\frac{\partial I}{\partial \mu_2} = 0. \tag{4.18}$$

This case corresponds to the scenario when both users are active. The pair (μ_1, μ_2) must satisfy (4.17) and (4.18) simultaneously.

From (4.13) and (4.14), we know that (4.17) and (4.18) are a pair of nonlinear equations. The solution can be obtained efficiently by numerical methods. Under certain conditions, we can make further analysis and draw definite conclusions. These analysis will be presented below.

After obtaining solutions from these three cases, we can then compare the rate obtained from them and set the solution to the one that results in the largest rate.

4.2.2 Special Cases

In this subsection, we further analyze (4.17) and (4.18) and analytically show that there are finite number of solutions for some interesting scenarios.

Asymptotic Analysis

In this subsection we show that when the transmission power of one user is sufficiently higher than the other, then there is no solution to (4.17) and (4.18), and hence single user transmission is optimal.

Lemma 16. *For any $\mu_1 \in (0, 1)$ and $\mu_2 \in (0, 1)$, if $a_m \to \infty$ for any $m \in \{1, 2\}$, then $\frac{\partial I}{\partial \mu_2} \to -\infty$.*

Proof.

$$\begin{aligned}
\lim_{a_m\to\infty}\frac{\partial I}{\partial \mu_2} &= \lim_{a_m\to\infty}\sum_{m=1}^{2}\Big(-(1-\mu_1)\phi(\lambda_m)-\mu_1\phi(a_m+\lambda_m)\\
&\quad +(1-\mu_1)\phi(b_m+\lambda_m)+\mu_1\phi(a_m+b_m+\lambda_m)\\
&\quad -b_m(\log(a_m\mu_1+b_m\mu_2+\lambda_m)+1)\Big)\\
&= \lim_{a_m\to\infty}\sum_{m=1}^{2}(1-\mu_1)\Big(\phi(b_m+\lambda_m)+\phi(\lambda_m)\Big)\\
&\quad +\lim_{a_m\to\infty}\sum_{m=1}^{2}\Big(\mu_1(a_m+\lambda_m)\log\left(\frac{b_m}{a_m+\lambda_m}+1\right)+\mu_1 b_m\log(a_m+b_m+\lambda_m)\\
&\quad -b_m\log(a_m\mu_1+b_m\mu_2+\lambda_m)+1\Big)
\end{aligned}$$

$$\begin{aligned}
&\overset{(a)}{\leq} c+\lim_{a_m\to\infty}\sum_{m=1}^{2}\left(\mu_1 b_m+b_m\mu_1\log(a_m)+\mu_1 b_m\log\left(\frac{b_m+\lambda_m}{a_m}+1\right)\right.\\
&\left.-b_m\log(a_{1m}\mu_1)-b_m\log\left(\frac{b_m+\lambda_m}{a_m}+1\right)-b_m\right)\\
&= c+\lim_{a_m\to\infty}\sum_{m=1}^{2}\Big(\mu_1 b_m-b_m+b_m\mu_1\log(a_m)-b_m\log(a_m\mu_1)\Big)\\
&= c+\lim_{a_m\to\infty}\sum_{m=1}^{2}\Big(-b_m(1-\mu_1)+b_m(\mu_1\log(a_m)-\log(\mu_1)-\log(a_m))\Big)\\
&= c+\lim_{a_m\to\infty}\sum_{m=1}^{2}\Big(-b_m(1-\mu_1)-b_m(1-\mu_1)\log(a_m)-b_m\log(\mu_1)\Big)\\
&= -\infty.
\end{aligned}$$

where (a) follows from $\log$ inequalities and c is a positive constant. □

From Lemma 16, we may conclude that when $a_m \to \infty$ for any $m \in \{1, 2\}$, there is no solution for Case-3. Similarly, when $b_m \to \infty$ for any $m \in \{1, 2\}$, Case-3 does not lead to any solution. Hence in these scenarios, single user transmission is optimal.

Symmetric Channel

Here we show that for the symmetric channel where $a_m = b_m, \forall m \in [1, M]$, there are at most 2 solutions to (4.17) and (4.18).

Lemma 17. *If the channel is symmetric,* (4.17) *and* (4.18) *have at most two solutions. Furthermore, in these solutions,* $\mu_1 = \mu_2$.

Proof. Let $S_m A \triangleq a_m = b_m = S_m A$, $\frac{\partial I}{\partial \mu_1} = 0$ becomes

$$\begin{aligned}
&\sum_{m=1}^{2} \Big(-(1-\mu_2)\phi(\lambda_m) + (1-\mu_2)\phi(S_m A + \lambda_m) \\
&-\mu_2 \phi(S_m A + \lambda_m) + \mu_2 \phi(2S_m A + \lambda_m) \\
&-S_m A(\log(S_m A(\mu_1 + \mu_2) + \lambda_m) + 1)\Big) = 0.
\end{aligned}$$

This implies

$$\begin{aligned}
&\sum_{m=1}^{2} \Big(S_m A \log(S_m A(\mu_1 + \mu_2) + \lambda_m) + S_m A \Big) = \\
&\sum_{m=1}^{2} \Big(-(1-\mu_2)\phi(\lambda_m) + (1-\mu_2)\phi(S_m A + \lambda_m) \\
&-\mu_2 \phi(S_m A + \lambda_m) + \mu_2 \phi(2S_m A + \lambda_m)\Big). \qquad (4.19)
\end{aligned}$$

After plugging the value of $\sum_{m=1}^{2} \Big(S_m A \log(S_m A(\mu_1 + \mu_2) + \lambda_m) + S_m A \Big)$ from (4.19)

into $\frac{\partial I}{\partial \mu_2} = 0$ and rearranging terms, we obtain

$$\begin{aligned}
&\sum_{m=1}^{2} \Big(-(1-\mu_1)\phi(\lambda_m) - \mu_1\phi(S_mA+\lambda_m) \\
&+(1-\mu_1)\phi(S_mA+\lambda_m) + \mu_1\phi(2S_mA+\lambda_m)\Big) \\
&= \sum_{m=1}^{2} \Big(-(1-\mu_2)\phi(\lambda_m) + (1-\mu_2)\phi(S_mA+\lambda_m) \\
&-\mu_2\phi(S_mA+\lambda_m) + \mu_2\phi(2S_mA+\lambda_m)\Big). \qquad (4.20)
\end{aligned}$$

(4.20) implies that $\mu_1 = \mu_2$, as the left side and right side of (4.20) are the same linear functions of μ_1 and μ_2 respectively.

We can now replace the value of $\mu_1 = \mu_2 = \mu$ in (4.19) and obtain:

$$\begin{aligned}
&\sum_{m=1}^{2} \Big[\phi(\lambda_m) - 2\phi(S_mA+\lambda_m) + \phi(2S_mA+\lambda_m) \\
&-S_mA\log(2S_mA\mu+\lambda_m) - S_mA \Big] = 0. \qquad (4.21)
\end{aligned}$$

It is easy to verify that the left side of (4.21) is a strictly convex function of μ, while the right side is a constant. Therefore, there can be at most two values of $\mu \in (0,1)$ that satisfies the above equation. □

4.3 MIMO-MAC Analysis

In this section, using the results obtained in the SIMO-MAC case discussed in Section 4.2, we study the general case of MIMO-MAC where all transmitters and receiver are equipped with multiple antennas.

Similar to SIMO-MAC, the continuous-time continuous-input discrete-output Poisson MIMO-MAC can be converted to discrete-time binary-input binary-output MAC. In

particular, the input waveform of each antenna can be limited to be piecewise constant waveforms with two levels 0 or A_{nj} for the j^{th} antenna of the n^{th} transmitter. Depending on the on-off states of each antenna of user n, there are 2^{J_n} states at user n. In the following, we use $i_n \in [1, \cdots, 2^{J_n}]$ to index each of these 2^{J_n} states at user n. We will use $P_n(i_n)$ to denote the probability that user n lies in state i_n and $\mathbf{p}_n \triangleq [P_n(1), \cdots, P_n(2^{J_n})]$ to denote the vector of probabilities of states at user n. We will use the binary variable $b_{nj}(i_n)$ to indicate whether the j^{th} antenna of the n^{th} user is on or off at state i_n, i.e., $b_{nj}(i_n) = 1$ if the j^{th} antenna of the n^{th} user is on for state i_n and is 0 otherwise. The sum-rate achievable using $(\mathbf{p}_1, \mathbf{p}_2)$ is given by

$$I_{\mathbf{X}_N;Y}(\mathbf{p}_1, \mathbf{p}_2) = \sum_{i_1=1}^{2^{J_1}} \sum_{i_2=1}^{2^{J_2}} \left[P_1(i_1) P_2(i_2) \sum_{m=1}^{M} \left[\zeta \left(\sum_{n=1}^{2} \sum_{j=1}^{J_n} S_{njm} A_{nj} b_{nj}(i_n), \lambda_m \right) \right] \right] - \sum_{m=1}^{M} \left[\zeta \left(\sum_{n=1}^{2} \sum_{j=1}^{J_n} S_{njm} A_{nj} \mu_{nj}, \lambda_m \right) \right]. \tag{4.22}$$

It is easy to see that

$$\mu_{nj} = \sum_{i_n=1}^{2^{J_n}} P_n(i_n) b_{nj}(i_n). \tag{4.23}$$

To characterize the sum-rate capacity, we need to solve the following optimization problem:

$$\textbf{(P1-Multi):} \quad C_{sum}^{MIMO-MAC} = \max_{\mathbf{p}_1, \mathbf{p}_2} I_{\mathbf{X}_N;Y}(\mathbf{p}_1, \mathbf{p}_2), \tag{4.24}$$

$$\text{s.t} \quad 0 \leq P_n(i_n) \leq 1, \tag{4.25}$$

$$i_n = 1, \cdots, 2^{J_n}, n = 1, 2, \tag{4.26}$$

$$\sum_{i_n=1}^{2^{J_n}} P_n(i_n) = 1, n = 1, 2. \tag{4.27}$$

Problem (**P1-Multi**) is a complex non-convex optimization problem with a large number of variables. In particular, the number of variables $2^{J_1} + 2^{J_2}$ increases exponentially with the number of antennas. The main result of this section is the following theorem.

Theorem 18. *Solving problem (**P1-Multi**) is equivalent to solving the following problem*

$$\textbf{(P2-Multi)}: \quad C_{sum}^{MIMO-MAC} = \max_{0\leq\mu_1,\mu_2\leq 1} I(\mu_1,\mu_2), \tag{4.28}$$

with

$$\begin{aligned} I(\mu_1,\mu_2) = \sum_{m=1}^{M} \Big[& (1-\mu_1)(1-\mu_2)\varphi(\lambda_m) \\ & +\mu_1(1-\mu_2)\varphi(a_m+\lambda_m) + (1-\mu_1)\mu_2\varphi(b_m+\lambda_m) \\ & +\mu_1\mu_2\varphi(a_m+b_m+\lambda) - \varphi(a_m\mu_1+b_m\mu_2+\lambda_m)\Big], \end{aligned} \tag{4.29}$$

where

$$a_m \triangleq \sum_{j_1}^{J_1} S_{1j_1m}A_{1j_1}, \tag{4.30}$$

$$b_m \triangleq \sum_{j_2}^{J_2} S_{2j_2m}A_{2j_2}. \tag{4.31}$$

Note that the right hand side of problem **(P2-Multi)** has the same form as **(P0-Multi)** solved in the SIMO-MAC case discussed in Section 4.2. This theorem means that the sum-rate capacity of MIMO-MAC is the same as the sum-rate capacity of a properly constructed SIMO-MAC. The enabling element of our result is that in MIMO-MAC, we show that to achieve the sum-rate capacity, all antennas of the same transmitter must be simultaneously on or off. This enables us to view these antennas of the same transmitter as one antenna with properly modified parameters.

Using this theorem and results from the SIMO case, we know that are three different

cases for the optimal inputs to achieve the sum-rate capacity of the Poisson MIMO-MAC. The three optimal solution corresponds to 1) the scenario where only user 2 is active with both antennas being simultaneously on or off; 2) the scenario where only user 1 is active with both antennas being simultaneously on or off; and 3) the scenario where both users are active with both antennas at user 1 being simultaneously on or off and both antennas at user 2 being simultaneously on or off.

4.3.1 Proof of Theorem 18

The proof of Theorem 18 follows the same two-step structure as our recent work [60], and relies on propositions 19 and 20 presented below. The proof of proposition 19 is similar to the proof of Proposition 7 in [60]. The proof of proposition 20, however, is significantly different as the proof method used in [60] does not work once we have multiple antennas at the receiver.

For the presentation convenience, we focus on the case $M = 2$ in this section. The proof for the cases with $M > 2$ is the same.

In Step-1, we prove the following proposition that simplifies the optimization problem from $(\mathbf{p}_1, \mathbf{p}_2)$ to $\boldsymbol{\mu}$.

Proposition 19. *At the optimality, for each user, if the antenna with a smaller duty cycle is on then all antennas with a larger duty cycle must also be on.*

Proof. The proof of this proposition is similar to the proof of Proposition 7 in [60] with proper modification. We prove Proposition 19 by characterizing the optimal value of $(\mathbf{p}_1, \mathbf{p}_2)$ for any given $\boldsymbol{\mu}$. Hence, in this subsection, $\boldsymbol{\mu}$ is fixed. More specifically, we show that, at the optimality in the MIMO-MAC, if the antenna with the smaller duty cycle is on, then the other antenna should also be on.

From (4.22), it is clear that to optimize over $(\mathbf{p}_1, \mathbf{p}_2)$ for a given $\boldsymbol{\mu}$, we only need to

focus on

$$\begin{aligned}\mathcal{H} &\triangleq \sum_{i_1=1}^{2^{J_1}}\sum_{i_2=1}^{2^{J_2}} P_1(i_1)P_2(i_2)\sum_{m=1}^{2}\zeta\left(\sum_{n=1}^{2}\sum_{j=1}^{J_n} S_{njm}A_{nj}b_{nj}(i_n),\lambda_m\right)\\ &= \sum_{i_1=1}^{2^{J_1}} P_1(i_1)\mathcal{H}_1(i_1),\end{aligned} \tag{4.32}$$

where

$$\mathcal{H}_1(i_1) = \sum_{i_2=1}^{2^{J_2}} P_2(i_2)\sum_{m=1}^{2} d(i_1,i_2), \tag{4.33}$$

and

$$d(i_1,i_2) = \zeta\left(\sum_{j=1}^{J_1} S_{1jm}A_{1j}b_{1j}(i_1) + \sum_{j=1}^{J_2} S_{2jm}A_{2j}b_{2j}(i_2),\lambda_m\right). \tag{4.34}$$

We focus on finding the optimal values of $\mathbf{p}_2$ first. To facilitate the understanding, we list the labeling of states of user 2 and the corresponding values of b_{2j}s in Table 4.1.

	b_{21}	b_{22}
$(i_1,1)$	0	0
$(i_1,2)$	0	1
$(i_1,3)$	1	0
$(i_1,4)$	1	1

Table 4.1: The states of user 2 and the corresponding values of b_{2j}s.

Using the definition of ζ function, we can easily check that

$$\begin{aligned}&d(i_1,1) < \min\{d(i_1,2),d(i_1,3)\} \leq\\ &\max\{d(i_1,2),d(i_1,3)\} < d(i_1,4),\end{aligned}$$

which is simultaneously true for any value of i_1. As $\mathcal{H}_1(i_1)$ is simply a linear combination

of $d(i_1, i_2)$s, hence, for any given $\boldsymbol{\mu}$, maximizing $\mathcal{H}_1(i_1)$ is a linear programming problem, for which we have the following (assuming $\mu_{21} \geq \mu_{22}$, the other case being similar):

1. As $d(i_1, 4)$ is the largest, $P_2(4)$ should be as large as possible. Therefore, we assign $P_2(4) = \mu_{22}$.

2. As μ_{22} has been all used, we should set $P_2(2) = 0$.

3. As $d(i_1, 3) > d(i_1, 1)$, we assign the remaining part of μ_{21} to state $(i_1, 3)$ and hence $P_2(3) = \mu_{21} - \mu_{22}$.

4. For the last state related to the term $d(i_1, 1)$, allot the remaining probability. Hence $P_2(1) = 1 - \mu_{21}$.

This assignment implies that if the antenna with a smaller duty cycle is on, the antenna with a larger duty cycle should also be on. Note that the above arguments are true for all i_1s, and hence this assignment maximizes $\mathcal{H}_1(i_1)$ for all i_1 simultaneously. Furthermore, this assignment is independent of $\mathbf{p}_1$.

Notice that the above discussion for $J_2 = 2$, can be extended for $J_2 > 2$.

Similarly, by writing

$$\mathcal{H} \;=\; \sum_{i_2=1}^{2^{J_2}} P_2(i_2) \sum_{i_1=1}^{2^{J_1}} P_1(i_1) \sum_{m=1}^{2} \zeta \left(\sum_{j=1}^{J_1} S_{1jm} A_{1j} b_{1j}(i_1) + \sum_{j=1}^{J_2} S_{2jm} A_{2j} b_{2j}(i_2), \lambda_m \right),$$

then following the same procedure as above, we can calculate the optimal values of $\mathbf{p}_1$.

As the result, we know that (4.22) can be simplified to a function $\boldsymbol{\mu}$ depending on the relationships between the values of μ_{nj}s. For example, in the case of two transmitter antennas, we have four symmetric cases, i.e. $(\mu_{11} \geq \mu_{12}, \mu_{21} \geq \mu_{22}), (\mu_{11} \leq \mu_{12}, \mu_{21} \geq \mu_{22}), (\mu_{11} \geq \mu_{12}, \mu_{21} \leq \mu_{22})$ and $(\mu_{11} \leq \mu_{12}, \mu_{21} \leq \mu_{22})$. For the case of $(\mu_{11} \geq$

$\mu_{12}, \mu_{21} \geq \mu_{22}$), $I_{\mathbf{X}_N;Y}$ can be simplified to

$$
\begin{aligned}
I(\mu_{11}-\mu_{12}, \mu_{12}, \mu_{21}-\mu_{22}, \mu_{22}) \;=\; & \\
& \sum_{m=1}^{2} \Bigg[(1-\mu_{11})((1-\mu_{21})\varphi(\lambda_m) + (\mu_{21}-\mu_{22})\varphi(b_{1m}+\lambda_m) \\
& + \mu_{22}\varphi(b_{1m}+b_{2m}+\lambda_m)) + (\mu_{11}-\mu_{12})((1-\mu_{21})\varphi(a_{1m}+\lambda_m) \\
& + (\mu_{21}-\mu_{22})\varphi(a_{1m}+b_{1m}+\lambda_m) + \mu_{22}\varphi(a_{1m}+b_{1m}+b_{2m}+\lambda_m)) \\
& + \mu_{12}((1-\mu_{21})\varphi(a_{1m}+a_{2m}+\lambda_m) + (\mu_{21}-\mu_{22})\varphi(a_{1m}+a_{2m}+b_{1m}+\lambda_m) \\
& + \mu_{22}\varphi(a_{1m}+a_{2m}+b_{1m}+b_{2m}+\lambda_m)) - \varphi\left(\sum_{n=1}^{2}\sum_{j=1}^{J_n} S_{njm}A_{nj}\mu_{nj} + \lambda_m\right) \Bigg].
\end{aligned}
\tag{4.35}
$$

As the result, the objective function is simplified to characterizing

$$
\begin{aligned}
C_{sum}^{MIMO-MAC} = \max\big(& C_{\mu_{11}\geq\mu_{12},\mu_{21}\geq\mu_{22}}, C_{\mu_{11}\leq\mu_{12},\mu_{21}\geq\mu_{22}}, \\
& C_{\mu_{11}\geq\mu_{12},\mu_{21}\leq\mu_{22}}, C_{\mu_{11}\leq\mu_{12},\mu_{21}\leq\mu_{22}}\big),
\end{aligned}
\tag{4.36}
$$

in which

$$
\textbf{(P3-Multi):} C_{\mu_{11}\geq\mu_{12},\mu_{21}\geq\mu_{22}} = \max I(\mu_{11}-\mu_{12}, \mu_{12}, \mu_{21}-\mu_{22}, \mu_{22}), \tag{4.37}
$$

$$
\text{s.t.} \quad 0 \leq \mu_{12} \leq \mu_{11} \leq 1, \tag{4.38}
$$

$$
0 \leq \mu_{22} \leq \mu_{21} \leq 1. \tag{4.39}
$$

Other terms in (4.36) are defined in a similar manner. Due to symmetry, in the following, we only provide details on how to solve (**P3-Multi**). □

In Step-2, we show the following proposition that characterizes the optimal value of $\boldsymbol{\mu}$.

Proposition 20. *At the optimality, for each user, all antennas must have the same duty cycle and they must be on or off simultaneously.*

Proof. For the ease of calculation, we define $q_1 = \mu_{11} - \mu_{12}$, $q_2 = \mu_{12}$, $q_3 = \mu_{21} - \mu_{22}$ and $q_4 = \mu_{22}$ and let $\mathbf{q} = [q_1, q_2, q_3, q_4]$. Then (4.35) can be re-written as

$$\begin{aligned} I(\mathbf{q}) \;=\; & \sum_{m=1}^{2} \Big[(1-(q_1+q_2))((1-(q_3+q_4))\varphi(\lambda_m) + q_3\varphi(b_{1m}+\lambda_m) \\ & + q_4\varphi(b_{1m}+b_{2m}+\lambda_m)) + q_1((1-(q_3+q_4))\varphi(a_{1m}+\lambda_m) + q_3\varphi(b_{1m}+a_{1m}+\lambda_m) \\ & + q_4\varphi(b_{1m}+b_{2m}+a_{1m}+\lambda_m)) + q_2((1-(q_3+q_4))\varphi(a_{1m}+a_{2m}+\lambda_m) \\ & + q_3\varphi(b_{1m}+a_{1m}+a_{2m}+\lambda_m) + q_4\varphi(b_{1m}+b_{2m}+a_{1m}+a_{2m}+\lambda_m)) \\ & - \varphi(a_{1m}q_1 + (a_{1m}+a_{2m})q_2 + b_{1m}q_3 + (b_{1m}+b_{2m})q_4 + \lambda_m) \Big]. \end{aligned} \tag{4.40}$$

Correspondingly, (**P3-Multi**) is equivalent to

$$\textbf{(P4-Multi):} \quad C_{\mu_{11}\geq\mu_{12},\mu_{21}\geq\mu_{22}} \;=\; \max I(\mathbf{q}) \tag{4.41}$$

$$\text{s.t.} \quad q_k \geq 0,\ k = 1, \cdots, 4, \tag{4.42}$$

$$q_1 + q_2 \leq 1, \tag{4.43}$$

$$q_3 + q_4 \leq 1. \tag{4.44}$$

Now in order to find the optimal solution for (**P4-Multi**), we show that any sum-rate achievable when both of the antennas at both of the users 1 and 2 are active with different duty cycles (called scheme A), can be achieved by setting the duty cycles of antennas of the same user to be the same (called scheme B) in a properly constructed weaker channel. This implies that, for the original channel, we can restrict to the case where the antennas of the same user are simultaneously on or off for optimality.

For scheme A, let q_1 and q_2 be the duty cycles of each of the antennas at user 1 and q_3

and q_4 be the duty cycle of each antenna at user 2 respectively.

$$
\begin{aligned}
I_A(\mathbf{q}) \;=\; & \sum_{m=1}^{2}\Big[(1-(q_1+q_2))((1-(q_3+q_4))\varphi(\lambda_m)+q_3\varphi(b_{1m}+\lambda_m) \\
& +q_4\varphi(b_{1m}+b_{2m}+\lambda_m))+q_1((1-(q_3+q_4))\varphi(a_{1m}+\lambda_m)+q_3\varphi(b_{1m}+a_{1m}+\lambda_m) \\
& +q_4\varphi(b_{1m}+b_{2m}+a_{1m}+\lambda_m))+q_2((1-(q_3+q_4))\varphi(a_{1m}+a_{2m}+\lambda_m) \\
& +q_3\varphi(b_{1m}+a_{1m}+a_{2m}+\lambda_m)+q_4\varphi(b_{1m}+b_{2m}+a_{1m}+a_{2m}+\lambda_m)) \\
& -\varphi(a_{1m}q_1+(a_{1m}+a_{2m})q_2+b_{1m}q_3+(b_{1m}+b_{2m})q_4+\lambda_m)\Big].
\end{aligned}
\tag{4.45}
$$

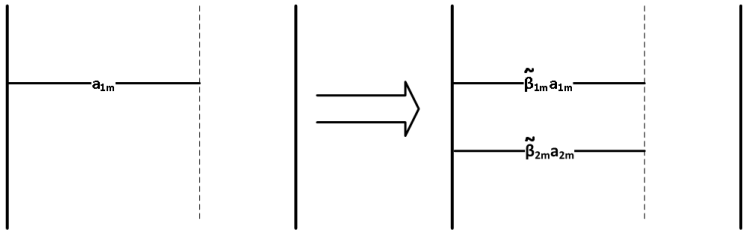

Figure 4.2: Transformation from Scheme A to Scheme B.

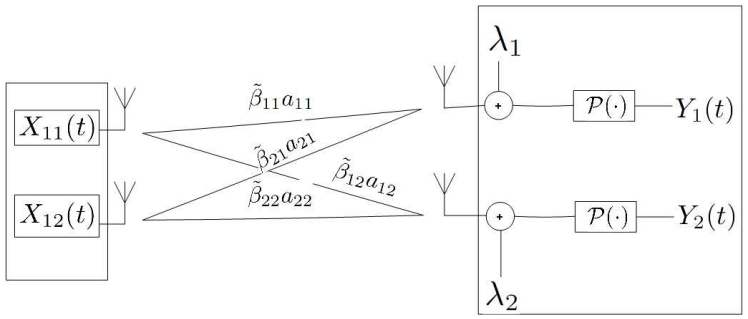

Figure 4.3: Scheme B elaborated.

Now we show that $I_A(\mathbf{q})$ can be achieved in a weakened channel but with both antennas to be simultaneously on or off. In particular, in the weakened channel, we restrict the channel gains for the stage of Scheme A when only the stronger antenna is active. For user 1, as shown in Fig. 4.3, we reduce each a_{jm} to $\tilde{\beta}_{jm}a_{jm}$ by reducing S_{1jm} to $\tilde{\beta}_{jm}S_{1jm}$

with $0 \leq \tilde{\beta}_{jm} \leq 1$. We choose the values of $\tilde{\beta}_{jm}$ such that

$$a_{11} = \tilde{\beta}_{11}a_{11} + \tilde{\beta}_{21}a_{21}, \tag{4.46}$$

$$a_{12} = \tilde{\beta}_{12}a_{12} + \tilde{\beta}_{22}a_{22}. \tag{4.47}$$

It is easy to check that we can always find $\tilde{\beta}_{jm}$s in $[0, 1]$ that satisfy (4.46) and (4.47).

Same can be done for user 2 by choosing $b_{1m} = \bar{\beta}_{1m}b_{1m} + \bar{\beta}_{2m}b_{2m}$ by restricting the channel gain at each of the channels for user 2. We know that this scheme is also feasible for $0 \leq \bar{\beta}_{1m}, \bar{\beta}_{2m} \leq 1$. Therefore, the sum-rate capacity for scheme B is:

$$\begin{aligned}
I_B(\mathbf{q}) \;=\; & \sum_{m=1}^{2} \Big[(1-(q_1+q_2))((1-(q_3+q_4))\varphi(\lambda_m) + q_3\varphi(\bar{\beta}_{1m}b_{1m} + \bar{\beta}_{2m}b_{2m} + \lambda_m) \\
& + q_4\varphi(b_{1m} + b_{2m} + \lambda_m)) + q_1((1-(q_3+q_4))\varphi(\tilde{\beta}_{1m}a_{1m} + \tilde{\beta}_{2m}a_{2m} + \lambda_m) \\
& + q_3\varphi(\bar{\beta}_{1m}b_{1m} + \bar{\beta}_{2m}b_{2m} + \tilde{\beta}_{1m}a_{1m} + \tilde{\beta}_{2m}a_{2m} + \lambda_m) \\
& + q_4\varphi(b_{1m} + b_{2m} + \tilde{\beta}_{1m}a_{1m} + \tilde{\beta}_{2m}a_{2m} + \lambda_m)) \\
& + q_2((1-(q_3+q_4))\varphi(a_{1m} + a_{2m} + \lambda_m) + q_3\varphi(\bar{\beta}_{1m}b_{1m} + \bar{\beta}_{2m}b_{2m} + a_{1m} + a_{2m} + \lambda_m) \\
& + q_4\varphi(b_{1m} + b_{2m} + a_{1m} + a_{2m} + \lambda_m)) \\
& - \varphi(a_{1m}q_1 + (a_{1m} + a_{2m})q_2 + b_{1m}q_3 + (b_{1m} + b_{2m})q_4 + \lambda_m) \Big].
\end{aligned} \tag{4.48}$$

Clearly, we have $I_A = I_B$. Therefore, we can conclude that any sum-rate achievable by both of the antennas at each user be active, at different duty cycles, can also be achieved by letting both antennas of each user to be simultaneously on or off. Note that scheme A represents a channel model with strong channel gains and scheme B represents a channel model with weak channel gains. Hence, we conclude that in order to achieve the sum-rate capacity, the duty cycles of antennas of the same user should be simultaneously on or

off. □

4.4 Extension to General Poisson MIMO-MAC

One of the natural extension of the case discussed above is to consider a MAC channel with more than two transmitting users. With the above discussion, it is clear that the sum-rate capacity for N users can be calculated by following the similar steps for 2 users. Let's take an example of a Poisson MAC channel with 3 transmitting users, then the candidates for optimal solution to achieve sum-rate capacity will be:

1. Only user 1 is active.
2. Only user 2 is active.
3. Only user 3 is active.
4. User 1 and user 2 both are active, while user 3 is inactive.
5. User 1 and user 3 are active, while user 2 is inactive.
6. User 3 and user 2 are active, while user 1 is inactive.
7. All three of the users are active.

Therefore, we can conclude that for N users, there are $\sum_{i=1}^{N} C_i^N$ possible candidates for the optimal solution, where $C_i^N = \frac{N!}{i!(N-i!)}$. As N increases, the number of possibilities for optimal solution increases exponentially. Although the approach used to analyze the 2 users case can be used in this scenario, but the complexity would by much higher.

4.5 Numerical Results

In this section, we present numerical examples to illustrate the results for Poisson MIMO-MAC channel.

In the first example, we set $a_1 = a_2 = 5, b_1 = b_2 = 5, \lambda = 0.25$. The sum-rate achieved by three different cases are

Case - 1: $\tilde{\mu}_1 = 0, \tilde{\mu}_2 = 0.25 \rightarrow I(\tilde{\mu}_1, \tilde{\mu_2}) = 2.616$.

Case - 2: $\bar{\mu}_1 = 0.25, \bar{\mu}_2 = 0 \rightarrow I(\bar{\mu}_1, \bar{\mu}_2) = 2.616$.

Case - 3: $\mu_1 = 0.2987, \mu_2 = 0.2987 \rightarrow I(\mu_1, \mu_2) = 3.6057$.

Therefore, for this channel, Case-3 where both users are active achieves the sum-rate capacity.

For the next example, we set $a_1 = a_2 = 4, b_1 = b_2 = 10, \lambda = 0.25$. The sum-rate achieved by three different cases are

Case - 1: $\tilde{\mu}_1 = 0, \tilde{\mu}_2 = 0.3888 \rightarrow I(\tilde{\mu}_1, \tilde{\mu_2}) = 6.3720$.

Case - 2: $\bar{\mu}_1 = 0.4041, \bar{\mu}_2 = 0 \rightarrow I(\bar{\mu}_1, \bar{\mu}_2) = 2.276$.

Case - 3: Does not result in a solution, therefore $I_(\mu_1, \mu_2) = 0$.

Therefore, for this channel, Case-1 where only user 2 is active achieves the sum-rate capacity. This confirms our conclusion that if the power of one user is relatively high, it is optimal for only this user to be active to achieve the sum-rate capacity.

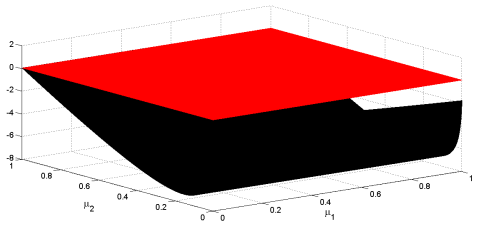

Figure 4.4: $\frac{\partial I}{\partial \mu_2}$ and the zero plane.

Fig. 4.4 illustrates Lemma 16. In this figure, the red surface is the zero plane, and

the black surface is $\frac{\partial I}{\partial \mu_2}$ for different values of μ_1 and μ_2. In generating this figure, we set $a_1 = a_2 = 450$, $b_1 = b_2 = 1$ and $\lambda_1 = \lambda_2 = 0.25$. From the figure, we can see that, for this set of parameters, $\frac{\partial I}{\partial \mu_2}$ has no intersection with the zero plane (except on the boundary). This confirms our conclusion that, if the power of one user is relatively high, Case-3 does not yield a solution.

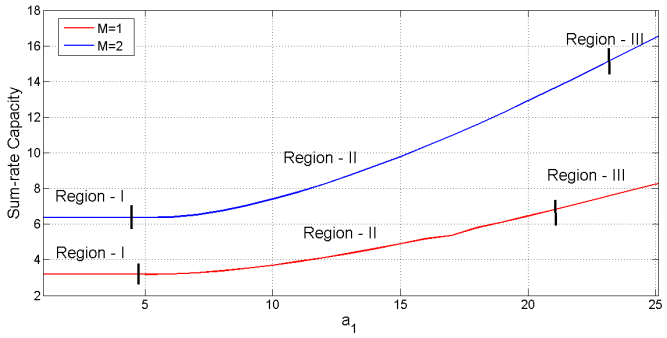

Figure 4.5: Sum-rate capacity with respect to transmission power at user 1 when $M = 1$ and $M = 2$. Region I corresponds to the case when only user 2 is transmitting, Region II is when both of the users are transmitting and Region III is when only user 1 is transmitting.

Fig. 4.5 illustrates how the sum-rate capacities for channels with different number of receiving antennas increases as the transmission power increases. In generating Fig. 4.5, we set $b_1 = b_2 = 10$ and $\lambda_1 = \lambda_2 = 0.25$, while increasing the value of $a_1 = a_2$. The sum-rate capacity increases as the available transmission power at user 1 increases but this slope is larger when the receiver has multiple receiving antennas. In the figure, we also mark three regions corresponding to different input scenarios that achieve the-rate capacity. In Region-I, when the value of a_1 is small, it is optimal to allow only user-2 to be active. When $a_1 = 4.7$ for $M = 1$ and $a_1 = 4.5$ for $M = 2$, both curves transit into Region-II where both users must be active to achieve the sum-rate capacity and when the value of a_1 is high enough ($a_1 = 21.1$ for $M = 1$ and $a_1 = 23$ for $M = 2$), the curves are in Region-III where it is optimal for only user-1 to be active.

Chapter 5

Summary and Future Work

5.1 Summary

For this research, motivated by the applications of visible light communication, we have analyzed Poisson channels under a variety of setups.

In Chapter 2, we have studied Poisson fading channels with varying noise levels for a scenario when a single user communicates with a single receiver. We have considered cases with and without strict delay constraints. For the case without a strict delay constraint, we have characterized the optimal power allocation scheme that achieves the ergodic capacity. For the case with a strict delay constraint, we have characterized the optimal power allocation strategy that minimizes the outage probability. We have also provided numerical results to illustrate the analytical results obtained in this research.

In Chapter 3, by solving non-convex optimization problems, we have characterized the sum-rate capacity for both non-symmetric Poisson SISO-MAC and non-symmetric Poisson MISO-MAC. We have shown that under certain channel conditions, it is optimal for both users to be active and we have also established conditions under which it is optimal for only one user to be active.

In Chapter 4, we have extended our analysis to the sum-rate capacity of the Poisson MIMO-MAC. We have shown that the sum-rate capacity of a Poisson MIMO MAC can be characterized by studying a carefully constructed Poisson SIMO MAC. We have also shown that there are three possible operating scenarios for achieving the sum-rate capacity of the Poisson SIMO MAC. We have shown that similar to SISO-MAC and MISO-MAC, it is optimal for a single user to transmit under certain channel parameters and under certain parameters, it is optimal for both of the users to transmit.

5.2 Future Work

In this section, we discuss a few interesting open directions along the lines of the results presented in this study and potential challenges associated with these problems.

After characterizing the sum-rate capacity in Chapter 3 and Chapter 4, a natural next step is to characterize all boundary points on the capacity region. Towards this goal,in the case of a single receiving antenna, we can follow the same approach developed in this chapter to solve the following optimization problem to obtain any boundary rate pair (R_1, R_2) for a given $0 \leq \gamma \leq 1/2$

$$\max \qquad \gamma R_1 + (1-\gamma) R_2. \tag{5.1}$$

Here,

$$R_1 = I_{X_1;Y}, \quad R_2 = I_{X_2;Y|X_1}, \tag{5.2}$$

whose expression can be written out as functions of duty cycles of each antenna. Let $\mathcal{E}_1$ be the set of obtained rate pairs (R_1, R_2) by solving (5.1) with γ varying in $[0, 1/2]$. Similarly, we can obtain the set $\mathcal{E}_2$ by setting $R_1 = I_{X_1;Y|X_2}$ and $R_2 = I_{X_2;Y}$.

Let $\mathcal{E} = \mathcal{E}_1 \bigcup \mathcal{E}_2$. [52] shows that $\mathcal{E}$ is a description of the boundary points of the capacity region, if the set $\mathcal{R} \triangleq \{(R_1, R_2) : \exists (R_1^*, R_2^*) \in \mathcal{E}$ such that $0 \leq R_1 \leq R_1^*, 0 \leq R_2 \leq R_2^*\}$ is a convex set. However, although one can verify the convexity of $\mathcal{R}$ numerically, it turns out to be difficult to analytically verify such convexity even for the symmetric case considered in [52] and further for the non-symmetric case. Such an open problem is interesting and the solution to it requires more refined understanding of the structure of the set $\mathcal{R}$.

Another natural extension for the analysis conducted in Chapter 3 and Chapter 4 is to characterize the sum-rate capacity in the presence of the maximum power constraint as well as the average power constraint. The SISO-MAC Poisson problem, in the presence of both average power constraint and maximum power constraint, can then be written as:

$$\begin{aligned} C_{sum}^{SISO-MAC} = \max \quad & I_{X_1,X_2;Y}(\mu_1, \mu_2), \\ \text{s.t.} \quad & 0 \leq \mu_1 \leq 1, \\ & 0 \leq \mu_2 \leq 1, \\ & \mu_1 A_1 \leq \sigma_1, \\ & \mu_2 A_2 \leq \sigma_2, \end{aligned} \tag{5.3}$$

where $I_{X_1,X_2;Y}$ is defined in (3.9), σ_1 and σ_2 are the average power constraints at each user 1 and 2 correspondingly. To solve the above problem, we can follow the similar steps as that of Chapter 3 and Chapter 4, but the number of KKT cases to analyze would be much larger and hence the solution would be much more complex. Therefore, there is a need to find an alternative approach to solve this problem.

Appendix A

Proofs for Chapter 2

A.1 Proof of Lemma 1

The proof of Lemma 1 is divided into two parts.

Proof. We first show that $\mu_0 \leq 1$, which is equivalent to

$$\begin{aligned} &\frac{\left(1+\frac{\lambda(t)}{SA}\right)^{\left(1+\frac{\lambda(t)}{SA}\right)}}{\left(\frac{\lambda(t)}{SA}\right)^{\left(\frac{\lambda(t)}{SA}\right)}}e^{-1} \leq 1+\frac{\lambda(t)}{SA} \\ &\iff \\ \log&\left(\frac{\left(1+\frac{\lambda(t)}{SA}\right)^{\left(1+\frac{\lambda(t)}{SA}\right)}}{\left(\frac{\lambda(t)}{SA}\right)^{\left(\frac{\lambda(t)}{SA}\right)}}e^{-1}\right) \leq \log\left(1+\frac{\lambda(t)}{SA}\right) \\ &\iff \end{aligned} \tag{A.1}$$

$$\left(1+\frac{\lambda(t)}{SA}\right)\log\left(1+\frac{\lambda(t)}{SA}\right)-1-\frac{\lambda(t)}{SA}\log\left(\frac{\lambda(t)}{SA}\right)$$
$$\leq \log\left(1+\frac{\lambda(t)}{SA}\right),$$
$$\iff$$
$$\frac{\lambda(t)}{SA}\log\left(1+\frac{\lambda(t)}{SA}\right)-\frac{\lambda(t)}{SA}\log\left(\frac{\lambda(t)}{SA}\right)\leq 1,$$
$$\iff$$
$$\log\left(\frac{1+\frac{\lambda(t)}{SA}}{\frac{\lambda(t)}{SA}}\right)^{\frac{\lambda(t)}{SA}}\leq 1,$$
$$\iff$$
$$\left(\frac{1+\frac{\lambda(t)}{SA}}{\frac{\lambda(t)}{SA}}\right)^{\frac{\lambda(t)}{SA}}\leq e^1,$$

Which is true, as $lim_{x\to+\infty}\left(1+\frac{1}{x}\right)^x = e$ and $\left(1+\frac{1}{x}\right)^x$ is an increasing function of x. Hence μ_0 will always be less or equal to 1.

Now we show $\mu_0 \geq 0$, which is equivalent to

$$\begin{aligned}
\frac{\left(1+\frac{\lambda(t)}{SA}\right)^{\left(1+\frac{\lambda(t)}{SA}\right)}}{\left(\frac{\lambda(t)}{SA}\right)^{\left(\frac{\lambda(t)}{SA}\right)}}e^{-1} - \frac{\lambda(t)}{SA} &\geq 0, \\
&\Longleftrightarrow \\
\frac{\left(1+\frac{\lambda(t)}{SA}\right)^{\left(1+\frac{\lambda(t)}{SA}\right)}}{\left(\frac{\lambda(t)}{SA}\right)^{\left(\frac{\lambda(t)}{SA}\right)}} &\geq e\frac{\lambda(t)}{SA}, \\
&\Longleftrightarrow \\
\log\left(\frac{\left(1+\frac{\lambda(t)}{SA}\right)^{\left(1+\frac{\lambda(t)}{SA}\right)}}{\left(\frac{\lambda(t)}{SA}\right)^{\left(\frac{\lambda(t)}{SA}\right)}}\right) &\geq \log\left(e\frac{\lambda(t)}{SA}\right), \\
&\Longleftrightarrow \\
\left(1+\frac{\lambda}{SA}\right)\log\left(1+\frac{\lambda}{SA}\right) - \frac{\lambda}{SA}\log\left(\frac{\lambda}{SA}\right) &\geq \log\left(\frac{\lambda}{SA}\right)+1, \\
&\Longleftrightarrow \\
\left(1+\frac{\lambda}{SA}\right)\log\left(1+\frac{\lambda}{SA}\right) - \left(1+\frac{\lambda}{SA}\right)\log\left(\frac{\lambda}{SA}\right) &\geq 1, \\
&\Longleftrightarrow \\
\left(1+\frac{\lambda}{SA}\right)\log\left(\frac{1+\frac{\lambda}{SA}}{\frac{\lambda}{SA}}\right) &\geq 1,
\end{aligned}$$

which is true, as $\log(1+x) \geq \frac{x}{1+x}$for $x > 0$. □

A.2 Proof of Theorem 3

The proof of theorem 3 is given below.

Proof. The proof of Theorem 3 consists of the following steps.

Step 1: First we show that there exists an optimal solution that has the particular form specified in (2.27).

Lemma 21. *For any arbitrary μ with outage probability P_{out} and $\mathbb{E}[\mu] \leq \sigma$, we can*

construct another power allocation function $\mu^{'}$ *with the form:*

$$\mu^{'} = \begin{cases} \mu^{*} & \textit{with probability } w, \\ 0 & \textit{with probability } (1-w). \end{cases}$$

such that $\mathbb{E}[\mu^{'}] \leq \sigma$ *and* $P_{out}^{'} \leq P_{out}$.

Proof. Let μ to be an arbitrary power allocation function that satisfies $\mathbb{E}[\mu] \leq \sigma$. For this power allocation scheme, we have a region such that:

$$A(\mu, \lambda(t)) = \{\mu \in \mathbb{R} : I(\mu, \lambda(t)) \geq r_0\}. \tag{A.2}$$

Hence the outage probability is obtained as:

$$P_{out} = 1 - \Pr\{\mu \in A(\mu, \lambda(t))\}. \tag{A.3}$$

Let χ_A be the indicator function of $\{\mu \in A(\mu, \lambda(t))\}$, then we can define a weight function as:

$$w = \mathbb{E}[\chi_A | \lambda]. \tag{A.4}$$

Now, we construct a new power allocation function:

$$\mu^{'} = \begin{cases} \mu^{*} & \text{with probability } w, \\ 0 & \text{with probability } (1-w). \end{cases} \tag{A.5}$$

The outage power for such a function is

$$P_{out}^{'} = 1 - \mathbb{E}[w]. \tag{A.6}$$

The outage probability of this new power allocation function is

$$\begin{aligned} P_{out}^{'} &= 1 - \mathbb{E}[w] \\ &= 1 - \mathbb{E}[\mathbb{E}[\chi_A|\lambda]] \\ &= 1 - \mathbb{E}[\chi_A] \\ &= 1 - \Pr\{\mu \in A(\mu, \lambda(t))\} \\ &= P_{out}. \end{aligned} \tag{A.7}$$

Moreover, $\mu^{'}$ satisfies the long-term power constraint:

$$\begin{aligned} \sigma &\geq \mathbb{E}[\mu] \\ &\geq \mathbb{E}[\chi_A \mu] \\ &\overset{(a)}{\geq} \mathbb{E}[\chi_A \mu^*] \\ &= \mathbb{E}[\mathbb{E}[\chi_A \mu^* | \lambda(t)]] \\ &= \mathbb{E}[\mu^* \mathbb{E}[\chi_A | \lambda(t)]] \\ &= \mathbb{E}[\mu^* w] \\ &= \mathbb{E}[\mu^{'}], \end{aligned}$$

in which (a) is true because of (2.26). □

As the result, we can restrict ourselves to those power allocation functions that can be written in the form of (A.5).

Step 2: Among all power allocation functions that have the form of (A.5), we characterize the optimal power allocation function by characterizing the optimal choice of w. From the discussion above, we know that the optimal choice of w is the solution to the

following optimization problem:

$$\begin{cases} \text{maximize} & \mathbb{E}[w] \\ \text{subject to} & \mathbb{E}[w\mu] = \sigma \\ \text{and} & 0 \leq w \leq 1 \quad \text{with probability 1} \end{cases} \tag{A.8}$$

We need to show $\hat{w}$ specified in (2.28) is the solution to this problem.

First we note that $\hat{w}$ satisfies the constraint with equality as

$$\begin{aligned} \mathbb{E}[\mu^* \hat{w}(\mu)] &= \sum(p^*) + w^* p^* \text{Pr}\{\mu = p^*\} \\ &= \sum(p^*) + \frac{\sigma - \sum(p^*)}{\overline{\sum}(p^*) - \sum(p^*)} p^* \text{Pr}\{\mu = p^*\} \\ &= \sigma. \end{aligned} \tag{A.9}$$

The objective function $\mathbb{E}[\hat{w}(\mu)]$ is

$$\mathbb{E}[\hat{w}(\mu)] = \sum(p^*) + w^* \text{Pr}\{\mu = p^*\}. \tag{A.10}$$

In the following, we show the optimality of $\hat{w}(\mu)$ by showing that for any other $0 \leq w(\mu) \leq 1$, such that $\mathbb{E}[w(\mu)]$ is larger than $\mathbb{E}[\hat{w}(\mu)]$ specified in (A.10), the power constraint will be voliated. In particular, we have:

$$\begin{aligned} \mathbb{E}[\mu w(\mu)] - \sigma &= \mathbb{E}[\mu w(\mu)] - \mathbb{E}[\mu \hat{w}(\mu)], \\ &\geq p^* \{\mathbb{E}[w(\mu)] - \mathbb{E}[\hat{w}(\mu)]\}. \end{aligned}$$

Hence if, $\mathbb{E}[w(\mu)] > \mathbb{E}[\hat{w}(\mu)]$, then we get $\mathbb{E}[\mu w(\mu)] > \sigma$, which means that it violates the average power constraint. □

Appendix B

Details of Equal Power Allocation Scheme

To carry out the comparison with the adaptive power control discussed in Chapter 2 and an equal power allocation scheme, we first derive the optimal duty cycle value for the equal power allocation scheme, as we were unable to find any existing literature that discusses this issue. To maximize the ergodic case for the two transmit antennas and one receive antenna, the optimal (fixed over time) duty cycle for the equal power allocation scheme is the solution of the following problem:

$$\begin{aligned} \max_{\mu_1,\mu_2} \quad & \mathbb{E}_\lambda[I(\mu_1,\mu_2;\lambda(t))] \\ \text{s.t} \quad & 0 \leq \mu_1 \leq 1 \\ & 0 \leq \mu_2 \leq 1 \end{aligned} \tag{B.1}$$

As in the numerical results presented in the manuscript we have assumed the $\lambda(t) \sim \mathcal{U}[1,2]$, so to be consistent, we assume the same distribution for solving (B.1) (the same analysis can be carried for other distributions).

There are two possible outcomes for this problem: either $\mu_1 \geq \mu_2$ or $\mu_2 \geq \mu_1$. As the case $\mu_1 \geq \mu_2$ is similar to $\mu_2 \geq \mu_1$, we present only one of them here. For $\mu_1 \geq \mu_2$, if we take $\mu_1 - \mu_2 = x_1$ and $\mu_2 = x_2$, then:

$$
\begin{aligned}
\mathbb{E}_\lambda[I] = \\
& x_1 \left[\frac{S_1^2 A_1^2 + 4S_1A_1 + 4}{2} \log(S_1A_1 + 2) - \frac{S_1^2 A_1^2 + 2S_1A_1 + 1}{2} \log(S_1A_1 + 1) - \frac{1}{2} S_1A_1 - 2 \right] \\
& + x_2 \left[\frac{(S_1A_1 + S_2A_2)^2 + 4(S_1A_1 + S_2A_2) + 4}{2} \log((S_1A_1 + S_2A_2) + 2) \right. \\
& \left. - \frac{(S_1A_1 + S_2A_2)^2 + 2(S_1A_1 + S_2A_2) + 1}{2} \log((S_1A_1 + S_2A_2) + 1) - \frac{1}{2}(S_1A_1 + S_2A_2) - 2 \right] \\
& - \left[\frac{((x_1 + x_2)S_1A_1 + x_2S_2A_2)^2 + 4((x_1 + x_2)S_1A_1 + x_2S_2A_2) + 4}{2} \log((x_1 + x_2)S_1A_1 + x_2S_2A_2 + 2) \right. \\
& - \frac{((x_1 + x_2)S_1A_1 + x_2S_2A_2)^2 + 2((x_1 + x_2)S_1A_1 + x_2S_2A_2) + 1}{2} \log((x_1 + x_2)S_1A_1 + x_2S_2A_2 + 1) \\
& \left. - \frac{1}{2}((x_1 + x_2)S_1A_1 + x_2S_2A_2) - 2 \right]
\end{aligned}
\tag{B.2}
$$

At optimality (After solving KKT conditions), we find that $\mu_1^* = \mu_2^* = x_2$ and they must satisfy the following equation:

$$
\begin{aligned}
& \left[\frac{(S_1A_1 + S_2A_2)^2 + 4(S_1A_1 + S_2A_2) + 4}{2} \log((S_1A_1 + S_2A_2) + 2) \right. \\
& \left. - \frac{(S_1A_1 + S_2A_2)^2 + 2(S_1A_1 + S_2A_2) + 1}{2} \log((S_1A_1 + S_2A_2) + 1) - \frac{1}{2}(S_1A_1 + S_2A_2) - 2 \right] \\
& - \frac{2x_2(S_1A_2 + S_2A_2)^2 + 4(S_1A_1 + S_2A_2)}{2} \log(x_2(S_1A_1 + S_2A_2) + 2) \\
& + \frac{2x_2(S_1A_2 + S_2A_2)^2 + 2(S_1A_1 + S_2A_2)}{2} \log(x_2(S_1A_1 + S_2A_2) + 1) = 0,
\end{aligned}
$$

which can be solved numerically.

In the numerical analysis we have compared proposed power allocation scheme with the above mentioned power allocation scheme.

Appendix C

Proofs for Chapter 3

C.1 Concavity of $I_{X_1,X_2;Y}(\mu_1, \mu_2)$

In this Appendix, we show that $I_{X_1,X_2;Y}(\mu_1, \mu_2)$ is not necessarily concave for general values of S_1A_1, S_2A_2 and λ. For $I_{X_1,X_2;Y}(\mu_1, \mu_2)$ to be concave, $\bigtriangledown^2 I$ needs to be negative semi-definite. For $\bigtriangledown^2 I$ to be negative semi-definite, there are two conditions to be satisfied [63]. The first condition is that its first order principle minor must be non-positive. As $\frac{\partial^2 I}{\partial \mu_1^2} = -\frac{S_1^2 A_1^2}{S_1A_1\mu_1+S_2A_2\mu_2+\lambda} < 0$, this condition holds. The second condition is that the determinant of the Hessian matrix must be non-negative. It is easy to check that

$$
\begin{aligned}
|\bigtriangledown^2 I| &= (\varphi(\lambda) - \varphi(S_1A_1 + \lambda) - \varphi(S_2A_2 + \lambda) + \varphi(S_1A_1 + S_2A_2 + \lambda)) \\
&\left(\frac{2S_1A_1S_2A_2}{S_1A_1\mu_1 + S_2A_2\mu_2 + \lambda} - (\varphi(\lambda) - \varphi(S_1A_1 + \lambda) - \varphi(S_2A_2 + \lambda) + \varphi(S_1A_1 + S_2A_2 + \lambda))\right).
\end{aligned}
$$

The two terms on the right hand side can be dealt separately. First, we show the following.

Lemma 22. $\varphi(\lambda) - \varphi(S_1A_1 + \lambda) - \varphi(S_2A_2 + \lambda) + \varphi(S_1A_1 + S_2A_2 + \lambda) > 0$.

Proof. Using the definition of φ, it is easy to see that φ' is a strictly increasing function. Let $a = \lambda, b = S_1A_1 + \lambda, c = S_2A_2 + \lambda$ and $d = S_1A_1 + S_2A_2 + \lambda$. then using the mean

value theorem, we have:

$$\begin{aligned} \exists x_1 \in (a,b) \quad \text{s.t. } \varphi^{'}(x_1) &= \frac{\varphi(b)-\varphi(a)}{b-a}, \\ \exists x_2 \in (c,d) \quad \text{s.t. } \varphi^{'}(x_2) &= \frac{\varphi(d)-\varphi(c)}{d-c}. \end{aligned}$$

Without loss of generality we can assume that $S_1A_1 < S_2A_2$, then we will have $a < b < c < d$. As $\varphi^{'}$ is an increasing function and $x_1 < x_2$, we have $\varphi^{'}(x_1) < \varphi^{'}(x_2)$ and $b-a = d-c$, then:

$$\begin{aligned} \frac{\varphi(b)-\varphi(a)}{b-a} &< \frac{\varphi(d)-\varphi(c)}{d-c} \\ \varphi(b)-\varphi(a) &< \varphi(d)-\varphi(c). \end{aligned} \tag{C.1}$$

Hence $\varphi(d)+\varphi(a) > \varphi(b)+\varphi(c)$. □

As the first term is always greater than 0, for the function to be concave, the second term, $\frac{2S_1A_1S_2A_2}{S_1A_1\mu_1+S_2A_2\mu_2+\lambda} - (\varphi(\lambda) - \varphi(S_1A_1+\lambda) - \varphi(S_2A_2+\lambda) + \varphi(S_1A_1+S_2A_2+\lambda))$, must also be non-negative. This, however, is not true. For example, taking $\mu_1 = 0.9, \mu_2 = 0.7$ and setting $S_1A_1 = 50, S_2A_2 = 100$ and $\lambda = 0.5$, the second term results in the value of -6.2943. Hence, we can conclude that $I_{X_1,X_2;Y}(\mu_1,\mu_2)$ is not always concave.

C.2 Proof of Lemma 9

In this section we present the asymptotic analysis of (3.16) and (3.19). As the case $S_1A_1 \to \infty$ is similar to analysis for $S_2A_2 \to \infty$ due to symmetry, we restrict our analysis to $S_2A_2 \to \infty$ in this section. We will show that as $S_2A_2 \to \infty$, $f(\mu_1)$ and $g(\mu_1)$ do not intersect. Denoting S_2A_2 as x, we calculate $\lim_{x\to\infty} g(0)$, $\lim_{x\to\infty} g(1)$ and $\lim_{x\to\infty} f(0)$ as

$\lim_{x\to\infty} f(0) = \lim_{x\to\infty} f(1)$.

$$\begin{aligned}
\lim_{x\to\infty} g(0) &= \lim_{x\to\infty} \left(\frac{1}{x} \exp\left(\frac{1}{x} \left(-\varphi(\lambda) + \varphi(x+\lambda) - x \right) \right) + \frac{\lambda}{x} \right) \\
&= \lim_{x\to\infty} \left(\frac{1}{xe} \exp\left(\log(\lambda)^{\frac{-\lambda}{x}} + \log(x+\lambda)^{\frac{x+\lambda}{x}} \right) \right) \\
&= \lim_{x\to\infty} \left(\frac{1}{xe} \lambda^{\frac{-\lambda}{x}} (x+\lambda)^{\left(\frac{x+\lambda}{x}\right)} \right) \\
&= \lim_{x\to\infty} \left(\frac{1}{e} \lambda^{\frac{-\lambda}{x}} \frac{1}{x} \frac{x^{\frac{\lambda}{x}}}{x^{\frac{\lambda}{x}}} (x+\lambda)^{\left(\frac{x+\lambda}{x}\right)} \right) \\
&= \lim_{x\to\infty} \left(\frac{1}{e} \lambda^{\frac{-\lambda}{x}} x^{\frac{\lambda}{x}} \left(1 + \frac{\lambda}{x} \right)^{\left(1+\frac{\lambda}{x}\right)} \right).
\end{aligned}$$

As $\lim_{x\to\infty} \lambda^{\frac{-\lambda}{x}} = 1$, and

$$\lim_{x\to\infty} x^{\frac{\lambda}{x}} = \lim_{x\to\infty} e^{\log\left(x^{\frac{\lambda}{x}}\right)} = \lim_{x\to\infty} e^{\frac{\lambda}{x}\log(x)} = 1,$$

and

$$\lim_{x\to\infty} \left(1 + \frac{\lambda}{x} \right)^{\left(1+\frac{\lambda}{x}\right)} = 1.$$

Hence, we obtain $\lim_{x\to\infty} g(0) = \frac{1}{e}$.

Similarly

$$\begin{aligned}
\lim_{x\to\infty} g(1) &= \lim_{x\to\infty}\left(\frac{1}{x}\exp\left(\frac{1}{x}\left(-\varphi(S_1A_1+\lambda)+\varphi(S_1A_1+x+\lambda)-x\right)\right)+\frac{S_1A_1+\lambda}{x}\right)\\
&= \lim_{x\to\infty}\left(\frac{1}{xe}\exp\left(\log(S_1A_1+\lambda)^{\frac{-(S_1A_1+\lambda)}{x}}+\log(S_1A_1+x+\lambda)^{\frac{S_1A_1+x+\lambda}{x}}\right)\right)\\
&= \lim_{x\to\infty}\left(\frac{1}{xe}(S_1A_1+\lambda)^{\frac{-(S_1A_1+\lambda)}{x}}(S_1A_1+x+\lambda)^{(\frac{S_1A_1+x+\lambda}{x})}\right)\\
&= \lim_{x\to\infty}\left(\frac{1}{e}(S_1A_1+\lambda)^{\frac{-(S_1A_1+\lambda)}{x}}\frac{1}{x}\frac{x^{\frac{(S_1A_1+\lambda)}{x}}}{x^{\frac{(S_1A_1+\lambda)}{x}}}(S_1A_1+x+\lambda)^{(\frac{S_1A_1+x+\lambda}{x})}\right)\\
&= \lim_{x\to\infty}\left(\frac{1}{e}(S_1A_1+\lambda)^{\frac{-(S_1A_1+\lambda)}{x}}x^{\frac{(S_1A_1+\lambda)}{x}}\left(1+\frac{S_1A_1+\lambda}{x}\right)^{\left(1+\frac{S_1A_1+\lambda}{x}\right)}\right)\\
&= \frac{1}{e}.
\end{aligned}$$

Now for the $f(\mu_1)$, we notice that $\lim_{x\to\infty} f(0) = \lim_{x\to\infty} f(1)$. Hence we calculate $\lim_{x\to\infty} f(0)$.

$$\begin{aligned}
&\lim_{x\to\infty} f(0)\\
&= \lim_{x\to\infty}\frac{\zeta(S_1A_1,\lambda)+\frac{S_1A_1}{x}\zeta(x,\lambda)}{\zeta(x,S_1A_1+\lambda)-\zeta(x,\lambda)}\\
&\overset{(a)}{=} \lim_{x\to\infty}\frac{\frac{-S_1A_1}{x^2}\lambda\log\left(1+\frac{x}{\lambda}\right)+\frac{S_1A_1}{x+\lambda}+\frac{S_1A_1\lambda}{x(x+\lambda)}}{\log(1+\frac{S_1A_1}{x+\lambda})}\\
&\overset{(b)}{=} \lim_{x\to\infty}\frac{-S_1A_1\lambda\log\left(1+\frac{x}{\lambda}\right)+2S_1A_1x}{2x(x+\lambda)\log\left(1+\frac{S_1A_1}{x+\lambda}\right)+(x)^2\log\left(1+\frac{S_1A_1}{x+\lambda}\right)-\frac{x^2S_1A_1}{S_1A_1+x+\lambda}}\\
&= \lim_{x\to\infty}\frac{\frac{-S_1A_1\lambda}{2x}\log\left(1+\frac{x}{\lambda}\right)+S_1A_1}{(x+\lambda)\log\left(1+\frac{S_1A_1}{x+\lambda}\right)+\frac{x}{2}\log\left(1+\frac{S_1A_1}{x+\lambda}\right)-\frac{xS_1A_1}{2(S_1A_1+x+\lambda)}}\\
&= 1,
\end{aligned}$$

where (a) follows from the L'hospital rule and (b) follows from multiplying by $\frac{x^2(x+\lambda)}{x^2(x+\lambda)}$ and L'hospital rule.

C.3 Proof of Lemma- 11

In this section we will prove that when $S_1A_1 = S_2A_2$, we have $g(1) < 1$ and $g(0) > 0$.

Proof. Using $S_1A_1 = S_2A_2$, we will show that

$$g(1) - 1 < 0.$$

By plugging $\mu_1 = 1$ in (3.19), this is equivalent to show

$$\begin{aligned}
& \frac{1}{S_1A_1}\exp\left(\frac{1}{S_1A_1}\left(-\varphi(S_2A_2+\lambda)+\varphi(S_1A_1+S_2A_2+\lambda)-S_1A_1\right)\right)-2-\frac{\lambda}{S_1A_1}<0,\\
\Leftrightarrow \quad & \frac{1}{S_1A_1}\exp\left(-(1+\frac{\lambda}{S_1A_1})\log(S_1A_1+\lambda)+(2+\frac{\lambda}{S_1A_1})\log(2S_1A_1+\lambda)\right).e^{-1}<2+\frac{\lambda}{S_1A_1},
\end{aligned}$$

which is equivalent to show

$$\begin{aligned}
\exp\left(\log\left(\frac{(2S_1A_1+\lambda)^{\left(2+\frac{\lambda}{S_1A_1}\right)}}{(S_1A_1+\lambda)^{\left(1+\frac{\lambda}{S_1A_1}\right)}}\right)\right) &< (2S_1A_1+\lambda)e,\\
\Leftrightarrow \frac{(2S_1A_1+\lambda)^{\left(2+\frac{\lambda}{S_1A_1}\right)}}{(S_1A_1+\lambda)^{\left(1+\frac{\lambda}{S_1A_1}\right)}} &< (2S_1A_1+\lambda)e,\\
\Leftrightarrow \left(1+\frac{S_1A_1}{S_1A_1+\lambda}\right)^{\left(1+\frac{\lambda}{S_1A_1}\right)} &< e,\\
\Leftrightarrow \left(1+\frac{\lambda}{S_1A_1}\right)\log\left(1+\frac{S_1A_1}{S_1A_1+\lambda}\right) &< 1,
\end{aligned}$$

which is true as $\log(1+x) < x$. Following the similar steps, $g(0) > 0$ can also be proved. □

C.4 Proof of Proposition 15

The proof strategy is to analyze different cases corresponding to whether η_ks are zero or not. By exploiting the structure of the problem, we will show that, except for three cases, all other cases are not optimal. It will be clear in the sequel, while some cases are easy to handle, it needs significant amount of work to rule out certain cases.

Case-1: $\eta_1 \neq 0, \eta_2 \neq 0, \eta_3 \neq 0, \eta_4 \neq 0 \Rightarrow$

$$\eta_k \neq 0 \rightarrow q_k = 0.$$

This implies that none of the users are active. It is clear that $I(0,0,0,0)$ can not the optimal solution.

Case-2: $\eta_1 \neq 0, \eta_2 \neq 0, \eta_3 \neq 0, \eta_4 = 0 \Rightarrow$

$$\begin{aligned} \eta_1 \neq 0 \rightarrow q_1 &= 0, \\ \eta_2 \neq 0 \rightarrow q_2 &= 0, \\ \eta_3 \neq 0 \rightarrow q_3 &= 0, \\ \frac{\partial I}{\partial q_4} &= 0. \end{aligned}$$

These equations imply that user 1 is inactive while at user 2 both transmitting antennas are active with a same duty cycle. These equations lead to

$$\zeta(B_2, \lambda) - B_2(\log(B_2 q_4 + \lambda) + 1) = 0,$$

from which we solve q_4:

$$\tilde{q}_4' = \alpha(B_2/\lambda).$$

As $0 \leq \alpha(B_2/\lambda) \leq 1$, we obtain a feasible candidate $(0, 0, 0, \tilde{q}_4)$.

Case-3: $\eta_1 \neq 0, \eta_2 \neq 0, \eta_3 = 0, \eta_4 \neq 0 \Rightarrow$

$$\begin{aligned} \eta_1 \neq 0 \rightarrow q_1 &= 0, \\ \eta_2 \neq 0 \rightarrow q_2 &= 0, \\ \frac{\partial I}{\partial q_3} &= 0, \\ \eta_4 \neq 0 \rightarrow q_4 &= 0. \end{aligned}$$

These equations imply that user 1 is inactive and at user 2 only one antenna is active. As user 1 is inactive, the scenario is same as a single-user MISO Poisson channel. It is easy to check that, for a single-user MISO Poisson channel, the maximal rate achievable using only a single antenna is less than the maximal rate achievable when both antennas are active, which is Case-2 mentioned above. Hence, Case-3 cannot be the optimal solution.

Case-4: $\eta_1 \neq 0, \eta_2 \neq 0, \eta_3 = 0, \eta_4 = 0 \Rightarrow$

$$\begin{aligned} \eta_1 \neq 0 \rightarrow q_1 &= 0, \\ \eta_2 \neq 0 \rightarrow q_2 &= 0, \\ \frac{\partial I}{\partial q_3} &= 0, \\ \frac{\partial I}{\partial q_4} &= 0. \end{aligned}$$

This case refers to the scenario when user 1 is inactive and user 2 transmits with both antennas having different duty cycles. Plugging $q_1 = 0$ and $q_2 = 0$ into the last two

equations leads to the following two equations:

$$\begin{aligned} S_{21}A_{21}\log\frac{\left(1+\alpha\left(\frac{S_{21}A_{21}}{\lambda}\right)\left(\frac{S_{21}A_{21}}{\lambda}\right)\right)}{1+\frac{S_{21}A_{21}}{\lambda}q_3+\frac{B_2}{\lambda}q_4} &= 0, \\ B_2\log\frac{\left(1+\alpha\left(\frac{B_2}{\lambda}\right)\left(\frac{B_2}{\lambda}\right)\right)}{1+\frac{S_{21}A_{21}}{\lambda}q_3+\frac{B_2}{\lambda}q_4} &= 0, \end{aligned}$$

which requires:

$$\begin{aligned} \frac{S_{21}A_{21}}{\lambda}q_3+\frac{B_2}{\lambda}q_4 &= \alpha\left(\frac{S_{21}A_{21}}{\lambda}\right)\left(\frac{S_{21}A_{21}}{\lambda}\right), \\ \frac{S_{21}A_{21}}{\lambda}q_3+\frac{B_2}{\lambda}q_4 &= \alpha\left(\frac{B_2}{\lambda}\right)\left(\frac{B_2}{\lambda}\right). \end{aligned}$$

It is easy to check that $z(x) \triangleq \alpha(x)x$ is a monotonically increasing function. As the result, there does not exist (q_3, q_4) that satisfies these two equations simultaneously as $S_{21}A_{21} < B_2$. Hence, Case-4 is not possible.

Case-5: $\eta_1 \neq 0, \eta_2 = 0, \eta_3 \neq 0, \eta_4 \neq 0 \Rightarrow$

$$\begin{aligned} \eta_1 \neq 0 \rightarrow q_1 &= 0, \\ \frac{\partial I}{\partial q_2} &= 0, \\ \eta_3 \neq 0 \rightarrow q_3 &= 0, \\ \eta_4 \neq 0 \rightarrow q_4 &= 0. \end{aligned}$$

These imply that user 2 is inactive and at user 1 both antennas are active with a same duty cycle. From these equations, we obtain

$$\zeta(B_1, \lambda) - B_1(\log(B_1 q_2 + \lambda) + 1) = 0,$$

from which we solve q_2:

$$\tilde{q}_2 \;=\; \alpha(B_1/\lambda).$$

Hence, the obtained feasible candidate for optimal solution from this case is $(0, \tilde{q}_2, 0, 0)$.

Case-6: $\eta_1 \neq 0, \eta_2 = 0, \eta_3 \neq 0, \eta_4 = 0 \Rightarrow$

$$\begin{aligned} \eta_1 \neq 0 \rightarrow q_1 &= 0, \\ \frac{\partial I}{\partial q_2} &= 0, \qquad \text{(C.2)} \\ \eta_3 \neq 0 \rightarrow q_3 &= 0, \\ \frac{\partial I}{\partial q_4} &= 0. \qquad \text{(C.3)} \end{aligned}$$

This case corresponds to the scenario when all of the antennas are active and both antennas at user 1 have same duty cycle and both antennas at user 2 have same duty cycle.

By plugging $q_1 = 0$ and $q_3 = 0$ into (C.2) and (C.3), these two equations have the same form as (3.13) and (3.14) (with S_1A_1 replaced by B_1 and S_2A_2 replaced by B_2 respectively). Hence, (C.2)-(C.3) can be solved in the same manner as (3.13)-(3.14). In particular, these two nonlinear equations can be converted into a linear equation and a convex equation, therefore we know that there can be only two such values of q_2 and q_4 that satisfy the equations simultaneously. Lets those values be $(0, \bar{q}_2, 0, \bar{q}_4)$ and $(0, \bar{q}_2', 0, \bar{q}_4')$. If the solutions lies outside the range of $(0,1) \times (0,1) \times (0,1) \times (0,1)$, we replace it with $(0,0,0,0)$ for the sake of presentations convenience.

Case-7: $\eta_1 \neq 0, \eta_2 = 0, \eta_3 = 0, \eta_4 \neq 0 \Rightarrow$

$$\begin{aligned} \eta_1 \neq 0 \rightarrow q_1 &= 0, \\ \frac{\partial I}{\partial q_2} &= 0, \\ \frac{\partial I}{\partial q_3} &= 0, \\ \eta_4 \neq 0 \rightarrow q_2 &= 0. \end{aligned}$$

This case refers to the scenario when both of the antennas at user 1 are active with a same duty cycle but at user 2 only the antenna with the larger duty cycle is active. In Appendix C.5.1, we show that any sum-rate achieved in this case can also be achieved by the letting both antennas of each user to be simultaneously on or off, which is Case-6. Hence, Case-7 can be ruled out.

Case-8: $\eta_1 \neq 0, \eta_2 = 0, \eta_3 = 0, \eta_4 = 0 \Rightarrow$

$$\begin{aligned} \eta_1 \neq 0 \rightarrow q_1 &= 0, \\ \frac{\partial I}{\partial q_2} &= 0, \\ \frac{\partial I}{\partial q_3} &= 0, \\ \frac{\partial I}{\partial q_4} &= 0. \end{aligned}$$

This case corresponds to the scenario when both antennas at the user 2 are active and have different duty cycles but at user 1 both transmitting antennas have the same duty cycle.

Following a similar approach as how to obtain (3.15), we can combine $\frac{\partial I}{\partial q_3} = 0$ and $\frac{\partial I}{\partial q_4} = 0$ to obtain a linear equation in terms of q_1 and q_2. By plugging $q_1 = 0$ to the

obtained linear equation, we solve

$$q_2 \;=\; \frac{c_1}{c_1+c_2}, \tag{C.4}$$

where $c_1 = h_1(\lambda), c_2 = -h_1(B_1+\lambda)$ with

$$h_1(x) \;=\; \left(1+\frac{S_{22}A_{22}}{S_{21}A_{21}}\right)\zeta(S_{21}A_{21},x) - \zeta(B_2,x).$$

Now for q_2 to be feasible, we need $0 \le q_2 \le 1$, which requires c_1 and c_2 to have the same sign. To rule out this case, we need the following lemma.

Lemma 23. $h_1(x) < 0$ *for* $x > 0$.

Proof. Please see Appendix C.5.2. □

Using this lemma, we know $c_1 < 0$ and $c_2 > 0$, so $q_2 \notin [0,1]$. Hence this case not a valid choice.

Case-9: $\eta_1 = 0, \eta_2 \neq 0, \eta_3 \neq 0, \eta_4 \neq 0 \Rightarrow$

$$\begin{aligned}
\frac{\partial I}{\partial q_1} &= 0,\\
\eta_2 \neq 0 \rightarrow q_2 &= 0,\\
\eta_3 \neq 0 \rightarrow q_3 &= 0,\\
\eta_4 \neq 0 \rightarrow q_4 &= 0.
\end{aligned}$$

In this case user 2 is inactive and at user 1 only the antenna with a larger duty cycle is active. As user 2 is inactive, the scenario is same as the single-user MISO Poisson channel. It is easy to check that, for a single-user MISO Poisson channel, the maximal rate achievable using only a single antenna is less than the maximal rate achievable when both antennas are active, which is Case-5 mentioned above. Hence, Case-9 cannot be the

optimal solution.

Case-10: $\eta_1 = 0, \eta_2 \neq 0, \eta_3 \neq 0, \eta_4 = 0 \Rightarrow$

$$\begin{aligned} \frac{\partial I}{\partial q_1} &= 0, \\ \eta_2 \neq 0 \rightarrow q_2 &= 0 \\ \eta_3 \neq 0 \rightarrow q_3 &= 0 \\ \frac{\partial I}{\partial q_4} &= 0. \end{aligned}$$

This case refers to the scenario when both antennas at user 2 are active with a same duty cycle, while at user 1 only one antenna is active. This case can be ruled out using the same reason as Case-7.

Case-11: $\eta_1 = 0, \eta_2 \neq 0, \eta_3 = 0, \eta_4 \neq 0 \Rightarrow$

$$\begin{aligned} \frac{\partial I}{\partial q_1} &= 0, \\ \eta_2 \neq 0 \rightarrow q_2 &= 0, \\ \frac{\partial I}{\partial q_3} &= 0, \\ \eta_4 \neq 0 \rightarrow q_4 &= 0. \end{aligned}$$

In this case, only one antenna at both of the users are active. Following similar argument as that in Case-7, we know this case cannot be the optimal solution.

Case-12: $\eta_1 = 0, \eta_2 \neq 0, \eta_3 = 0, \eta_4 = 0 \Rightarrow$

$$\begin{aligned} \frac{\partial I}{\partial q_1} &= 0, \\ \eta_2 \neq 0 \rightarrow q_2 &= 0, \\ \frac{\partial I}{\partial q_3} &= 0, \\ \frac{\partial I}{\partial q_4} &= 0. \end{aligned}$$

This case occurs when both antennas at user 2 are active and have different duty cycles while at user 1 only one antenna is active. Following the same steps in Case-8, we obtain

$$q_1 = \frac{c_1}{c_1 + c_3},$$

in which $c_1 = h_1(\lambda)$ and $c_3 = -h_1(S_{11}A_{11} + \lambda)$. Using Lemma 23, we know that $q_1 \notin [0, 1]$, hence we may conclude that Case-12 is not a valid case.

Case-13: $\eta_1 = 0, \eta_2 = 0, \eta_3 \neq 0, \eta_4 \neq 0 \Rightarrow$

$$\begin{aligned} \frac{\partial I}{\partial q_1} &= 0, \\ \frac{\partial I}{\partial q_2} &= 0, \\ \eta_3 \neq 0 \rightarrow q_3 &= 0, \\ \eta_4 \neq 0 \rightarrow q_4 &= 0. \end{aligned}$$

In this case user 2 is inactive while at user 1 both antennas transmit with different duty cycles. By plugging $q_3 = 0$ and $q_4 = 0$ into $\frac{\partial I}{\partial q_1} = 0$ and $\frac{\partial I}{\partial q_2} = 0$, we have that (q_1, q_2)

must satisfy the following two equations simultaneously:

$$\begin{aligned} S_{11}A_{11}\log\frac{\left(1+\alpha\left(\frac{S_{11}A_{11}}{\lambda}\right)\left(\frac{S_{11}A_{11}}{\lambda}\right)\right)}{1+\frac{S_{11}A_{11}}{\lambda}q_1+\frac{B_1}{\lambda}q_2} &= 0, \\ B_1\log\frac{\left(1+\alpha\left(\frac{B_1}{\lambda}\right)\left(\frac{B_1}{\lambda}\right)\right)}{1+\frac{S_{11}A_{11}}{\lambda}q_1+\frac{B_1}{\lambda}q_2} &= 0. \end{aligned}$$

As mentioned in Case-4, $z(x) = \alpha(x)x$ is a monotonically increasing function. As $S_{11}A_{11} \neq B_1$, we may conclude that there does not exist such (q_1, q_2) pair and hence this case is not possible.

Case-14: $\eta_1 = 0, \eta_2 = 0, \eta_3 \neq 0, \eta_4 = 0 \Rightarrow$

$$\begin{aligned} \frac{\partial I}{\partial q_1} &= 0, \\ \frac{\partial I}{\partial q_2} &= 0, \\ \eta_3 \neq 0 \rightarrow q_3 &= 0, \\ \frac{\partial I}{\partial q_4} &= 0. \end{aligned}$$

This case corresponds to the scenario when at user 1 both antennas are active with different duty cycles and at user 2 both antennas have same duty cycle.

Following the same steps in Case-8, we obtain

$$q_4 = \frac{\left(1+\frac{S_{12}A_{12}}{S_{11}A_{11}}\right)\zeta(S_{11}A_{11},\lambda) - \zeta(B_1,\lambda)}{\zeta(B_2,B_1+\lambda) - \left(1+\frac{S_{12}A_{12}}{S_{11}A_{11}}\right)\zeta(B_2,S_{11}A_{11}+\lambda) + \frac{S_{12}A_{12}}{S_{11}A_{11}}\zeta(B_2,\lambda)}. \quad \text{(C.5)}$$

However, it is difficult to make any definitive conclusion about q_4 from this form. To rule out this case, we use the following lemma.

Lemma 24.

$$\text{(C.5)} = \frac{c_4}{c_4 + c_5},$$

in which $c_4 = h_2(\lambda)$ *and* $c_5 = -h_2(B_2 + \lambda)$ *with*

$$h_2(x) \;=\; \left(1 + \frac{S_{12}A_{12}}{S_{11}A_{11}}\right)\zeta(S_{11}A_{11}, x) - \zeta(B_1, x).$$

Proof. Please see Appendix C.5.3. □

Similar to Lemma 23, we can show that $h_2(x) < 0$ when $x > 0$. As the result, $q_4 \notin [0, 1]$. Hence, we know that Case-14 is not a valid choice.

Case-15: $\eta_1 = 0, \eta_2 = 0, \eta_3 = 0, \eta_4 \neq 0 \Rightarrow$

$$\begin{aligned} \frac{\partial I}{\partial q_1} &= 0, \\ \frac{\partial I}{\partial q_2} &= 0, \\ \frac{\partial I}{\partial q_3} &= 0, \\ \eta_4 \neq 0 \rightarrow q_4 &= 0. \end{aligned}$$

This case corresponds to the scenario when both antennas at user 1 are active with a different duty cycles while at user 2 only the antenna with the larger duty cycle is active. Following the same steps in Case-8, we obtain the value of q_3 as:

$$q_3 = \frac{\left(1 + \frac{S_{12}A_{12}}{S_{11}A_{11}}\right)\zeta(S_{11}A_{11}, \lambda) - \zeta(B_1, \lambda)}{\zeta(S_{21}A_{21}, B_1 + \lambda) - \left(1 + \frac{S_{12}A_{12}}{S_{11}A_{11}}\right)\zeta(S_{21}A_{21}, S_{11}A_{11} + \lambda) + \frac{S_{12}A_{12}}{S_{11}A_{11}}\zeta(S_{21}A_{21}, \lambda)} \quad \text{(C.6)}$$

Similar to Case-14, it is difficult to directly make any conclusion about the value of q_3.

Following similar steps as in Lemma 24, we can show that

$$\text{(C.6)} = \frac{c_4}{c_4 + c_6},$$

in which $c_4 = h_2(\lambda)$ and $c_6 = -h_2(S_{21}A_{21} + \lambda)$. Hence, similar to Case-14, we can conclude that $q_3 \notin [0, 1]$, and hence this case is not a valid choice.

Case-16: $\eta_1 = 0, \eta_2 = 0, \eta_3 = 0, \eta_4 = 0 \Rightarrow$

$$\frac{\partial I}{\partial q_k} = 0, k = 1, \cdots, 4$$

This case refers to the scenario when both of the antennas of each user is active and have different duty cycles. Following similar argument in Appendix C.5.1, we can rule this case out.

In summary, we are left with only three candidates for the optimality, i.e. Case-2, Case-5 and Case-6. Case-2 corresponds to the scenario where only user 2 is active with both antennas are simultaneously on or off with duty cycle $\alpha(B_2/\lambda)$ and hence the optimal value of $\mathbf{q}$ is $(0, 0, 0, \alpha(B_2/\lambda))$. Case-5 is the scenario where only user 1 is active with both antennas are simultaneously on or off with duty cycle $\alpha(B_1/\lambda)$ and therefore $\mathbf{q} = (0, \alpha(B_1/\lambda), 0, 0)$. Case-6 is the scenario where both users are active with both antennas at user 1 are simultaneously on or off and both antennas at user 2 are also simultaneously on or off and hence $\mathbf{q} = (0, \mu_1, 0, \mu_2)$ where μ_1 and μ_2 are obtained by solving (3.13) and (3.14) with S_1A_1 replaced by $B_1 = S_{11}A_{11} + S_{12}A_{12}$ and S_2A_2 replaced by $B_2 = S_{21}A_{21} + S_{22}A_{22}$. It is clear that results obtained for MISO-MAC are the same as a SISO-MAC with properly chosen parameter.

C.5 Proofs of Lemmas used in the Proof of Proposition 15

C.5.1 Proof of Case-7

In this section we show that any sum-rate achievable for scheme A, where both of the antennas at user 1 are active with a same duty cycle but at user 2 only the antenna with the larger duty cycle is active, can also be achieved by scheme B, where both antennas of each user are simultaneously on or off.

Let p^* be the duty cycle used by both antennas of user 1 and x^* be the duty cycle used by the antenna with the larger duty cycle of user 2. Then the sum-rate achieved by scheme A is

$$\begin{aligned} I_A &= (1-p^*)(1-x^*)\varphi(\lambda) + (1-p^*)x^*\varphi(S_{21}A_{21}+\lambda) \\ &\quad +p^*(1-x^*)\varphi(S_{11}A_{11}+S_{12}A_{12}+\lambda) + p^*x^*\varphi(S_{21}A_{21}+S_{11}A_{11}+S_{12}A_{12}+\lambda) \\ &\quad -\varphi((S_{11}A_{11}+S_{12}A_{12})p^* + S_{21}A_{21}x^* + \lambda). \end{aligned}$$

Now consider scheme B, in which both antennas of user 1 to be simultaneously on-off with duty-cycle p^*, for user 2, we let both antennas to be simultaneously on or off with duty cycle x^* but with reduced amplitude. In particular, for antenna 1, it uses $\beta_1 A_{21}$. For antenna 2, it uses $\beta_2 A_{22}$. We select β_1 and β_2 such that $\beta_1 S_{21}A_{21} + \beta_2 S_{22}A_{22} = S_{21}A_{21}$. It is easy to check that there always exists $0 \leq \beta_1 \leq 1$ and $0 \leq \beta_2 \leq 1$ such that this relationship holds. Hence, scheme B is a valid scheme. For this scheme, the achievable sum-rate is

$$\begin{aligned} I_B &= (1-p^*)(1-x^*)\varphi(\lambda) + (1-p^*)x^*\varphi(\beta_1 S_{21}A_{21}+\beta_2 S_{22}A_{22}+\lambda) \\ &\quad p^*(1-x^*)\varphi(S_{11}A_{11}+S_{12}A_{12}+\lambda) + p^*x^*\varphi(\beta_1 S_{21}A_{21}+\beta_2 S_{22}A_{22}+S_{11}A_{11}+S_{12}A_{12}+\lambda) \\ &\quad -\varphi((S_{11}A_{11}+S_{12}A_{12})p^* + (\beta_1 S_{21}A_{21}+\beta_2 S_{22}A_{22})x^* + \lambda). \end{aligned}$$

As $\beta_1 S_{21} A_{21} + \beta_2 S_{22} A_2 2 = S_{21} A_{21}$, we have $I_A = I_B$. Therefore, we can conclude that any sum-rate achievable by letting both of the antennas at user 1 to be active with a same duty cycle but letting only one antenna of user 2 to be active can also be achieved by letting both antennas of each user to be simultaneously on or off.

C.5.2 Property of Lemma 23

To lighten up the notation, we set $a = S_{22} A_{22}$ and $b = S_{21} A_{21}$. We have

$$\begin{aligned} h_1(x) &= \left(1 + \frac{b}{a}\right) \zeta(a, x) - \zeta(a + b, x) \\ &= \zeta(a, x) + \frac{b}{a} \zeta(a, x) - \zeta(a + b, x) \\ &= (a + x) \log(a + x) - x \log x + \frac{b}{a} (a + x) \log(a + x) \\ &\quad - \frac{b}{a} x \log x - (a + b + x) \log(a + b + x) + x \log x \\ &= -(a + x) \log \left(\frac{a + b + x}{a + x} \right) - b \log \left(\frac{a + b + x}{a + x} \right) + \frac{b}{a} x \log \left(\frac{a + x}{x} \right). \end{aligned}$$

Using the fact that for $x > 0$,

$$\frac{x}{1 + x} < \ln(1 + x) < x,$$

we obtain

$$h_1(x) < \frac{1}{\ln(2)} \left(-(a + x) \frac{b}{a + b + x} - \frac{b^2}{a + b + x} + \frac{b}{a} x \frac{a}{x} \right) = 0.$$

C.5.3 Proof of Lemma 24

In order to come to a firm conclusion about the value of q_4, we will write the value of $I(\mathbf{q})$ in (4.40) in a different form. In (4.40), all the terms are written separated by q_1 and

q_2 terms, we will now write $I(\mathbf{q})$ written separated by q_3 and q_4. Clearly $I(\mathbf{q})$ in (4.40) can be written as

$$
\begin{aligned}
I(\mathbf{q}) &= (1-(q_3+q_4))\Big((1-(q_1+q_2))\varphi(\lambda)+q_1\varphi(S_{11}A_{11}+\lambda)+q_2\varphi(B_1+\lambda)\Big)\\
&+q_3\Big((1-(q_1+q_2))\varphi(S_{21}A_{21}+\lambda)+q_1\varphi(S_{11}A_{11}+S_{21}A_{21}+\lambda)+q_2\varphi(B_1+S_{21}A_{21}+\lambda)\Big)\\
&+q_4\Big((1-(q_1+q_2)\varphi(B_2+\lambda)+q_1\varphi(S_{11}A_{11}+B_2+\lambda)+q_2\varphi(B_1+B_2+\lambda)\\
&-\varphi(S_{11}A_{11}q_1+B_1q_2+S_{21}A_{21}q_3+B_2q_4+\lambda). \qquad \text{(C.7)}
\end{aligned}
$$

Using this new form, then we have:

$$
\begin{aligned}
\frac{\partial I}{\partial q_1} &= (1-(q_3+q_4))\zeta(S_{11}A_{11},\lambda)+q_3\zeta(S_{11}A_{11},S_{21}A_{21}+\lambda)+q_4\zeta(S_{11}A_{11},B_2+\lambda)\\
&\quad -S_{11}A_{11}\left(\log\left(S_{11}A_{11}q_1+B_1q_2+S_{21}A_{21}q_3+B_2q_4+\lambda\right)+1\right),\\
\frac{\partial I}{\partial q_2} &= (1-(q_3+q_4))\zeta(B_1,\lambda)+q_3\zeta(B_1,S_{21}A_{21}+\lambda)+q_4\zeta(B_1,B_2+\lambda)\\
&\quad -B_1\left(\log(S_{11}A_{11}q_1+B_1q_2+S_{21}A_{21}q_3+B_2q_4+\lambda)+1\right),\\
\frac{\partial I}{\partial q_3} &= \zeta(S_{21}A_{21},\lambda)+q_1\Big(\zeta(S_{11}A_{11},S_{21}A_{21}+\lambda)-\zeta(S_{11}A_{11},\lambda)\Big)+q_2\Big(\zeta(B_1,S_{21}A_{21}+\lambda)\\
&\quad -\zeta(B_1,\lambda)\Big)-S_{21}A_{21}(\log\left(S_{11}A_{11}q_1+B_1q_2+S_{21}A_{21}q_3+B_2q_4+\lambda\right)+1),
\end{aligned}
$$

and

$$
\begin{aligned}
\frac{\partial I}{\partial q_4} &= \zeta(B_2,\lambda)+q_1\Big(\zeta(S_{11}A_{11},B_2+\lambda)-\zeta(S_{11}A_{11},\lambda)\Big)+q_2\Big(\zeta(B_1,B_2+\lambda)\\
&\quad -\zeta(B_1,\lambda)\Big)-B_2(\log\left(S_{11}A_{11}q_1+B_1q_2+S_{21}A_{21}q_3+B_2q_4+\lambda\right)+1).
\end{aligned}
$$

Recall that we need to solve

$$\begin{aligned} \frac{\partial I}{\partial q_1} &= 0, \\ \frac{\partial I}{\partial q_2} &= 0, \\ q_3 &= 0, \\ \frac{\partial I}{\partial q_4} &= 0. \end{aligned}$$

By combining $\frac{\partial I}{\partial q_1} = 0$ and $\frac{\partial I}{\partial q_2} = 0$, we can eliminate the term with $\log$ and obtain a linear equation in terms of q_3 and q_4. By plugging $q_3 = 0$ to the obtained linear equation, we obtain an alternative form of (C.5):

$$q_4 = \frac{c_4}{c_4 + c_5},$$

in which $c_4 = h_2(\lambda)$ and $c_5 = -h_2(B_2 + \lambda)$ with

$$h_2(x) = \left(1 + \frac{S_{12}A_{12}}{S_{11}A_{11}}\right)\zeta(S_{11}A_{11}, x) - \zeta(B_1, x).$$

Appendix D

Proofs for Chapter 4

D.1 Detailed Poisson SIMO-MAC:

In order to find out the optimal solution to the given problem, in this section, under different constraints we have following 16 cases.

Case-1: $\eta_1 = 0, \eta_2 \neq 0, \eta_3 = 0, \eta_4 = 0 \Rightarrow$

$$\begin{aligned} \frac{\partial I}{\partial \mu_1} + \eta_2 &= 0, \\ \frac{\partial I}{\partial \mu_2} &= 0 \\ \eta_2 \neq 0 \Rightarrow \mu_1 &= 0. \end{aligned}$$

Therefore the candidate for the optimal solution is $(0, \mu_2)$, where μ_2 satisfies $\frac{\partial I}{\partial \mu_2}\Big|_{(0,\mu_2)} = 0$. This case corresponds to the scenario when user 1 is inactive and user 2 is active.

Case-2: $\eta_1 = 0, \eta_2 = 0, \eta_3 = 0, \eta_4 \neq 0 \Rightarrow$

$$\begin{aligned} \frac{\partial I}{\partial \mu_1} &= 0, \\ \frac{\partial I}{\partial \mu_2} + \eta_4 &= 0, \\ \eta_4 \neq 0 \Rightarrow \mu_2 &= 0. \end{aligned}$$

Therefore the optimal pair must satisfy $\frac{\partial I}{\partial \mu_1}\Big|_{(\mu_1,0)} = 0$. This case corresponds to the scenario when user 1 is active and user 2 is inactive.

Case-3: $\eta_1 = 0, \eta_2 = 0, \eta_3 = 0, \eta_4 = 0 \Rightarrow$

$$\begin{aligned} \frac{\partial I}{\partial \mu_1} &= 0, \\ \frac{\partial I}{\partial \mu_2} &= 0. \end{aligned}$$

This case corresponds to the scenario when it is optimal for both of the users to transmit. The pair (μ_1, μ_2) must satisfy both of the equations simultaneously.

Case-4: $\eta_1 = 0, \eta_2 = 0, \eta_3 \neq 0, \eta_4 = 0 \Rightarrow$

$$\begin{aligned} \frac{\partial I}{\partial \mu_1} &= 0, \\ \frac{\partial I}{\partial \mu_2} - \eta_3 &= 0, \\ \eta_3 \neq 0 \Rightarrow \mu_2 &= 1. \end{aligned}$$

Then the optimal solution must satisfy $\frac{\partial I}{\partial \mu_1}\Big|_{(\mu_1,1)} = 0$. As $I(\mu_1, 0) \geq I(\mu_1, 1)$, therefore we may conclude that this case does not result in a candidate for the optimal solution.

Case-5: $\eta_1 = 0, \eta_2 = 0, \eta_3 \neq 0, \eta_4 \neq 0 \Rightarrow$

$$\begin{aligned} \frac{\partial I}{\partial \mu_1} &= 0, \\ \frac{\partial I}{\partial \mu_2} - \eta_3 + \eta_4 &= 0, \\ \eta_3 \neq 0 \Rightarrow \mu_2 &= 1, \\ \eta_4 \neq 0 \Rightarrow \mu_2 &= 0. \end{aligned}$$

It is clear that this case is not possible.

Case-6: $\eta_1 = 0, \eta_2 \neq 0, \eta_3 = 0, \eta_4 \neq 0 \Rightarrow$

$$\begin{aligned} \frac{\partial I}{\partial \mu_1} + \eta_2 &= 0, \\ \frac{\partial I}{\partial \mu_2} + \eta_4 &= 0, \\ \eta_2 \neq 0 \Rightarrow \mu_1 &= 0, \\ \eta_4 \neq 0 \Rightarrow \mu_2 &= 0. \end{aligned}$$

It is clear that this case does not result in a candidate for the optimal solution.

Case-7: $\eta_1 = 0, \eta_2 \neq 0, \eta_3 \neq 0, \eta_4 = 0 \Rightarrow$

$$\begin{aligned} \frac{\partial I}{\partial \mu_1} + \eta_2 &= 0, \\ \frac{\partial I}{\partial \mu_2} - \eta_3 &= 0, \\ \eta_2 \neq 0 \Rightarrow \mu_1 &= 0, \\ \eta_3 \neq 0 \Rightarrow \mu_2 &= 1. \end{aligned}$$

It is clear that $\mu_1 = 0, \mu_2 = 1$ is not a candidate for the optimal solution.

Case-8: $\eta_1 = 0, \eta_2 \neq 0, \eta_3 \neq 0, \eta_4 \neq 0 \Rightarrow$

$$\begin{aligned} \frac{\partial I}{\partial \mu_1} + \eta_2 &= 0, \\ \frac{\partial I}{\partial \mu_2} - \eta_3 + \eta_4 &= 0, \\ \eta_2 \neq 0 \Rightarrow \mu_1 &= 0, \\ \eta_3 \neq 0 \Rightarrow \mu_2 &= 1, \\ \eta_4 \neq 0 \Rightarrow \mu_2 &= 0. \end{aligned}$$

It is clear that it is not a feasible case.

Case-9: $\eta_1 \neq 0, \eta_2 = 0, \eta_3 = 0, \eta_4 = 0 \Rightarrow$

$$\begin{aligned} \frac{\partial I}{\partial \mu_1} - \eta_1 &= 0, \\ \frac{\partial I}{\partial \mu_2} &= 0, \\ \eta_1 \neq 0 \Rightarrow \mu_1 &= 1. \end{aligned}$$

Similar to Case-4, this case does not result in a candidate for optimal solution because $I(0, \mu_2) \geq I(1, \mu_1)$.

Case-10: $\eta_1 \neq 0, \eta_2 = 0, \eta_3 = 0, \eta \neq 0 \Rightarrow$

$$\begin{aligned} \frac{\partial I}{\partial \mu_1} - \eta_1 &= 0, \\ \frac{\partial I}{\partial \mu_2} + \eta_4 &= 0, \\ \eta_1 \neq 0 \Rightarrow \mu_1 &= 1, \\ \eta_4 \neq 0 \Rightarrow \mu_2 &= 0. \end{aligned}$$

It is clear that $I(1,0)$ does not result in a candidate for the optimal value of sum-rate.

Case-11: $\eta_1 \neq 0, \eta_2 = 0, \eta_3 \neq 0, \eta_4 = 0 \Rightarrow$

$$\begin{aligned} \frac{\partial I}{\partial \mu_1} - \eta_1 &= 0, \\ \frac{\partial I}{\partial \mu_2} - \eta_3 &= 0, \\ \eta_1 \neq 0 \Rightarrow \mu_1 &= 1, \\ \eta_3 \neq 0 \Rightarrow \mu_2 &= 1. \end{aligned}$$

It is clear that this this case does not result in the optimal candidate.

Case-12: $\eta_1 \neq 0, \eta_2 = 0, \eta_3 \neq 0, \eta_4 \neq 0 \Rightarrow$

$$\begin{aligned} \frac{\partial I}{\partial \mu_1} - \eta_1 &= 0, \\ \frac{\partial I}{\partial \mu_2} - \eta_3 + \eta_4 &= 0, \\ \eta_1 \neq 0 \Rightarrow \mu_1 &= 1, \\ \eta_3 \neq 0 \Rightarrow \mu_2 &= 1, \\ \eta_4 \neq 0 \Rightarrow \mu_2 &= 0. \end{aligned}$$

This case is not feasible due to conflicting values of μ_2.

Case-13: $\eta_1 \neq 0, \eta_2 \neq 0, \eta_3 = 0, \eta_4 = 0 \Rightarrow$

$$\begin{aligned} \frac{\partial I}{\partial \mu_1} - \eta_1 + \eta_2 &= 0, \\ \frac{\partial I}{\partial \mu_2} &= 0, \\ \eta_1 \neq 0 \Rightarrow \mu_1 &= 1, \\ \eta_2 \neq 0 \Rightarrow \mu_1 &= 0. \end{aligned}$$

Clearly this case is also not feasible.

Case-14: $\eta_1 \neq 0, \eta_2 \neq 0, \eta_3 = 0, \eta_4 \neq 0 \Rightarrow$

$$\begin{aligned}
\frac{\partial I}{\partial \mu_1} - \eta_1 + \eta_2 &= 0, \\
\frac{\partial I}{\partial \mu_2} + \eta_4 &= 0, \\
\eta_1 \neq 0 \Rightarrow \mu_1 &= 1, \\
\eta_2 \neq 0 \Rightarrow \mu_1 &= 0, \\
\eta_4 \neq 0 \Rightarrow \mu_2 &= 0.
\end{aligned}$$

This case is also not feasible.

Case-15: $\eta_1 \neq 0, \eta_2 \neq 0, \eta_3 \neq 0, \eta_4 = 0 \Rightarrow$

$$\begin{aligned}
\frac{\partial I}{\partial \mu_1} - \eta_1 + \eta_2 &= 0, \\
\frac{\partial I}{\partial \mu_2} - \eta_3 &= 0, \\
\eta_1 \neq 0 \Rightarrow \mu_1 &= 1, \\
\eta_2 \neq 0 \Rightarrow \mu_1 &= 0, \\
\eta_3 \neq 0 \Rightarrow \mu_2 &= 1.
\end{aligned}$$

This case is also not feasible.

Case-16: $\eta_1 \neq 0, \eta_2 \neq 0, \eta_3 \neq 0, \eta_4 \neq 0 \Rightarrow$

$$\begin{aligned}
\frac{\partial I}{\partial \mu_1} - \eta_1 + \eta_2 &= 0, \\
\frac{\partial I}{\partial \mu_2} + \eta_4 &= 0, \\
\eta_1 \neq 0 \Rightarrow \mu_1 &= 1, \\
\eta_2 \neq 0 \Rightarrow \mu_1 &= 0, \\
\eta_3 \neq 0 \Rightarrow \mu_2 &= 1, \\
\eta_4 \neq 0 \Rightarrow \mu_2 &= 0.
\end{aligned}$$

This case is also not feasible.

Bibliography

[1] J. Mitola III and G. Maguire Jr, "Cognitive radio: making software readios more personal," *IEEE Personal Communications*, vol. 6, pp. 13–18, Aug. 1999.

[2] I. F. Akyildiz, W.-Y. Lee, M. Vuran, and S. Mohanty, "A survey on spectrum management in cognitive radio networks," *IEEE Communications Magazine*, vol. 46, pp. 40–48, Apr. 2008.

[3] N. Devroye, M. Vu, and V. Tarokh, "Cognitive radio networks," *IEEE Signal Processing Magazine*, vol. 25, pp. 12–13, Nov. 2008.

[4] A. Ghasemi and E. S. Sousa, "Spectrum sensing in cognitive radio networks: requirements, challenges and design trade-offs," *IEEE Communications Magazine*, vol. 46, pp. 32–39, Apr. 2008.

[5] K. B. Lataief and W. Zhang, "Cooperative communications for cognitive radio networks," *Proceedings of the IEEE*, vol. 97, pp. 878–893, May 2009.

[6] Ain-ul-Aisha, J. Qadir, and A. Baig, "Mitigating the effect of malicious users in cognitive networks," in *Proc. IEEE Frontiers of Information Technology*, (Islamabad, Pakistan), pp. 1–5, Dec. 2013.

[7] G. Corbellini, K. Aksit, S. Schmid, S. Mangold, and T. Gross, "Connecting networks of toys and smartphones with visible light communication," *IEEE Communications Magazine*, vol. 52, pp. 72–78, July 2014.

[8] T. Komine and M. Nakagawa, "Fundamental analysis for visible-light communication system using LED lights," *IEEE Trans. on Consumer Electronics*, vol. 50, pp. 100–107, Feb. 2004.

[9] D. C. O'Brien, "Visible light communications: Challenges and potential," in *IEEE Photonic Society*, pp. 365–366, Oct. 2011.

[10] D. C. O'Brien, L. Zeng, H. Le-Minh, G. Faulkner, J. W. Walewski, and S. Randel, "Visible light communications: Challenges and possibilities," in *Proc. IEEE Intl. Symposium on Personal, Indoor and Mobile Radio Communications*, (Cannes, France), pp. 1–5, Sept. 2008.

[11] M. Afgani, H. Haas, H. Elgala, and D. Knipp, "Visible light communication using OFDM," in *IEEE International Conference on Testbeds and Research Infrastructures for the Development of Networks and Communities*, (Castelldefels, Spain), July 2006.

[12] H. Kaushal and G. Kaddoumtitle, "Optical communication in space: Challenges and mitigation techniques," *IEEE Communications Surveys and Tutorials*, vol. 19, pp. 57–96, Aug. 2017.

[13] X. Liu, "Free-space optics optimization models for building sway and atmospheric interference using variable wavelength," vol. 57, pp. 492–498, Feb. 2009.

[14] W. R. Leeb, "Space laser communications: Systems, technologies, and applications," available at https://pdfs.semanticscholar.org/0be8/757d1c81f0a1d8401542c2c6f7d5f4bf0d70.pdf.

[15] X. Zhu and J. M. Kahn, "Free-space optical communication through atmospheric turbulence channels," *IEEE Trans. Communications*, vol. 50, pp. 1293–1300, Aug. 2002.

[16] H. Henniger and O. Wilfert, "An introduction to free-space optical communications," *RadioEngineering*, vol. 19, pp. 203–212, Nov. 2010.

[17] F. Khan, S. R. Jan, M. Tahir, and S. Khan, "Applications, limitations, and improvements in visible light communication systems," in *IEEE Conference on Connected Vehicles and Expo*, (Shenzhen, China), pp. 259–260, Oct. 2015.

[18] T. Q. Wang, Y. A. Sekercioglu, and J. Armstrong, "Analysis of an optical wireless receiver using a hemispherical lens with application in MIMO visible light communications," *Journal of Lightwave Technology*, vol. 31, pp. 1744–1754, Apr. 2013.

[19] S. M. Haas and J. H. Shapiro, "Capacity of wireless optical communications," *IEEE Journal on Selected Areas in Communications*, vol. 21, pp. 1346–1357, Oct. 2003.

[20] S. Bross, M. Burnashev, and S. Shamai (Shitz), "Error exponents for the two-user poisson multiple-access channel," *IEEE Trans. Inform. Theory*, vol. 47, pp. 1999–2016, July 2001.

[21] S. Bross and S. Shamai (Shitz), "Capacity and decoding rules for the poisson arbitrarily varying channel," *IEEE Trans. Inform. Theory*, vol. 49, pp. 3076–3093, Nov. 2003.

[22] E. Bayraktar, S. Dayanik, and I. Karatzas, "The standard Poisson disorder problem revisited," *Stochastic Processes and Their Applications*, vol. 115, pp. 1437–1450, Mar. 2005.

[23] E. Bayraktar and H. V. Poor, "Quickest detection of a minimum of two Poisson disorder times," *SIAM Journal on Control and Optimization*, vol. 46, pp. 308–331, Mar. 2007.

[24] S. M. Haas, *Capacity of and Coding for Multiple-Aperture, Wireless, Optical Communications*. PhD thesis, Massachusetts Institute of Technology, 2003.

[25] D. Guo, Y. Wu, S. Shamai (Shitz), and S. Verdu, "Estimation in Gaussian noise: Properties of the minimum mean-square error," *IEEE Trans. Inform. Theory*, vol. 57, pp. 2371–2385, Jan. 2011.

[26] A. D. Wyner, "Capacity and error exponent for the direct detection photon channel - Parts I and II," *IEEE Trans. Inform. Theory*, vol. 34, pp. 1449–1471, Nov. 1988.

[27] R. Atar and T. Weissman, "Mutual information, relative entropy, and estimation in the Poisson channel," *IEEE Trans. Inform. Theory*, vol. 58, pp. 1302–1318, Mar. 2012.

[28] D. Guo, S. Shamai (Shitz), and S. Verdu, "Mutual information and conditional mean estimation in Poisson channel," *IEEE Trans. Inform. Theory*, vol. 54, pp. 1837–1849, May 2008.

[29] M. Frey, "Information capacity of the Poisson channel," *IEEE Trans. Inform. Theory*, vol. 37, pp. 244–256, Mar. 1991.

[30] M. Frey, "Capacity of the l_p norm-constrainted Poisson channel," *IEEE Trans. Inform. Theory*, vol. 38, pp. 445–450, Mar. 1992.

[31] K. Chakraborty, "Capacity of the MIMO optical fading channel," in *Proc. IEEE Intl. Symposium on Inform. Theory*, (Adelaide, Australia), pp. 530–534, Sept. 2005.

[32] K. Chakraborty, S. Dey, and M. Franceschetti, "Outage capacity of MIMO Poisson fading channels," *IEEE Trans. Inform. Theory*, vol. 54, pp. 4887–4907, Nov. 2008.

[33] Ain-ul-Aisha, L. Lai, and Y. Liang, "Optimal power allocation for Poisson channels with time-varying background light," *IEEE Trans. Communications*, vol. 63, pp. 4327–4338, Nov. 2015.

[34] Y. Kabanov, "Capacity of a channel of the Poisson type," *Theory of Probability and its Applications*, vol. 23, pp. 143–147, Jan. 1978.

[35] M. Davis, "Capacity and cutoff rate for Poisson-type channels," *IEEE Trans. Inform. Theory*, vol. 26, pp. 710–715, Nov. 1980.

[36] S. Shamai (Shitz) and A. Lapidoth, "Bounds on the capacity of a spectrally constrained Poisson channel," *IEEE Trans. Inform. Theory*, vol. 39, pp. 19–29, Jan. 1993.

[37] S. Dayanik, H. V. Poor, and S. O. Sezer, "Sequential multi-hypothesis testing for compound Poisson processes," *Stochastics*, vol. 80, pp. 19–50, June 2008.

[38] A. Lapidoth, J. H. Shapro, V. Venkatesan, and L. Wong, "The discrete-time Poisson channel at low input powers," *IEEE Trans. Inform. Theory*, vol. 57, pp. 3260–3272, June 2011.

[39] A. Lapidoth and S. Moser, "On the capacity of the discrete-time Poisson channel," *IEEE Trans. Inform. Theory*, vol. 55, pp. 303–322, Oct. 2009.

[40] L. Wang and G. W. Wornell, "A refined analysis of the Poisson channel in the high-photon-efficiency regime," *IEEE Trans. Inform. Theory*, vol. 60, pp. 4299–4311, July 2014.

[41] K. Chakraborty, S. Dey, and M. Franceschetti, "Outage capacity of MIMO Poisson fading channels," *IEEE Trans. Inform. Theory*, vol. 54, pp. 4887–4907, Nov. 2008.

[42] K. Chakraborty, *Relaiable Communication over Optical Fading Channels*. PhD thesis, University of Maryland, 2005.

[43] K. Chakraborty and P. Narayan, "The Poisson fading channel," *IEEE Trans. Inform. Theory*, vol. 35, pp. 2349–2364, Jul. 2007.

[44] E. J. Lee and V. W. S. Chan, "Part I: Optical communication over the clear turbulent atmospheric channel using diversity," *IEEE Journal on Selected Areas in Communications*, vol. 22, pp. 1896–1906, Nov. 2004.

[45] Y. He and S. Dey, "Throughput maximization in Poisson fading channels with limited feedback," *IEEE Trans. Communications*, vol. 61, pp. 4343–4355, Oct. 2013.

[46] M. Sapari, M. M. Rad, and M. Uysal, "Multi-hop relaying over the atmospheric Poisson channel: Outage analysis & optimization," *IEEE Trans. Communications*, vol. 60, pp. 817–829, Mar. 2013.

[47] M. Alem-Karladani, L. Sepahi, M. Jazayerifar, and K. Kalbasi, "Optimum power allocation in parallel Poisson optical channel," in *Proc. Intl. Conf. on Telecommunications*, (Zagreb, Croatia), pp. 285–288, June 2009.

[48] S. Bross, A. Lapidoth, and L. Wang, "The Poisson channel with side information," in *Proc. Allerton Conf. on Communication, Control, and Computing*, (Monticello, Illinois), pp. 574–578, Oct. 2009.

[49] A. Lapidoth, I. E. Telatar, and R. Urbanke, "On wide-band broadcast channels," *IEEE Trans. Inform. Theory*, vol. 49, pp. 3250–3258, Dec. 2003.

[50] H. Kim, B. Nachman, and A. E. Gamal, "Superposition coding is almost always optimal for the Poisson broadcast channel," *IEEE Trans. Inform. Theory*, vol. 62, pp. 1782–1794, Apr. 2016.

[51] A. Sokolovsky and S. Bross, "Attainable error exponents for the Poisson broadcast channel with degraded message sets," *IEEE Trans. Inform. Theory*, vol. 51, pp. 364–374, Jan. 2005.

[52] A. Lapidoth and S. Shamai (Shitz), "The Poisson multiple-access channel," *IEEE Trans. Inform. Theory*, vol. 44, pp. 488–501, Mar. 1998.

[53] S. A. M. Ghanem and M. Ara, "The MAC Poisson Channel: Capacity and optimal power allocation," in *IAENG Transactions on Engineering Technologies*, pp. 45–60, Springer, 2013.

[54] S. Bross, A. Lapidoth, and L. Wang, "The Poisson channel with side information," in *Proc. Allerton Conf. on Communication, Control, and Computing*, (Monticello, IL.), pp. 574–578, Oct. 2009.

[55] L. Lai, Y. Liang, and S. Shamai (Shitz), "On the sum capacity of Poisson Z-interference channels," in *IEEE International Conference on Communications in China*, (Xian, China), Aug. 2013.

[56] J. Cao, J. Chen, and S. Hranilovic, "Discreteness of sum-capacity-achieving distributions for discrete-time Poisson multiple access channels with peak constraints," *IEEE Communications Letters*, vol. 17, pp. 1644–1647, Aug. 2013.

[57] J. Cao, S. Hranilovic, and J. Chen, "Capacity achieving distributions for the discrete-time Poisson channel - Part I: general properties and numerical techniques," *IEEE Trans. Communications*, vol. 62, pp. 194–202, Jan. 2014.

[58] M. A. Kashani and M. Uysal, "Outage performance and diversity gain analysis of free-space optical multi-hop parallel relaying," *IEEE Trans. Communications*, vol. 5, pp. 901–909, Aug. 2013.

[59] G. Caire, G. Taricco, and E. Biglieri, "Optimum power control over fading channels," *IEEE Trans. Inform. Theory*, vol. 45, pp. 1468–1489, Jul. 1999.

[60] Ain-ul-Aisha, L. Lai, Y. Liang, and S. Shamai (Shitz), "On the sum-rate capacity of Poisson multi antenna multiple access channels," *IEEE Trans. Inform. Theory*. Submitted, available at http://users.wpi.edu/∼aaisha.

[61] A. W. Roberts and D. E. Varberg, *Convex functions*. Academic Press Inc., 1973.

[62] Ain-ul-Aisha, Y. Liang, L. Lai, and S. Shamai (Shitz), "On the sum-rate capacity of non-symmetric Poisson multiple access channel," in *Proc. IEEE Intl. Symposium on Inform. Theory*, (Barcelona, Spain), pp. 375–379, July 2016.

[63] H. R. Varian, *Symbolic Optimization*. New York: Springer, 1993.